بسم الله الرحمن الرحيم

Sudan University of Science and Technology

College of Graduate Studies & Scientific Research

Fatigue life improvement of Aluminum alloy by using laser and ultrasonic techniques

تحسين عمر الكلال لسبيكة الألمنيوم باستخدام تقنيات الليزر والموجات فوق الصوتية

A THESIS SUBMITTED IN FULFILMENT OF THE DEGREE OF DOCTOR OF PHILOSOPHY (phD) IN MECHANICAL ENGINEERING

Presented by: **Ali Yousuf Khenyab**

B.Sc. (1989), M.Sc. (2013) Mechanical Engineering

Supervisor: Dr. Alkhawad A . Alfaky
Co-supervisor: Dr.(Prof.) Hussain J. Al-Alkawi

November 2016

بسم الله الرحمن الرحيم

وَبَشِّرِ الَّذِينَ آمَنُواْ وَعَمِلُواْ الصَّالِحَاتِ أَنَّ لَهُمْ جَنَّاتٍ تَجْرِي مِن تَحْتِهَا الأَنْهَارُ كُلَّمَا رُزِقُواْ مِنْهَا مِن ثَمَرَةٍ رِّزْقاً قَالُواْ هَـذَا الَّذِي رُزِقْنَا مِن قَبْلُ وَأُتُواْ بِهِ مُتَشَابِهاً وَلَهُمْ فِيهَا أَزْوَاجٌ مُّطَهَّرَةٌ وَهُمْ فِيهَا خَالِدُونَ .

صدق الله العظيم

سورة البقرة الآية (25)

Dedication

Mercy of God to help me,

TO the soul of my parents, my brother and my sister,

TO my family, to my wife, my son and my daughters

TO all who admired this piece of a work,

Acknowledgement

I would like to record my sincere gratitude and indebtedness to my supervisors ***Prof. Dr. Alalkawi H.J.M and Dr. Elkhawad Ali Elfaki*** *for all the support they gave me.*

I would like to thank the head of Electromechanical Engineering Department of Technology, the engineers in strength of Materials Laboratory and Laser Department for their help during the experimental work.

I would like to thank all of those who assisted me in any way during the completion the research.

Abstract

Laser Peening (LP) and Ultrasonic Peening (UP) treatments with fatigue interaction were studied for 2017A-T3 Aluminum alloy under room temperature (RT) and stress ratio R = -1.

Experimental mechanical properties and fatigue behavior of the above alloy were obtained for different conditions of LP & UP surface treatments. The mechanical properties ultimate strength ($\boldsymbol{\sigma_u}$) and yield stress ($\boldsymbol{\sigma_y}$) were enhanced by 8.7% and 20.4% respectively, while the above parameters were improved by 10.3% and 30.7% for ultrasonic peening (UP).

Constants fatigue behavior for the mentioned treatments have been also determined. The fatigue endurance limit was increased by 38% for LP and 61% for UP. The fatigue life for both treatments was significantly improved compared to as-received metal. Cumulative fatigue damage testing were carried out for two steps loading and it is observed that the fatigue life for LP and UP treated specimens were improved compared to the unpeened results. Two proposed cumulative non-linear models were presented one for LP and other for UP. These models showed that safe and satisfactory predications of fatigue life but the ultrasonic model gave 1.8 factor of safety while the laser model showed 1.2 factor of safety.

المستخلص

تمت دراسة تداخل الكلال مع التصليد الليزري (LP) والتصليد بالموجات فوق الصوتيه (UP) لسبيكة الالمنيوم (2017A-T3) عند درجة حرارة الغرفه (RT) ونسبة الإجهاد (R = -1).
تم استخراج المواصفات الميكانيكية والكلالية لظروف مختلفة من تعاملات السطح بواسطة (LP) و(UP) تم الحصول على تحسن في المواصفات الميكانيكية, المقاومة العظمى (σ_u) تحسنت بنسبة (**8.7%**) اما اجهاد الخضوع (σ_y) فتحسن بمقدار (20.4%) على التوالي عند التصليد الليزري , بينما هذه المواصفات اعلاه تحسنت بمقدار (10.3%) و (30.7%) في حالة التصليد بالموجات فوق الصوتية (UP).
تم ايجاد تصرف الكلال ثابت السعة للمعاملات آنفة الذكر. حيث ازداد حد الكلال بمقدار (38%) عند التصليد الليزري (LP) و (61%) عند التصليد بالموجات فوق الصوتية (UP). اعمار الكلال لكلا المعاملتين تحسنت بشكل ملحوظ مقارنة مع حالة المعدن المستلم بدون تصليد. تم تقديم انموذجين للكلال التراكمي الاول للتصليد الليزري والثاني للتصليد بالموجات فوق الصوتية هذان النموذجان ابدوا تخمينات أمينة ومقنعة لاعمار الكلال ولكن انموذج التصليد بالموجات فوق الصوتية أعطى عامل أمان يساوي (1.8) بينما الانموذج الليزري اعطى عامل أمان يساوي (1.2).

Contents

Figures & Tables

Tables ***Page***

Nomenclature

A, α : Material constant
D : Damage
E : Young's elastic modulus
N : Number of applied cycles
N_f : Number of cycles to failure
R : Stress ratio
$\Delta\sigma$: Stress range
a : Curve fitting parameters
σ_{EL} : Endurance limit stress at 10^7 cycle
σ_H : High stress
σ_L : Low stress
σ_u : Ultimate tensile strength
σ_u : Yield stress
ASM : American society for Metals
ASTM: American society for Testing and Materials
HCF : High cycle fatigue
LCF : Low cycle fatigue
H-L : High- Low
L-H : low -High
LRD : Liner damage Rules
S-N : Stress-No. of cycles
LP : Laser peening
BLP : Black laser peening
WLP : water laser peening
UP : Ultrasonic peening
1UP : one line Ultrasonic peening
2UP : Two lines Ultrasonic peening
3UP : Three lines Ultrasonic peening

Chapter 1
Introduction

1.1 Introduction

Engineering materials are subjected to fluctuating stresses, taking place at relatively high frequencies and under these conditions, failure is found to occur at stress value much lower than would apply for static loading. The phenomenon is known as fatigue failure.

It has been found experimentally that when a material is subjected to dynamic stresses, it fails at stress below the yield point stresses; such type of failure of a material is known as fatigue.

The failure is caused by means of a progressive crack for motion which are usually fine and of microscope size. The failure may be occur even without any prior indication.

If the stress is kept below a certain value, the material will not fail whatever may be the number of cycles; this stress is known as endurance limit.

This study light on the effective modern means to prolong fatigue life, Such Laser and Ultrasonic techniques which will be selected to enhance the mechanical properties and fatigue resistance of 2017A-T3 aluminum alloy.

1.2 Background

Many machine parts have been subjected to fluctuating stresses, happened at relatively high frequencies, and under these stats, failure is found by [Ryder (1982)].

It has been found experimentally that a material fails at stresses below the yield point stresses, when it is subjected to repeated stresses. That type of failure of a material is known as fatigue. The failure is caused by means of a progressive crack formation which are usually fine and of microscopic size. The failure may occur even without any prior indication. The fatigue of material is affected by the size of the component, relative magnitude of static and fluctuating loads and the number of load reversals. If the stress is kept below a certain value, the material will not fail whatever may be the number of cycles. This stress is known as endurance or fatigue limit. It is defined as maximum value of the completely reversed bending stress which a polished standard specimen can withstand without failure, for infinite number of cycles (usually 10^7 cycles) [Khurml (1990)].

Wrought aluminum, is widely used in automotive and aerospace industry due to its light weight and excellent specific strength. As industry develops, higher quality properties of products become more and more required in those industries. To meet those requirements, several researches have been carried out to improve mechanical performance by grain refinement and precipitation hardening by severe plastic deformation process, by [Choa (2012)] .

This study light on the effective modern means to prolong fatigue life, Such Laser and Ultrasonic techniques which will be selected to enhance the mechanical properties and fatigue resistance of 2017A-T3 aluminum alloy.

Ultrasonic technique provides severe plastic deformation via repetitive sliding impact, may be produce a number of beneficial properties of surface layers in different metallic material. They are the following (i) nancrystalline structure. (ii) Surface compressive residual stresses, (iii) strain hardening of the surface layer. These enhanced properties of the surface layer are shown to be attributing to the obtained superior fatigue behavior of processed materials during fatigue test [Bohdan (2007)].

Ultrasonic peening treatment (UPT) has recently had significantly more attention in several manufacturing processes. UPT modifies the surface of a material and enhances the mechanical and/or chemical properties. This is especially true for welded components when working under fatigue dynamic loading conditions by [Massoud (2015)].

Laser technique is an emerging surface modification technology which introduces deeper compressive residual stresses and less occurrence of defects in the material surface. It can significantly improve the mechanical performance and reduce fatigue crack growth rate on a number of metals [Anoop (2012)].

Laser shock peening (LSP) is an effective laser-based surface processing technique used to treat metallic materials for the enhanced surface strength, improved wear and corrosion resistance, and extended fatigue life. These superior mechanical properties are mainly attributed to the laser-induced surface compressive residual stress and work-hardened layer by [Yiliang (2016)].

1.2.3. Selected material

Aluminum alloy 2017 (2017 A-T3) has high strength with excellent fatigue strength. Alloy 2017A-T3 also has very good machining characteristics. It is suitable for welding only by resistance welding. This alloy is used for various applications from

high strength structural components, aircraft, machine construction, military equipment, rivets according to [WWW.aircraftmaterials.com (2013)].

1.3 **Research Problems**

The fatigue failure is one of the most common kind of failure for engineering parts that are exposed to variable loads, and because of the use of aluminum alloys in aircraft structures, missiles and other air equipment that is always exposed to variable amplitude loading, it needs to surface enhancement technologies, which are employed to improve the properties of components including fatigue, stress corrosion cracking, wear, and fretting. Among these surface enhancement technologies, shot peening is a conventional and widely applied process to increase fatigue performance of parts, which has been applied for many years in aircraft components. Laser peening and ultrasonic peening are a recently developed process and are being investigated in this study. Due to its accurate positioning and precise operation, laser peening and ultrasonic peening can be applied to many aircraft components such as fuselage, blades and wing with good repeatability and reliability, although it costs more than shot peening due to its low production rate. Laser peening and ultrasonic peening induces deep compressive residual stress in the surface layer by pulse laser impact energy and plastic deformation occurs in the surface layer, this prevents cracks or stop their growth, then increases fatigue resistance and increase the life of the functioning.

1.4 Research Importance

Technology to improve the surface which is mainly engaged to modify the surface integrity of parts using a wide range to improve the properties of the components, including fatigue, corrosion and stresses, between these technologies:

1. Laser peening which is a sophisticated technique can be used to hardener metallic surfaces such as aluminum due to accuracy and good specifications of the laser, which produces residual stresses layer to improve the mechanical specifications that through this research can be investigated**.**
2. Ultrasonic peening on the metal surface used , it is a moderns techniques that apply of most often on a limited area and produces surfaces with few roughness and this will investigate in our research, and also can be used to surface treatment of engineering components in their original positions.

1.5 Research Objectives

The objectives of this research are to investigate the following aspects:

1. Study the effect of surface treatment for the Aluminum alloy 2017A-T3 by laser and Ultrasonic peening after that comparison each other and with original metal.
2. To obtain the optimum case for improving the surface properties mechanical and fatigue behavior to help the designers and workers in this field.
3. Compare between the two surface treatments technique and to reach the best of enhancement.
4. To propose mathematical model describes the behavior of fatigue optimize at these two techniques.

1.6 Methodology

A- Theoretical part

i. Survey of modern research in laser hardening techniques and ultrasonic to improve fatigue life for metals and aluminum alloys.

ii. Survey of mathematical models describes the behavior of fatigue for Al-alloy, and put propose mathematical model.

B. Practical part

i. Manufacture of required specimens for fatigue test.

ii. Conducting chemical tests to find out the chemical composition of alloy 2017A-T3 Al-alloy.

iii. Manufacturing required specimens for tensile tests.

iv. Measuring the roughness of specimens.

v. Tensile tests.

vi. Fatigue tests with constant and variable amplitude without any treatment (Laser or Ultrasonic):

vii. Fatigue test with constant and variable amplitude after treatment by Laser peening and ultrasonic peening respectively.

viii Application of proposed model to laser and ultrasonic peening cumulative testing.

ix Comparison between mechanical properties and fatigue behavior of 2017A-T3 under laser & ultrasonic peening.

Chapter 2
Literature Survey and Theoretical Considerations

2.1 Importance of aluminum alloys, Fatigue failure, Laser Peening and Ultrasonic peening

Aluminum alloys with a wide range of properties are used in engineering structures. Alloy systems are classified by a number system (ANSI) or by names indicating their main alloying constituents (DIN and ISO). Selecting the right alloy for a given application entails considerations of its tensile strength, density, ductility, formability, workability, weld ability, and corrosion resistance, to name a few. A brief historical overview of alloys and manufacturing technologies is given in [Sanders (2001)]. Aluminum alloys are used extensively in aircraft due to their high strength-to-weight ratio. On the other hand, pure aluminum metal is much too soft for such uses, and it does not have the high tensile strength that is needed for airplanes and helicopters.

Fatigue is the weakening of a material caused by repeatedly applied loads. It is the progressive and localized structural damage that occurs when a material is subjected to cyclic loading. The nominal maximum stress values that cause such damage may be much less than the strength of the material typically quoted as the ultimate tensile stress limit, or the yield stress limit by [Kim (1978)].

Laser peening (LP), is a surface engineering processes used to impart beneficial residual stresses in materials. The deep, high magnitude compressive residual stresses induced by laser peening increase the resistance of materials to surface-related failures, such as fatigue, fretting fatigue and stress corrosion cracking. The physics of the laser shock peening process can also be used to strengthen thin sections, work-harden surfaces, shape or straighten parts (known as laser peen forming), break up hard materials, compact powdered metals and for other applications where high pressure, short duration shock waves offer desirable processing results [https://en.wikipedia.org (2015).] .

Ultrasonic peening (UP) in our process of strengthening metal to combat fatigue failure, stress corrosion cracking, and any number of other potential problems that can weaken metal and decrease equipment lifespan. The process of ultrasonic peening is a fatigue improvement technique which is applied via ultrasonic and mechanical impulses to the high-stressed locations in the weld.

As a result of the ultrasonic peening process, which modifies the metal weld at its very atomic level, the stress concentrations and residual stress are relieved, and the integrity and strength of the structure is increased dramatically [www.appliedultrasonics.com (2015)].

2.1.1 Aluminum alloys

Aluminum alloys are alloys in which aluminum (AL) is the predominant metal. The typical alloying elements are copper, magnesium, manganese, silicon and zinc. They are two principle classifications, namely casting alloys, and wrought alloys.

Aluminum alloys are widely used in engineering structures and components where light or corrosion resistance is required **[**Kaufman **(2006]).**

- wrought Aluminum alloys

Wrought aluminum alloys can be mainly classified in two groups as shown in fig (2.1), non-precipitation-hardenabale and precipitation hardenable aluminum alloys **[**polmear **(1996)].**

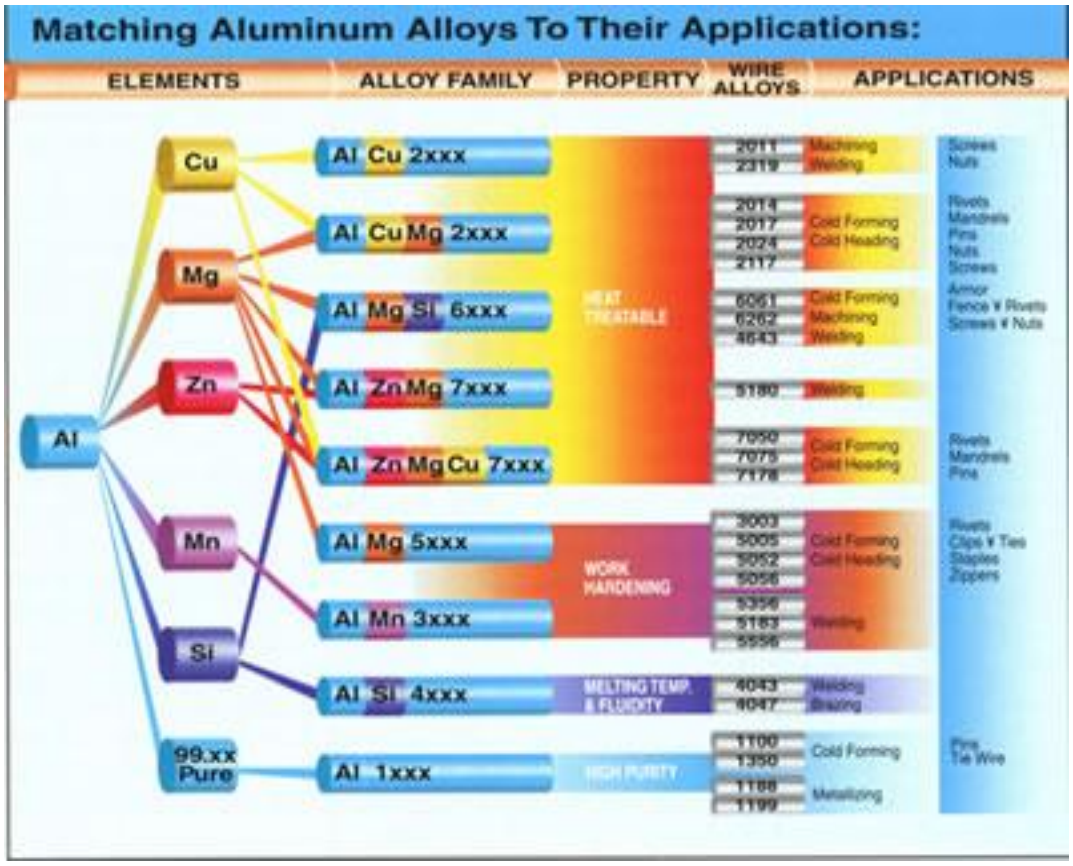

Fig. (2.1): Classification of wrought aluminum alloys

a. **Non precipitation-hardenable aluminum alloys**

The non-precipitation- hardenable wrought aluminum alloy (1XXX, 3XXX, 4XXX, 5XXX) contain manganese and magnesium as the major additions. In these alloys, the increase of strength is principally due to lattice distortion by the atoms in solid solution.

When dislocations move on a slip plane, the strain field obstructs movement leading to a pining effect. Strength can be also developed be work hardening (increasing dislocation density) usually be cold working during fabrication. Dislocations interact with other dislocation and with other barriers to their motion through the lattice. Strengthening of aluminum alloys in this group is considerably produced with magnesium in solid solution because of its high solid solubility.

b. Precipitation-hardenable aluminum alloys

The wrought aluminum alloys which respond to strengthening by precipitation are covered by three (2XXX, 6XXX, 7XXX). As shown in figure (2.1). Precipitation-hardenable aluminum alloys usually contain elements, such as (Cu, Mg, Si and Zn) which have high solid solubility at high temperature, but rather lower solubility at room temperature. Heat treatment of these alloys generally involves the flowing state:

1. Solid solution treatment at a relative high temperature within the single phase region to dissolve the alloying elements.
2. Quenching, usually to room temperature to obtain a supersaturated solid solution of these elements in aluminum.
3. Controlled decomposition of the supersaturated solid solution to form finely dispersed precipitates by the ageing treatment**.**

- Temper designation of Aluminum alloys

The temper designation follows the cast or wrought designation number with a dash, a letter and potentially a one to three digit number; The definitions for the tempers are:

F: As fabricate.

O: Annealed (full soft).

H: Strain hardened (cold worked) with or without thermal statement.

T: Heat treated to produce stable tempers. Apply to products that are thermally treated with or without supplementary strain hardening to produce stable tempers. The T is always followed by one or more digits.

T1: cooled from hot working and naturally aged (at room temperature).

T2: cooled from hot working, cold-worked and naturally aged.

T3: solution heat treated and cold worked

T4: solution heat treated and naturally aged.

T5: cooled from hot working and artificially aged (at elevated temperature).

T6: solution heat treated and artificially aged.

T7: solution heat treated and stabilized.

T8: solution heat treated, cold worded and artificially aged.

T9: solution heat treated, artificially aged, and cold worked.

T10: cooled from working, cold worked, and artificially aged.

W: solution heat treated only.

The most widely used temper designations above are the **H** and **T** categories, and these are always flowed by from one to four numeric digits that provide more detail about how the alloy has been fabricated **[**Kaufman (2006).**]**

- Engineering use and aluminum alloys properties

Aluminum alloys typically have an elastic modulus of about 70 GPa which is about one-third of the elastic modulus of most kinds of steel and steel alloys. Therefore, for a given load, a component or unit made of an aluminum alloy will experience a greater deformation in the elastic regime than a steel part of identical size and shape. Though there are aluminum alloys with somewhat-higher tensile strengths than the commonly used kinds of steel, simply replacing a steel part with an aluminum alloy might lead to problems. With completely new metal products, the design choices are often governed by the choice of manufacturing technology. Extrusions are particularly important in this regard, owing to the ease with which aluminum alloys, particularly the Al–Mg–Si series, can be extruded to form complex profiles **[**https://en.wikipedia.org (2015)].

An important structural limitation of aluminum alloys is their lower fatigue strength compared to steel. In controlled laboratory conditions, steels display a fatigue limit, which is the stress amplitude below which no failures occur – the metal does not continue to weaken with extended stress cycles. Aluminum alloys do not have this lower fatigue limit and will continue to weaken with continued stress cycles. Aluminum alloys are therefore sparsely used in parts that require high fatigue strength in the high cycle regime (more than 10^7stres cycles).The main application of metallic scandium by weight is in aluminum-scandium alloys for minor aerospace industry components. These alloys contain between 0.1% and 0.5% (by weight) of scandium. They were used in the Russian military aircraft Mig 21 and Mig 29. [*Ahmad (2003*] and [*Schwarz* (2004)].

- Aluminum Industry Today

The production of primary aluminum is a young industry - just over 100 years old. But it has developed to the point where scores of companies in some 35 countries are smelting aluminum and thousands more are manufacturing the many end products to which aluminum is so well suited.

For its first half century the aluminum industry pursued the dual role of improving and enlarging production processes to reduce the price of the metal and, at the same time, proving the worth and feasibility of aluminum in a wide range of markets. Such was the dynamic approach of the industry to this problem that the consumption of aluminum gained the remarkable record of doubling every ten years. The strong demand for aluminum stimulated the rapid expansion of productive capacity to meet it.

The First World War had a dramatic effect on aluminum production and consumption. In the six years between 1914 and 1919 world output soared from 70,800 tons to 132,500 tons a year and it is a striking testimony to the adaptability of the metal that after the very large expansion occasioned by war the ground was held. Once the changeover to civilian production had been carried through the increased capacity was occupied before very long in supplying the normal demands of industry. And this happened again, on a much larger scale, as a result of the Second World War.

World production of primary aluminum increased from 704,000 tons in 1939 to a peak of 1,950,000 tons in 1943, after which it declined considerably. At the end of World War II, the western world industry had completed an unprecedented threefold expansion in capacity in the space of four to five years. Civilian markets had to be developed for this new capacity. The demand for aluminum proved to be elastic and the expanded facilities were working at near capacity in a matter of a few years.

Constant research and product development throughout the 1950's, 60's and 70's led to an almost endless range of consumer goods incorporating aluminum. Its basic benefits of lightness, strength, durability, formability, conductivity and finishability made it a much sought after product.

The necessity for the industry itself to pioneer the use of aluminum led to an integrated structure in the major companies from the mining of bauxite to, in some cases, the finished consumer product. As the total world production soared, countries with raw materials and especially those with cheap energy resources began to enter the market with primary metal for others to further the process. Today a significant proportion of metal is marketed in this way by [Ron (1997)].

- Properties at Low Temperatures

Aluminum and its alloys have no ductile to brittle transition at low temperatures, indeed, their strengths increase with decreasing temperature. The strengths of stable temper aluminum alloys are not influence by the time of exposure at low temperatures neither are the strengths at room temperature after exposure at low temperature. However, freshly solution treated heat treatable alloys can be held in this condition for long periods by storing them at a low temperature because of the retardation of the ageing process. This is used to good effect when placing aircraft rivets of the AlCuMgSi type which may be solution treated prior to use by heating to 495C for a period of time between 5 and 60 minutes, depending upon the size and quantity of rivets being processed, after which they are quenched in cold water. The rivets remain soft after quenching for up to two hours at ambient, but at minus 50C this is extended to forty-five hours and at minus 150C to one hundred and fifty hours.

The increase in strength of aluminum alloys at low temperatures is negligible down to minus 500C but begins to increase significantly below minus 1000C (Figure 2.2**).** The elongations of most aluminum alloys also increase with the reduction in temperature down to minus 196°C whereupon some alloys notably with higher magnesium content (4.5% and above) begin to reduce again but not below the ambient figure.

Shear, compression and bearing strengths - all improve at low temperatures, also the module of elasticity under tensile, compressive and shear loading are 12% higher at minus 1960C than at room temperature **[**Ron (1997**)]**

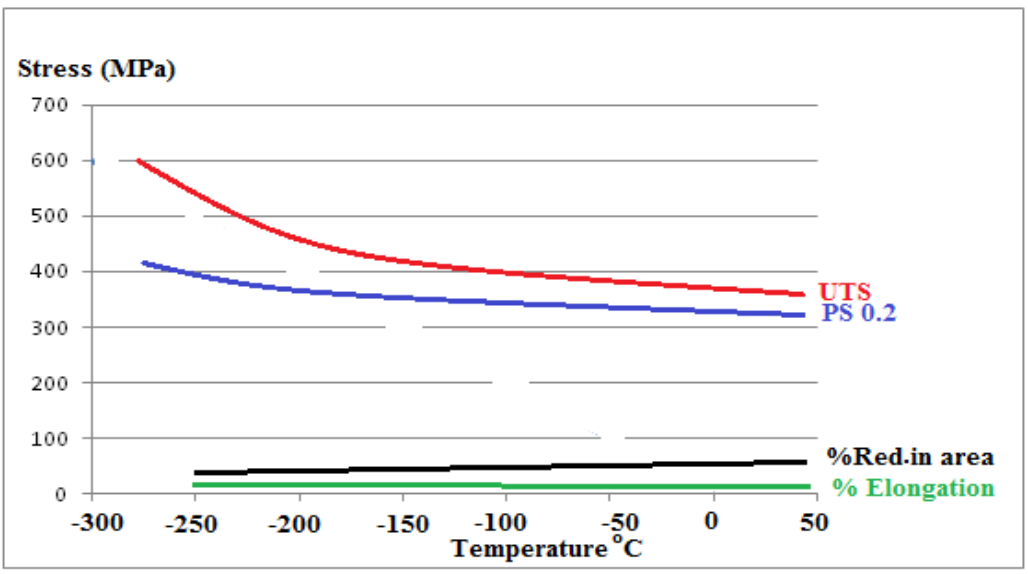

Fig.(2.2): Tensile properties of 6061 Al-alloy at low temperature

2.1.2 Fatigue

- Historical overview of fatigue

The word "fatigue" was introduced in the 1840s and 1850s describe failures occurring from repeated stresses. This word has continued to be used for the normal description of fracture due to repeated stresses. The first systematic investigation of fatigue by "August" Wohler" In Germany at 1860s and he introduced the concept of the S-N diagram and the fatigue limit. In 1886 showed that the yield strength in tension or compression was reduced after applying a load of the opposite sign that caused inelastic deformation. This was the first indication that a single reversal of inelastic strain could change the stress- strain behavior of metals. In 1900s, Ewing used the optical microscope to pursue the study of fatigue mechanisms. In 1910 showed that alternating stress versus number of cycles to failure (S-N) in the finite life region could be represented as a Log-Log linear relationship. During World War II the deliberate use of compressive residual stresses become common in the design of aircraft engines and armored vehicles. In Paris 1960s.low - cycle strain- controlled fatigue behavior became prominent with the Manson relationship between plastic strain amplitude and fatigue life.

Paris in 1960s showed that the fatigue crack growth rate, da/dn, could best be described using the stress intensity factor range Δk_1. During 1975s, 1980s and1990s many researchers were investigating the complex problem of in-phase and out-of-phase multi axial fatigue. The critical plane method suggested by Brown and Miller, motivated anew philosophy concerning this problem, and many additional critical plane models were developed [Stephens (2001)].

- Fatigue Failure

A fatigue failure is particularly insidious because it occurs without any obvious warning. Fatigue results in a brittle- appearing Fracture, with no gross deformation at the fracture. On a macroscopic scale the fracture surface is usually normal to the direction of the principal tensile stress. A fatigue failure can usually be recognized from the appearance of the fracture surface, which shows a smooth region, due to the rubbing action as the crack propagated through the section, and a rough region, where the member has failed in a ductile manner when the cross section was no longer able to carry the load. Frequently the progress of the fracture is indicated by a series of rings, or "beach marks" progressing in ward from the point of initiation of the failure. Three basic factors are necessary to cause fatigue failure:

a. Maximum tensile stress of sufficiently high value.

b. Large enough variation of fluctuation in the applied stress.

c. Sufficiently large number of cycles of the applied stress.

In addition there are a host of other variables, such as stress concentration, corrosion, temperature, metallurgical structure, residual stresses, and combined stresses, which tend to alter the condition for fatigue [Mahir (2009)].

- Metal fatigue

A phenomenon which results in the sudden fracture of a component after a period of cyclic is loading in the elastic regime. Failure is the end result of a process involving the initiation and growth of a crack, usually at the site of a stress concentration on the surface. Occasionally, a crack may initiate at a fault just below the surface. Eventually the cross sectional area is so reduced that the component ruptures under a normal service load, but one at a level which has been satisfactorily withstood on many previous occasions before the crack propagated. The final fracture may occur in a ductile or brittle mode depending on the characteristics of the material. Fatigue fractures have a characteristic appearance which reflects the initiation site and the progressive development of the crack front, culminating in an area of final overload fracture.

Fatigue strength is determined by applying different levels of cyclic stress to individual test specimens and measuring the number of cycles to failure. Standard laboratory test use various methods for applying the cyclic load, e.g. rotating bend, cantilever bend, axial push-pull and torsion. The data are plotted in the form of a stress-number of cycles to failure (S-N) curve, fig (2.3). Owing to the statistical nature of the failure, several specimens have to be tested at each stress level. Some materials, notably low-carbon steels, exhibit a flattening off at a particular stress level as at (a) in Fig.(2.3) which is referred to as the fatigue limit. As a rough guide, the fatigue limit is usually about 40% of the tensile strength. In principle, components designed so that the applied stresses do not exceed this level should not fail in service. The difficulty is a localized stress concentration may be present or introduced during service which leads to initiation, despite the design stress being normally below the 'safe' limit. Most materials, however, exhibit a continually falling curve as at (b) and the usual indicator of fatigue strength is to quote the stress below which failure will not be expected in less than a given number of cycles which is referred to as the endurance limit [ttp://www.totalmateria.com (2016)].

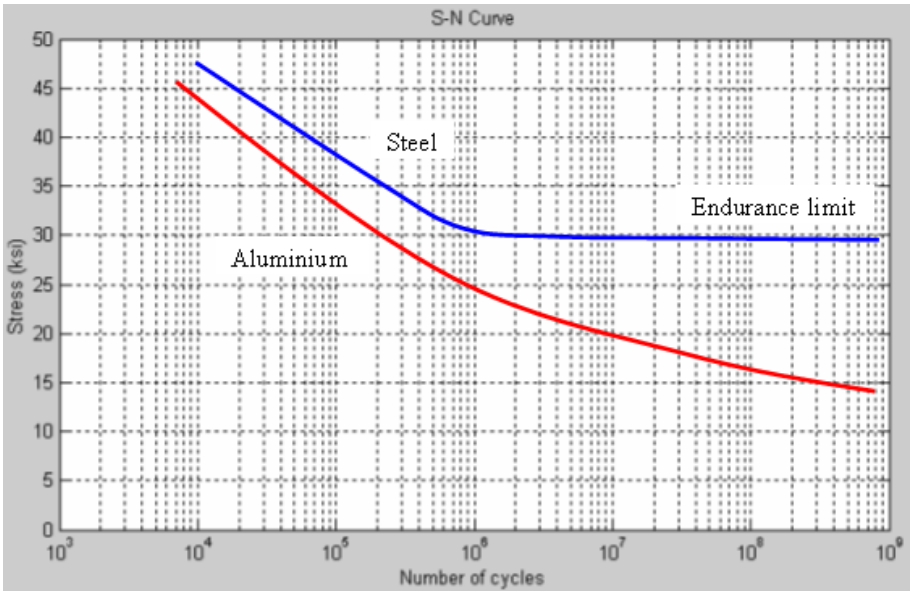

Fig. (2.3): Stress-number of cycles to failure (S-N) curve

Although fatigue data may be determined for different materials it is the shape of a component and the level of applied stress which dictate whether a fatigue failure is to be expected under particular service conditions. Surface condition is also important. Often complete components or assemblies, e.g. railway bogie frames or aircraft fuselage will be tested by subjecting them to an accelerated loading spectrum reproducing what they are likely to experience over their entire service lifetime **[**Technology.open.ac.uk (2007)].

2.1.3 Mechanical surface Treatments

Mechanical surface treatment is a localized (inhomogeneous) near- surface plastic deformation. Several properties as well as microstructures at the surface and in near-surface regions of metallic materials are altered by mechanical surface treatment, eg, Surface topography, plasticity induced phase transformations, increased dislocation densities, induced near-surface macroscopic compressive residual stresses as well as work hardening states. The amount and distribution of these altered near-surface properties depend strongly on the type of mechanical surface treatment as well as the process parameters. At this time for several industries, the most well- known method of mechanical surface treatments are treatments peening [Schulze (2005)].

Mechanical surface treatments, such as deep rolling, shot peening laser shock peening and ultrasonic peening, can significantly improve the fatigue behavior of highly-stressed metallic components.

Treatment is particularly attractive since it is possible to generate, near the surface, deep compressive residual stresses and work hardened layers while retaining a relatively smooth surface finish [Nalla (2003)].

- Laser peening

The use of laser-generated pressure pulses to improve fatigue life by inducing compressive residual stress near the surfaces of metal parts has been under development for more than 30 years [Clauer(1983)], and is gaining popularity as numerous successful aerospace and industrial applications demonstrate the benefits of the technique. Advantages of LSP over conventional shot peening include increased control in applying the process, reduced microstructure damage, and deeper penetration of the compressive residual stress field into the surface [Montross (2002)].

The aerospace industry is leading the integration of methods to apply laser peening to many aerospace products, such as turbine blades and rotor components discs, gear shafts and bearing components.

Laser peening could also be used to treat fastener holes in aircraft skins and to refurbish fastener holes in old aircraft in which cracks, not discernible by inspection, have initiated. General Electric Aircraft Engines in the USA treated the leading edges of turbine fan blades in F101-GE-102 turbine for the Rockwell B-1B bomber by laser peening in 1997, which enhanced fan blade durability and resistance to foreign object damage (FOD) without harming the surface finish .Protection of turbine engine components against FOD is a key priority of the US Air Force. In addition, it was reported that laser peening would be applied to treat engines used in the Lockheed Martin F-16C/D [Charles (2002)].

One of the keys to understanding and quantifying the effects of LSP on fatigue life is a clear knowledge of the residual stress state. As with shot peening, more LSP, or more intense LSP, is not necessarily better in terms of extending life. In the case of LSP, the resulting residual stress state also is known to exhibit a fair degree of variability [Martinez (2003).

- Mechanism of laser peening

Laser peening is a recently-developed surface treatment method designed to improve the performance and prolong the fatigue life of work-pieces. Laser peening which generates confined plasma on the surface of work-pieces use high power density and short pulse laser irradiation. The explosion of confined plasma leads to high pressure shock wave, which causes the compressive residual stress on the surface of work-pieces. Since 1970s, considerable attention has been paid to potential application of laser peening in the aviation industry and other industrial fields.

Figure (2.4) shows the fundamentals of laser-material-plasma interaction during laser peening processes [ZHAO (2013)].

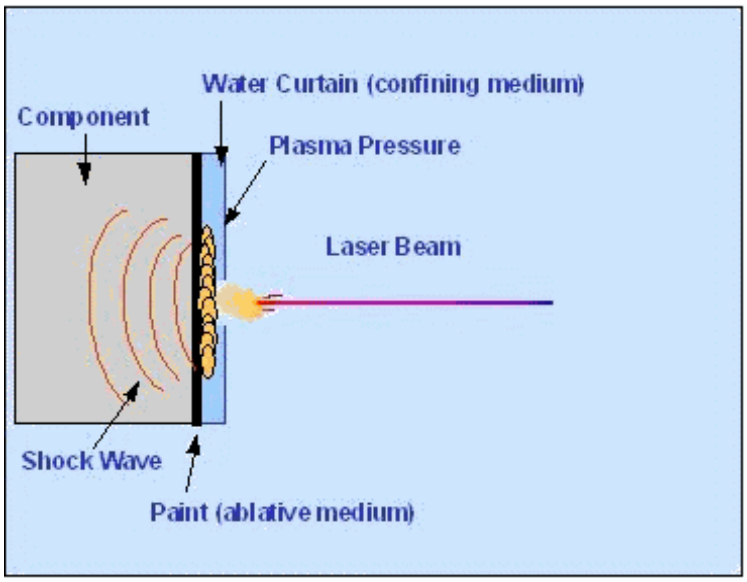

Fig.(2.4): laser peening mechanism

Fig.(2.4) shows the surface stresses in a 6.35 mm thick aluminum specimen treated with overlapping laser spots at an intensity of 4 GW/cm2. Significant variations in the surface stress are evident near the spot centers and boundaries, and in spot overlap areas, Surface stress variation in specimen subjected to 9-shot rosette LSP pattern. Stress values are in MPa [https://www.google.iq (2015)] and [Robert (2011)].

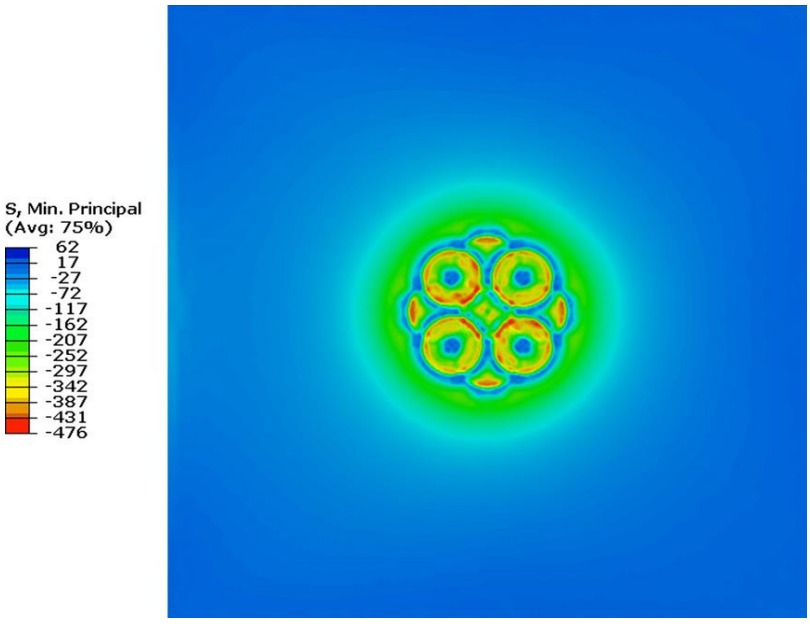

Fig.(2.5): Surface stress variation in specimen subjected to LSP pattern

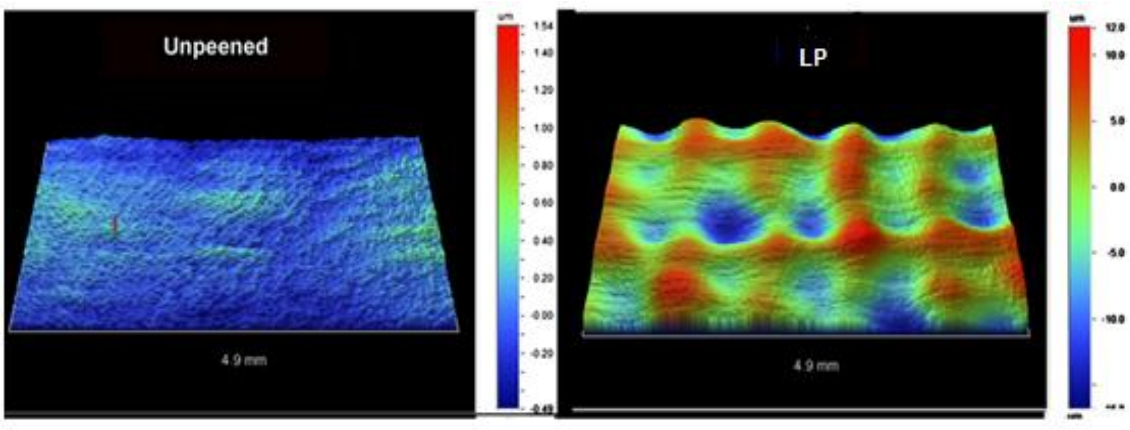

Fig.(2.6):specimen surface before and after laser peening

- Ultrasonic peening

Ultrasonic impact treatment (UIT) is a metallurgical processing technique, similar to work hardening, in which ultrasonic energy is applied to a metal object. This technique is part of the High Frequency Mechanical Impact (HFMI) processes. Other acronyms are also equivalent: Ultrasonic Needle Peening (UNP), Ultrasonic Peening (UP). Ultrasonic impact treatment can result in controlled residual compressive stress, grain refinement and grain size reduction.

Low and high cycle fatigue are enhanced and have been documented to provide increases up to ten times greater than non-UIT specimens.

In UIT, ultrasonic waves are produced by an electro-mechanical ultrasonic transducer, and applied to a work piece. An acoustically tuned resonator bar is caused to vibrate by energizing it with a magneto astrictive or piezoelectric ultrasonic transducer. The energy generated from these high frequency impulses is imparted to the treated surface through the contact of specially designed steel pins. These transfer pins are free to move axially between the resonant body and the treated surface. When the tool, made up of the ultrasonic transducer, pins and other components, comes into contact with the work piece it acoustically couples with the work piece, creating harmonic resonance. This harmonic resonance is performed at a carefully calibrated frequency, to which metals respond very favorably, resulting in compressive residual stress, stress relief and grain structure improvements **[**Fisher (2001)**].**

Depending on the desired effects of treatment a combination of different frequencies and displacement amplitude is applied. Depending on the tool and the Original Equipment Manufacturer, these frequencies range between 15 and 55 KHz.

The micro characteristics and fatigue properties of samples that underwent ultrasonic peening treatment (UPT) indicated that the results in addition to residual compressive stress, the UP process might also introduce short cracks, known as fold defects at the surface of metal samples.

Fold defects were observed in all samples, this may be due to the formation of small fold defects and the introduction of compressive stress in the metal. However, long treating times led to a significant reduction in the fatigue life to levels lower than those for untreated samples. [Yanyan (2016)].

- Residual Stress (RS) Modification by Ultrasonic Peening

Ultrasonic peening is one of the new and promising processes for effective redistribution of RS. During the different stages of its development the UP process was also known as ultrasonic impact treatment (UIT) and ultrasonic impact peening (UIP). The beneficial effect of UP is achieved mainly by relieving of harmful tensile RS and introducing of compressive RS into surface layers of metals and alloys, decreasing of stress concentration in weld toe zones and enhancement of mechanical properties of the surface layers of the material [Kudryavtsev (2010) **].** The UP technique is based on the combined effect of high frequency impacts of special strikers and ultrasonic oscillations in treated material. The developed system for UP treatment (total weight ~11 kg) includes an ultrasonic transducer, a generator and a laptop (optional item) with software for UP optimum application – maximum possible increase in fatigue life of parts and welded elements with minimum cost, labor and power consumption. In general, the basic UP system shown in Figures (2.7),(2.8) could be used for treatment of weld toe or welds and larger surface areas if necessary [www.appliedultrasonics.com (2015)].

Fig.(2.7): Basic UP-600 system for fatigue life improvement of parts elements

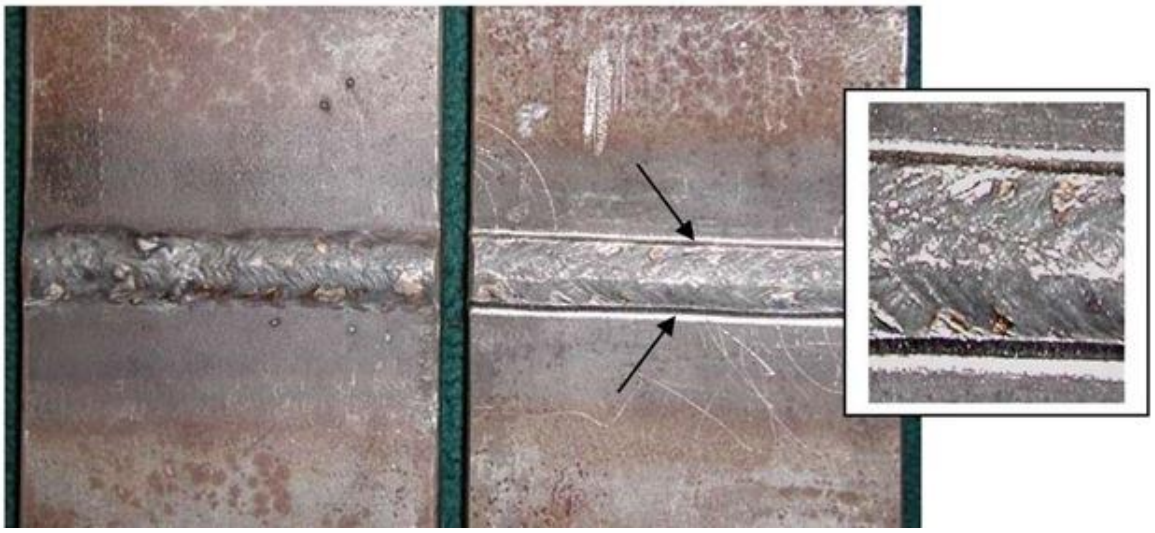

Fig. (2.8): The view of the butt welds before and after application of UP

The effects of different improvement treatments, including the UP treatment, on the fatigue life of welded elements depend on the mechanical properties of used material, the type of welded joints, parameters of cyclic loading and other factors. For effective application of the UP, depending on the above-mentioned factors, a software package for Optimum Application of UP was developed that is based on original predictive model. In the optimum application, a maximum possible increase in fatigue life of welded elements with minimum time/labor/cost is thought [Kudryavtsev (2009)].

The developed technology and computerized complex for UP were successfully applied for increasing of the fatigue life of welded elements, elimination of distortions caused by welding and other technological processes, relieving of residual stress, increasing of the

hardness of the surface of materials and surface nanocrystallization. The areas/industries where the UP was applied successfully include: Railway and Highway Bridges, Construction equipment, Shipbuilding, Mining, Automotive and aerospace to name a few. Mechanical properties of the surface layers of materials to attain the maximum possible increased in fatigue life of welded elements and structures [Kudryavtsev (2009)].

An important practical limitation on the use of peening improvement techniques that rely on the presence of compressive residual stresses is that the fatigue lives are strongly dependent on the applied mean stress. In particular, the degree of improvement decreases as the maximum applied stress approaches tensile yield. Thus, in general, the techniques are not suitable for structures operating at applied stress ratios R > 0.5 or maximum applied stresses above around 80% yield. The guideline gives special limitations for high stress ratio situations.

Even occasional application o high stresses in tension or compression as part of a variable amplitude fatigue history, can also be detrimental in terms of relaxing the compressive residual stress. Systematic guidelines are not yet developed. Special limitations also exist for improved large-scale structures. Halid provides a comprehensive evaluation of published data for high frequency mechanical impact treated welds subject to R = 0.1 constant amplitude loading. In total 228 experimental results for longitudinal, transverse and butt welds subject to axial loading have been reviewed. An increase in fatigue strength with yield strength was found. By choosing yield stress σ_Y = 355 MPa as a reference, approximately 12.5% increase in strength for every 200 MPa increase in σ_Y above σ_{Y0} was found. This correction significantly reduced the observed scatter in the data with respect to data without any yield strength correction. This value of was adopted as a basis for proposing design curves for high frequency mechanical impact treated welds. The proposed SN lines are conservative with respect to available data. Special cautions are given for high R-ratio or variable amplitude fatigue and alternate failure locations [Halid (2012).].

2.2 Previous work

2.2.1 Ultrasonic peening

Ultrasonic impact peening has been used to control the residual stress of the welded joints of 6005A-T6 AL- alloy. Investigational were tests display that ultrasonic impact treatment can produce compressive longitudinal and transverse residual stress in the welded joint, harden the surface, and increment the tensile strength of welded joints. Salt-fog corrosion tests had been conducted for both an as-welded sample and an ultrasonic impact-peened specimen. The surface of the peened sample was far fewer corrosion pits than that of the unpeening specimen. The peening specimen is higher strength and lower tensile residual stress than the

unpeened specimen during corrosion. Thus, ultrasonic impact peening is functional technique to develop the stress corrosion cracking resistance of the welded joints of 6005A-T6 aluminum alloy **[Gou (2016)].**

SP and UP have been used mechanical surface cure in the cars and aerospace industries to get better the fatigue life of metallic parts.
To enhance the mechanical properties of the 7475-T7351 AL- alloy by applying three different treating processes: Ultrasonic treating (UT) and Micro shot treatment with two different beads size (MSP). A systematic study was carried out on the roughness, surface hardening, residual stress shape and fatigue life. Uniaxial fatigue tests had been carried out. Residual stresses were estimated by X-ray diffraction. All of the surface peening enhanced the simples fatigue lives [**Ramos (2016)**].

Effect of ultrasonic treatment for different periods with steps surface structures, has been studied on low cycle fatigue behavior of the 7075 AL-alloy at RT. LCF tests were carried out at different total strain capacities Surface microstructures had been characterized. No phase change was found due to treatment. Surface region of the ultrasonically treated specimen was found to improve nanosize grains of 16-20 nm. Significant enhancement was spotted in LCF life of the simple subjected to treatment for 180 seconds, may be attributed to raised resistance of the treated specimen against fatigue crack initiation, because grain refinement in the surface zone [**Vaibhav (2016)].**

(Five groups of D36 steel plates with different surface topographies had been prepared to estimate the influence of topography and needle size on the surface quality after ultrasonic peening treatment. Factors such as the stress distribution, micro-hardness, and fold defects had been studied to quantify the surface quality. The numerical results show that fold overlapping has been dependent on the initial surface topography and the size of the peening needle could affect the morphology of the fold defects. The results further specific that fold defects had been closely related to the initial surface topography, with the aspect ratio being a key determining factor for the dimensions of fold defects [Yanyan **(2016)**].

.Nanostructure of 17 to 25 nm was improved in surface zone of the titanium alloy Ti–6Al–4V, up to the depth of ~ 30 μm, by USP. The effect of nanostructured surface has been studied on corrosion behavior of this alloy, in three different salt mixtures at 400, 500 and 600 °C. Samples were subjected to heating and cooling cycles with different fixed periods in three blocks for total display of 100 h. The main corrosion products formed in the different salt mixtures had been characterized as TiO_2, Al_2O_3, V_2O_3, Ti_2O_3 and V_2O_5 oxides. The

corrosion rate has been found to be lower in the ultrasonic shot peened specimens as compared to those in the non-shot treated ones [**Sanjeev (2016)**].

Ultrasonic shot peening treatment (USPT) has been suggested to correct welding buckling distortion. The residual stress distribution along the depth direction of the treated region was measured by an X-ray diffractometer. The microstructure of the peened samples was investigated by (SEM). The Vickers microhardness has been measured in different areas of welded joint before USPT and along the depth way of the weld after USPT. The experimental results shown that the welding buckling distortion of 5A06 aluminum alloy butt joint can be essentially corrected by USPT; the average correction rate amount 90.8% in this study. Furthermore, USPT improved samples by work hardening. The microstructure of the treated zone was enhanced [**zhang (2016)**].

The flash welded joint of U75V steel was widely used in high-speed railway. Considering the fact that fatigue failure has been the main failure mode of high-speed railway, ultrasonic peening treatment (UPT) was used to enhance the fatigue realization of the flash welded joint. Micro-structure, hardness, wear resistance, corrosion resistance and fatigue fracture mechanism of the flash welded joint before and after UPT had been analyzed in detail. Results indicated that nanocrystals form on the surface of the welded joint after UPT. Fatigue life, wear resistance and corrosion resistance of the welded joint had been enhance for the surface strengthening caused by UPT **[Yanjun (2016)].**

Ultrasonic impact peening (UIP) has been remarkable post-weld technique, which applies mechanical impacts in participate with ultrasonic oscillations into welded joints entering plastic deformation and beneficial compressive residual stress in the zone of the weld toe. The actual operation parameters and ultrasonic-induced material temperament, which has been appropriately adjusted to fit experimental results, are considered. The estimated residual stress distributions of a non-load-carrying cruciform joint before and after UIP have been compared with experimental results, showing a fairly good agreement with each other. In addition, an evaluation of fatigue life of welded joints based on crack mechanics is achieved. The results clearly distinguish the fatigue lives of as-weld and UIP processed weld joints [**Kuilin (2016)]**.

The effects of multiple ultrasonic impact peening (UIP) on the surface properties had been investigated. The results showed the effects of surface smoothing and hardening on the wear performance. A rise in the number of UIP resulted in a lower roughness and higher hardness. After three UIP, the surface roughness decreased from 0.694 to 0.112 μm, and the hardness

rose from 257.32 to 428.38 HV. The growth of surface morphology had been also analyzed in detail over multiple UIP, Moreover, the volume fraction of plastic deformation-induced marten site raise with the number of UIP of the surface. The samples peening three passes showed better wear resistance than untreated specimen under dry sliding conditions [**Liang (2016)**].

The effects of severe plastic deformation generated by ultrasonic impact treatment (UIT) and the electric discharge surface alloying with chromium have been studied. The surface micro relief and integrity have been analyzed. The structural formations in the sub-surface layers had been characterized. The samples underwent UIT processes demonstrate the fatigue life a quantities increased respectively by ~15, ~5 and ~30% on the base of 10^7 cycles in comparison with that for the pristine samples. The improvement fatigue life and extended lifetime of the low-carbon steel samples after UIT are concluded to be associated with the subsurface crack nucleation carried out by the following factors: (1) reduced surface roughness and enhanced integrity of the improved layer; (2) compressive residual stresses; and (3) hardening of surface connected with the alloying by chromium and with the formation of the dislocation-cell structure including the cell walls invincible to moving dislocations at cyclic loading [**Mordyuk (2016)]**.

Ultrasonic treatment (UT) has been known as a point to surface improvement process for industrial practice to manufacture components with high resistance fatigue realization, on which a compressive residual stress layer can be insert up to a typical depth of many micrometers. The wear resistance of UT processed stainless steel components has been notably enhanced; with anti- corrosion is observed. The multiple surface unity factors of both surface features and surface properties simultaneously achieved by the surface enhancement, exhibiting strong interactions between them, have been responsible for the high realization of components with combined characteristic [**Wang (2016)]**.

The quality of the ultrasonic shot peening treatment, has been strongly dependent on kind of strike. This movement of the beads clearly depends on their quantity, the agitation source, and the materials include the chamber. The average depth of strike marks in different arrangements has been measured by microscopy. A linear relationship is between plastic depth and incident speed. The results is indicted that the average strike velocities gained numerically have been strongly linked with average impact depths, there validating the numerical simulation for this shot peening configuration [**Nouguier (2012)**].

Ultrasonic peening is a cold surface treatment used to extend the fatigue life of material components. This process is performed in a closed chamber where spherical beads are moved by sonotrode vibration. The present study shows the effect of the number of beads used in the process on the treated surface. The surface analysis of the peened sample showed that the number of beads strongly affected the number of impacts and their depth distribution. The result showed that in the present peening configuration, an increasing number of beads concentrated the compressive residual stress onto the treated surface [**Thomas** (2015].

An ultrafine-grained surface layer with strong basal texture was produced during UIP-induced surface SPD of bulk Zr–2.5%Nb alloy. Average grain size is approx. 180 nm in the topmost surface layer of 10 μm thick. The mechanism for subdivision of α-grains is dislocation-mediated mainly. With ongoing UIP process (increase in the effective strains), accommodation of deformation in the topmost surface layer occurs through sequential changes in dislocation structures.XRD analysis reveals high compressive residual stresses and strong basal texture after the UIP process **[Mordyuk (2012)].**

The effects of high-frequency ultrasonic peening (HFUP) on the tribological characteristics of Cu-based material sintered on low carbon steel by a powder metallurgy (P/M) technique were investigated. The friction and wear properties of the Cu-based materials were studied using a pin-on-disk reciprocating tribotester sliding against a hardened steel ball under dry and oil-lubricated conditions. Experimental results showed that the HFUP process led to a reduction in friction and wear of the Cu-based materials in both dry and oil-lubricated conditions. This was attributed to the increase in hardness of the HFUP treated specimen. It was also found that the friction coefficient was independent of the normal load but decreased with increasing sliding speed **[Auezhan (2012)].**

2.2.2 Laser peening

The effects of massive laser shock peening (LSP) treatment on micro-hardness, residual stress and microstructure in four different zones of laser cladding coating was investigated. Furthermore, microhardness curves and residual stress distributions with and without massive LSP treatment were presented and compared, and typical microstructure in different zones of both coatings were characterized. Results and analyses showed that massive LSP treatment had an important influence on micro-hardness and residual stress of the cladding coating. Special attempt was made to the effects of massive LSP treatment on microstructure in three zones of the cladding coating. In addition, the underlying mechanism of massive

LSP treatment on microstructure and mechanical properties of the cladding coating was revealed clearly **[Luo (2016)].**

The effects of warm laser peening (WLP) on the thermal stability and mechanical properties of A356 alloy is study. The residual stress, micro-hardness and microstructures of samples treated by WLP were observed. The result shows that the temperature significantly affects the strengthening effect of laser peening (LP). The residual stress induced by WLP decreases with the increasing temperature. The micro-hardness and dislocation density increase first, and then decrease with the increases of temperature. The grain refinement degree of the samples treated by WLP is much higher than that of LP. In addition, after aging for 100 min at 220 _C, the samples treated by LP and WLP were comparatively investigated in thermal stability. Obviously, the residual compressive stress, micro-hardness and microstructure induced by WLP present a better thermal stability property than that of LP. The residual stress and micro-hardness of WLP samples are obviously improved, and the increasing degrees are 23.31% and 19.70%, respectively [**Chen (2016**)].

The effects of laser shock processing without protective coating on high-cycle fatigue crack growth and fracture toughness were investigated. Laser shock peening treatment was performed on compact tension specimens from both sides perpendicular to the crack growth direction, followed by subsequent grinding. Fatigue crack growth tests were performed at frequencies between 116 and 146 Hz, at R = 0.1 and a constant stress intensity range during the fatigue crack initiation phase and K-decreasing test. A lower number of cycles was required to initiate a fatigue precrack, and faster fatigue crack growth was found in tensile residual stress field of LSP-treated specimens. The crack growth threshold decreased by 60% after LSP treatment. The fracture toughness decreased by 28–33% after LSP treatment **[Zoran (2016)].**

The fatigue crack growth tests were introduced for studying the effect of Laser Shock Peening (LSP) on fatigue crack growth rate of AZ31B Magnesium (Mg) alloy. The surface layer structures of laser treated samples were analyzed. The results show that the nanometer grains (with an average size of 17.5 nm) can be generated in the surface layer by using the optimized laser parameters. Surface roughness decreased from 1.177 mm to 0.713 mm after LSP. The depth of compressive residual stress induced by LSP reached to about 0.8 mm from the top surface. Comparing with the original samples, the obviously lower fatigue crack growth rates for the LSP treated samples was observed due to a combination of grain

refinement, residual compressive stress and the barrier effect of surface nanocrystalline layer **[Mao (2016)]**.

The purpose of this study is to investigate the effects of Laser Shock Peening (LSP) on Al 6061-T6. Results showed that by the use of LSP, compressive residual stress could effectively be induced on the surface of treated material. It was also revealed that the hardened depth of the material, up to a maximum depth of 1875 μm, could be achieved due to work hardening and grain refinement. In addition, surface roughness measurements showed that the LSP could deteriorate surface quality depending on the LSP parameters. The influences of beam overlap rates, number of laser shots and scanning pattern on microhardness as well as surface roughness are discussed **[Salimianrizi (2016)].**

The warm laser peening without coating process utilizing decarburized surface as the protective ablation layer and is directly intended towards the experimental evolution of existing laser shock peening technology. The depth-wise compressive residual stress and its thermal relaxation behavior are comparatively prevailing. The scanning and transmission electron microscopic analysis identify the severe plastic deformation features of microstructures. So, the grain refinement and pinning force mechanisms on the mechanical properties are recognized. Further, the micro and nano-hardness studies provide a significant improvement in the surface and sub-surface mechanical properties. Moreover, the optimized fatigue life of low-alloy steel is achieved through the thermal engineering process. The present work increased the fatigue life of the specimen by 26 times and it is effectively repairing the partially pre-fatigued specimen [**Prabhakaran (2016)**].

To deeply understand the effect of laser peening (LP) with different laser pulse energies on 6061-T6 aluminum alloy, the fatigue fracture morphologies evolution process at various fatigue crack growth (FCG) stages and the corresponding strengthen mechanism were investigated. At the initial stage of FCG, more fatigue micro-cliffs were found after LP, while the fatigue striation spacing simultaneously reduced. A “stop-continue” phenomenon of crack propagation was discovered for laser peened samples. The fatigue striation spacing at the middle stage of FCG increased significantly while compared with that at the initial stage, in addition, the fatigue striation spacing decreased with an increase in laser pulse energy [**Sheng (2016)**].

The first part of the review involves the parameters controlling and optimization of low energy laser shock peening process. The second part presents the effect of laser peening without coating on ferrous, aluminum and titanium alloys. Therefore, the recently developed

techniques and challenges on it are discussed. Opportunities to tackle the current challenges are overviewed. Finally, in the third part, the future perspectives of low energy laser peening on metal matrix composites and single crystals for several typical applications are deliberated [**Kalainathan (2016).**].

A technique called elastic contact laser shock peening (ECLSP) is presented in this paper. In this technique, a metal foil with high dynamic yield strength is fixed between absorbing layer and workpiece, and the peak pressure of laser shock wave is a little less than the dynamic yield strength of metal foil, but higher than the Hugoniot Elastic Limit (HEL) of work piece. Surface roughness, microhardness and residual stress are investigated. Compared with regular laser shock peening (LSP), ECLSP can reduce the depth and area of secondary plastic deformation of overlapping region. This can effectively reduce surface roughness in overlapping LSP. Measurement of microhardness and residual stress shows that the work hardening effects and strengthening effect are similar as regular LSP [**Fengze (2016)**].

The room-temperature tensile properties and thermal stability of Ti834 alloy before and after laser shock peening (LSP) were investigated. Micro-hardness measurement of the untreated and LSP treated specimens were carried out by using a Vickers indenter. The characteristic of microstructures were analyzed by TEM. The results show that both of the strength and ductility decrease for the 600 °C/100 h exposed Ti834 alloy, especially the decrease of ductility is more pronounced than that of strength. The strength and micro-hardness of Ti834 alloy can be improved by LSP, which is attributed to the high-density dislocation and dislocation-cell formation in the near-surface of the specimen. LSP treatment has a detrimental effect on the thermal stability of Ti834 alloy because of the formation of high density defects in the surface of the alloy [**Weiju (2016)**].

The fatigue life of steam turbine blades is enhanced by subjecting its fir tree blade root section to mechanical treatments like shot peening and laser peening to introduce compressive stresses in the surface layers. This paper studies the effect of shot peening and laser peening on the fatigue crack growth of Ti6Al4V alloy at a stress ratio R of 0.1 and the changes observed in the fracture microstructure during the fatigue crack growth (FCGR). In specific, study of the striations developed during the FCGR on the fracture surface at regular intervals of crack movement has been recorded; an attempt has been made to correlate the striation spacing with crack front growth. It is observed that the fatigue life in the initial stages of FCGR testing is affected by the shot peening effect whereas it is more affected by laser peening effect at higher values of delta K (ΔK) [**Pant (2016).**]

Magnesium, as a biomaterial has the potential to replace conventional implant materials owing to its numerous advantages. However, high corrosion rate is a major obstacle that has to be addressed for its implementation as implants. This study aims to evaluate the feasibility and effects of High Repetition Laser Shock Peening (HRLSP) on biocompatibility and corrosion resistance of Mg samples and as well as to analyze the effect of operational parameters such as peening with overlap on corrosion rate. From the results obtained using hydrogen evolution and mass loss methods, it was found that corrosion rates of both 0% overlap and 66% overlap peened samples reduced by more than 50% compared to that of unpeened sample and sample peened with 66% overlap exhibited least corrosio**n** [**Vinodh (2017)**].

Two-sided and simultaneous laser shock peening impacts is considered as a novel surface treatment technology for the turbine blade and thin-walled component. In these paper, tensile properties of Mg–Al–Mn alloy specimens with different sheet thickness under two kinds of laser shock peening strategies were investigated, and an overlapping three-dimension axisymmetric numerical model was developed to analyze the effects of sheet thickness on residual stress distributions. Meanwhile, special attentions were paid to the in-depth microstructural evolution as a function of sheet thickness. Results showed that sheet thickness had an important influence on the tensile properties of Mg–Al–Mn alloy, and the generated residual stress distribution and grain arrangement were two important factors [**Luo (2016)**].

The purpose of this study was to develop a laser shock peening (LSP) surface treatment of a curved surface that adjusts the surface integrity of a MgCa alloy by varying the peening overlap ratio and determine the effect of LSP on the fatigue life. Surface integrity was characterized by topography, microstructure, and microhardness. Fatigue life of laser peened and unpeened samples were measured by rotating bending fatigue tests. It was found that LSP increased the fatigue life of the peened MgCa samples. Implementing LSP at high overlap ratios reduced the surface pile-up which resulted in a higher fatigue life. The fractured surfaces of the peened samples exhibited striation patterns which were more pronounced at higher peening overlap ratios[**Sealy (2016)].**

The goal of the present study is to investigate residual stress distributions and the accompanying deformation mechanisms during the process of laser peening without coating (LPwC), carried out on a Ti-2.5Cu alloy at a fixed power density of 6.97 GW cm^{-2} with overlap rates from 50 to 90% (in steps of 10%). Thermal softening near surface (confined to a depth of 50 μm) from laser beam-material interaction was observed. Work-hardening

increased with increase in overlap percentage till 80%. The maximum residual stress was found to be − 889 MPa for an optimal 70% overlap. Twinning was found to increase with the increase in overlap rates, indicating the hardening of the sample. The combined effect of adiabatic heating and thermal effects at the surface due to laser beam-material interaction (propagating inside the material), results in the softening of the material [**Umapathi (2016)**].

2.2.3 Concluding Remarks

1. From what has been presented in the above mentioned modern literatures it can be made that many efforts have been spent in establishing fatigue behaviors under laser and ultrasonic peening of aluminum alloys. All of which indicated about the importance of the use of these technologies to improve the fatigue life and mechanical properties.

2. Most of researches show that UP impact treatment can induce compressive residual stress, harden the surface, and increase the mechanical strength. The surface of the treated had far less corrosion, higher strength and lower tensile residual stress than the untreated surface. Therefore, ultrasonic impact treatment is an effective technique to raising the fatigue properties of the aluminum alloys.

3. LP treatment had an important influence on micro-hardness and residual stress of the surface coating improves the mechanical properties. Researcher results showed that the temperature significantly affects the strengthening effect of (LP). The residual stress induced by warm LP decreases with the increasing temperature, Also the Studies indicated that the LP used to improve the fatigue behavior which depends strongly on the generated surface profile and plastic deformation in the surface layers.

4. These most important points derived from previous research. The current research is talking about the use of these technologies UP & LP to increase fatigue life for 2017A-T3 aluminum alloy and improve the mechanical properties.

The present work deals with the process of enhancing the surface of 2017A-T3 aluminum alloy interims of strength and life which gives percentage improvement compared to the metal without treatment.

2.3 Theoretical Considerations

2.3.1 Fatigue loading

One of the major problems in fatigue process is concerning the fatigue damage to be proportioned to each cycle in the fatigue life. The fatigue damage is made more difficult

should the stress range vary in magnitude. The most widely used theory to assess damage is due to Palmgren and Miner [Fatemi (1998)].

Structural components are subjected to a variety of load (stress) histories. There are three typical fatigue stress; cycles (i) Reversed stress; (ii) repeated stress; and (iii) random stress cycle. Figure (2.9) serves to illustrate typical fatigue stress [Gyekenyesi (2005)]

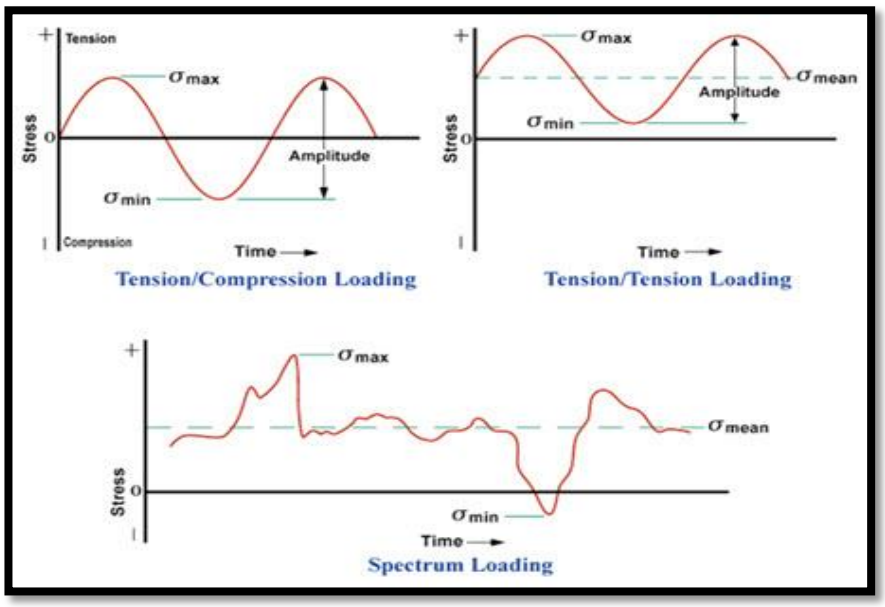

Fig.(2.9): typical Fatigue stress cycle under various loading conditions

The most complex fluctuating-load history is a variable-amplitude random sequence. The type of loading is experienced by many structures, including offshore drilling rigs, ships, aircraft, and earthmoving equipment [Knud (2000)].

- Constant amplitude loading

Load histories can be represented by a constant load (stress) range, Δp (Δσ); a mean stress, σ mean; an alternating stress amplitude, amp; and a stress ratio, R, as shown in figure (2.10) below.

The stress range is the algebraic difference between the maximum stress, σ max, and minimum stress, σ min, in the cycle [Knud (2000)].

$$\Delta \sigma = \sigma_{max} - \sigma_{min} \qquad (2.1)$$

The mean stress is the algebraic mean of σ max and σ min in the cycle.

$$\sigma_{mean} = \frac{\sigma max + \sigma min}{2} \qquad (2.2)$$

The alternating stress or stress amplitude is half the stress range in cycle.

$$\sigma_{amp} = \frac{\sigma max - \sigma min}{2} \qquad (2.3)$$

The stress ratio, R, represents the relative magnitude of the minimum and maximum stress in each cycle.

$$R = \frac{\sigma min}{\sigma max} \qquad (2.4)$$

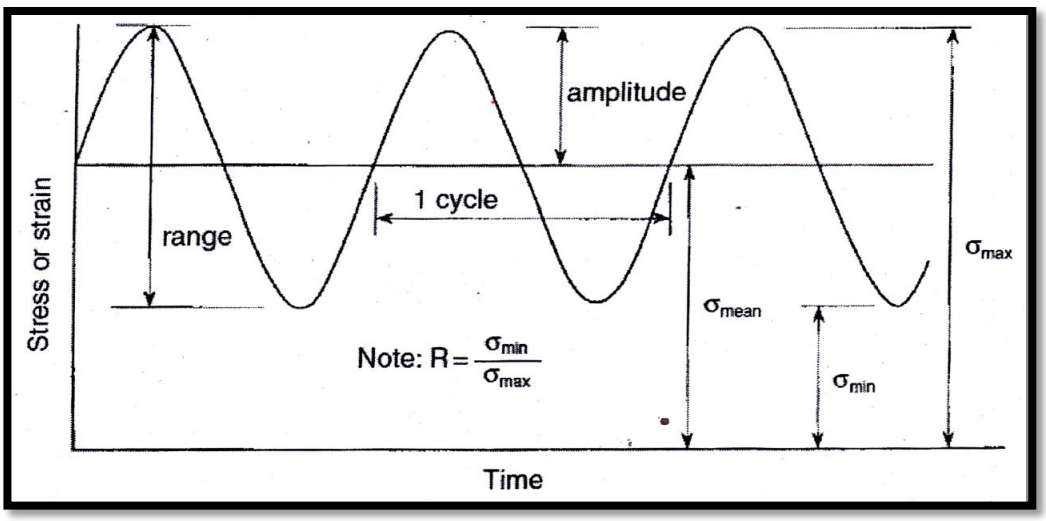

Fig.(2.10): Typical S-N curves

- Variable – amplitude loading

Various structures in service are subjected to variable – amplitude loading which can be a rather complex load –time history. Prediction on fatigue life should obviously be more complex than predication for constant amplitude loading. Example of this type of fatigue loading include wind loading on aircraft, wave loading or ship and offshore platforms, and true loading on bridges [Schijve (2009)].

- Endurance limits

Certain materials have a fatigue limit or endurance limit which represents a stress level below which the material does not fail and can be cycled infinitely. If the applied stress level is below the endurance limit of the material, the structure is said to have an infinite life. This is characteristic of steel and titanium in normal environmental conditions. A typical S-N curve corresponding to this type of material is shown curve A in Figure (4.3). Many non-ferrous metals and alloys, such as aluminum, magnesium, and copper alloys, do not exhibit well-defined endurance limits. These materials instead display a continuously decreasing S-N response, similar to curve B in Figure (2.11). In such cases a fatigue strength S_f for a given number of cycles must be specified. An effective endurance limit for these materials is sometime defined as the stress that causes failure at1x 10^8 or $5X10^8$ loading cycles.

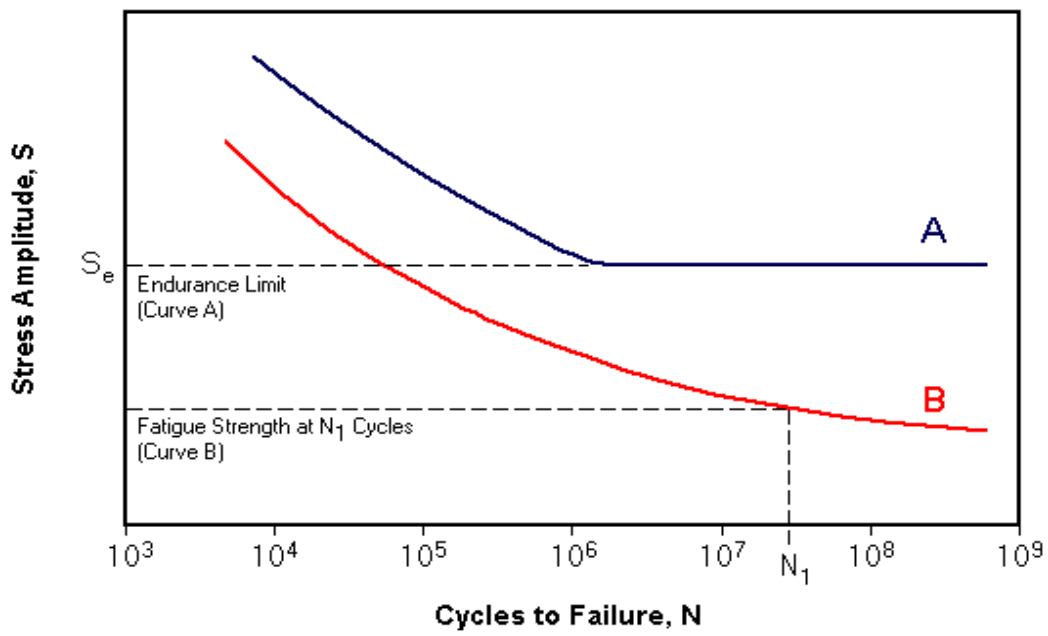

Fig.(2.11): Fatigue limit

- Relation between Endurance Limit and Ultimate Tensile strength.

It has been found experimentally that the endurance limit σ_{EL} of a material subjected to fatigue loading is a function of its ultimate tensile strength σ_u. Some empirical relations commonly used in Practice are; for steel, $\sigma_{EL} = 0.5\ \sigma_u$; for non-ferrous metals and alloy, $\sigma_{EL} = 0.3\sigma_u$. Furthermore, table (2.1) shows the approximate ratio of the endurance limit to ultimate tensile strength for several engineering metals. **[**Schijve (2009)]

Table (2.1): Ratio of the endurance limit to tensile strength for various materials

Material	Ratio
Aluminum	0.38
Beryllium copper (heat treated)	0.29
Copper, hard	0.33
Magnesium	0.38
Steel	0.46 - 0.54
Wrought iron	0.63

2.3.2 Cumulative fatigue damage

Instead of a single stress σ for n cycles, suppose apart is subjected to σ1 for n1 cycles, σ2 for n2 cycles, etc. Under these conditions, the problem is to estimate the fatigue life of a part subjected to these reversed stresses, or to estimate the factor of safety if the part has an infinite life. A search of the literature reveals that this problem has not been solved completely. Therefore the results obtained using either of the approaches presented here should be employed as guides to indicate how you might seek improvement. They should never be used to obtain absolute values unless your own experiments indicate the feasibility of doing so as Joseph Edward explained [Joseph (1986)].

Fatigue damage could increases with applied cycles in a cumulative manner which may lead to fracture. Cumulative fatigue damage is an old, but not yet resolved problem. More than 70 years ago, Palmgren suggested the concept which is now known as the 'liner rule'. In 1945, Miner first expressed this concept in a mathematical from as [Fatemi (1998)]:

$$\mathbf{D} = \sum \frac{\mathbf{n_i}}{N_{f_i}} \qquad (2.5)$$

Where:

D the damage

$\mathbf{n_i}$ applied cycles to failure under *ith* constant-amplitude loading level.

N_{f_i} Total cycles to failure under *ith* constant-amplitude loading level,

- Linear Damage Rule (LDR)

Miner first represented the Palmgren linear damage concept in a mathematical from as the LDR presented by [Fatemi (1998)]:

$$\mathbf{D} = \Sigma \boldsymbol{ri} = \Sigma \frac{\boldsymbol{ni}}{\boldsymbol{Nfi}} \qquad (2.6)$$

In the LDR, the measure of damage is simply the cycle ratio with basic assumptions of constant work absorption per cycle, and characteristic amount of work absorbed at failure. The energy accumulation, therefore, leads to a linear summation of cycle ratio or damage. Failure is deemed to occur when:

$$\mathbf{D} = \Sigma \boldsymbol{ri} = 1 \qquad (2.7)$$

Where: ***ri*** is the cycle ratio corresponding to the *ith* load level, or *ri* = (*n/Nfi*).
Experimental evidence under completely reversed loading condition often indicate that $\Sigma \boldsymbol{ri} > 1$ for a low-to-high (L-H) loading sequence, and $\Sigma ri < 1$ for a high-to-low (H-L) loading sequence [Fatemi (1998)].

- Corten- Dolan theory

The main assumptions of this theory are;

1. Initiation of crack need to a period of time.
2. The increase of applied stress, the increase in number of damaged nucleus.
3. Damage rate increase by increasing of number of applied cycles for the same stress.
4. Damage rate increase bystress increasing.
5. Total damage which causes failure at some number of cycles is constant for all types of loading.

Corten and Dolan suggested a quantitative expression for cumulative damage. The final from CD hypothesis is [Ail (2006)].

$$\mathbf{D} = \frac{\boldsymbol{n_1}}{\boldsymbol{N_1}} + \frac{\boldsymbol{n_2}}{\boldsymbol{N_2}}\left(\frac{\boldsymbol{\sigma_2}}{\boldsymbol{\sigma_1}}\right)^2 + \frac{\boldsymbol{n_3}}{\boldsymbol{N_3}}\left(\frac{\boldsymbol{\sigma_3}}{\boldsymbol{\sigma_2}}\right)^2 + \cdots = 1 \qquad (2.8)$$

Where $\boldsymbol{\sigma_1}$: maximum applied stress in the consequence.

$\mathbf{N_1}$: total number of cycles required to failure under constant (σ_1) effect.

$\boldsymbol{\sigma_1, \sigma_2}\ldots$: applied stress amplitudes (MPa)

- Manson double linear damage rule

Manson developed a semi empirical expression for determining the crack initiation and the crack propagation phases. It was assumed that the crack propagation period ΔN_f could be described in terms of the life N_f by the equation [Manson (1986)]

$$\Delta N_f = P N_f^{0.6}$$

Where p ; is an adjustable constant to be determined experimentally. Manson suggested that the crack initiation period be;

$$No = N_f - P N_f^{0.6}$$

Wherever $N_f > 750$ cycles and equal to zero for $N_f < 750$. Thus, the two equations for the double linear damage rule (DLDR) become.

for initiation

$$\sum\left(\frac{n}{N_o}\right) = \sum\left(\frac{n}{N_f - P N_f^{0.6}}\right) = 1 \qquad (2.9)$$

And For propagation

$$\sum\left(\frac{n}{\Delta N_f}\right) = \sum\left(\frac{n}{P N_f^{0.6}}\right) = 1 \qquad (2.10)$$

A convenient method for determining the value of P is to conduct a test at high load range for a part of the life then continues the test to failure at a lower range.

- Marsh Damage Theory

In this Theory, an applied stress of a value less than fatigue limit does not cause damage. Thus, when (σL<σf<σH) the resulted damage will be for higher stress (σH) only, while the lower stress (σL) will do not have any effect on Marsh expected life fatigue stress (σf) [Ail (2006)].

Thus:

$$N_m = \frac{\sigma_H - \sigma_f}{\sigma_H - \sigma_L} \times N_E \qquad (2.11)$$

Where N_m: Marsh expected life.

N_E: experimental fatigue life.

- Exponential model

The fatigue crack behavior in metals and alloys under constant amplitude test conditions is usually described by relationships between the crack growth rate da/dN and the stress intensity factor range ΔK. This model, an enhanced two-parameter exponential equation of fatigue crack growth was introduced in order to describe sub-critical crack propagation behavior of AL 2524-T3 alloy. It was demonstrated that besides adequately correlating the load ratio effects, the exponential model also accounts for the slight deviations from linearity. A comparison with other models allowed for verifying the better performance. According to Eq. (4.12) the superior performance of the exponential model is evident [Baptista (2012).]

$$\text{Residue (j)} = \sum_{i=l}^{p(j)} \sqrt{\left(\frac{da/dN_{i,exp} - da/dN_{i,calc}}{dald\ N_{i,exp}}\right)^2} / \text{P(j)} \qquad (2.12)$$

Δk : stress intensity factor range.

P (j) : the number of experimental point of curve " j ".

j = 1,….r. Thus the Logarithmic error for point " i ".

da/dN : crack growth rate.

- Garcia model

Fatigue damage accumulation in arrested crack holes with cold expansion process was studied. A detailed description of the damage stress model and the definition eq. (2.13) and eq. (2.3) for the damage stress and the determination of this one is described [Garcia (2005)]:

$$Di = \frac{\sigma_{(i)}\, d - \sigma i}{\sigma u - \sigma i} \qquad (2.13)$$

Where $\sigma_{(i)d}$ = stress of damage

σ_i = applied stress

σ_u = ultimate stress

The equivalent stress of damage at level i+1 is calculated with relation

$$Di = \frac{\sigma_{(i)}\, d - \sigma i}{\sigma u - \sigma i} = \frac{\sigma_{(i+1)}\, d - \sigma i+1}{\sigma u - \sigma i+1} \qquad (2.14)$$

Where $\sigma_{(i+1)}$d = equivalent stress of damage at level i+1

σ_i+1 = stress at the level i+1

- Lynn model

Computer software for the prediction of fatigue crack initiation has been developed. Based on a model derive from the closure behavior of microcracks and intrinsic resistance of metals and alloys to fatigue damage. The model had been previously proven successful for a number of material types and load spectra. The crack opening stress σop is dependent on cyclic yield stress and maximum and minimum stress corresponding to the largest rain flow cycle. The magnitude of σ_{op} in materials with high stress magnitude was observed to vary with σ_{max} and σ_{min} according to [Lynn (2012)].

$$\sigma_{op} = \alpha\sigma_{max}\,[1 - \sigma_{max}/\sigma y]^2 + \boldsymbol{\beta}\sigma_{min} \qquad (2.15)$$

Where α, B = The constants are typically determined using a differential compliance technique.

Table (2.2) crack opening constant

Alloy	α	β
Mild steel	0.45	0.8
Aluminum alloys	0.45	0.2

The life predication algorithm for software was designed to produce an EΔε life predication from inputs comprised of nominal stress spectrum, an absolute maximum nominal stress (s_{max}). A program is presented in figure (2.12).

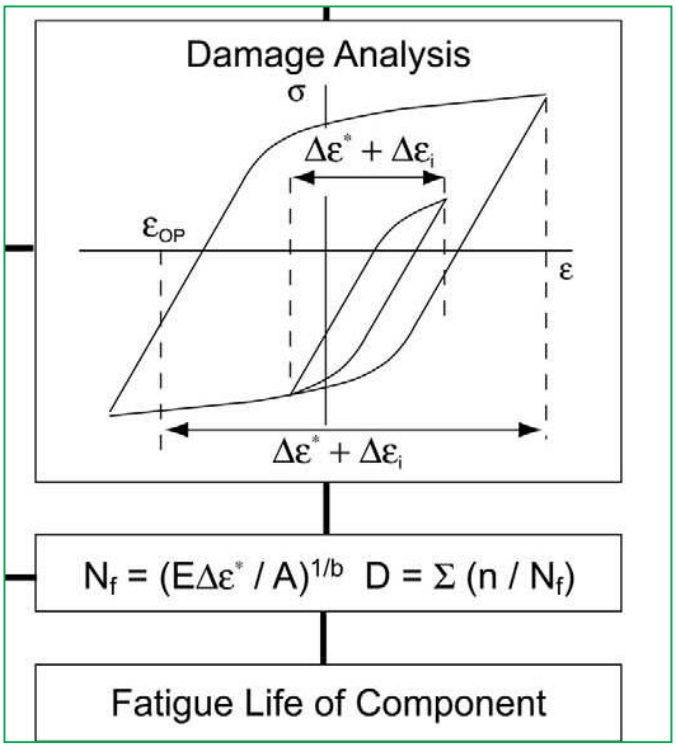

Fig.(2.12) fatigue life component

- Halford model

Nonlinear cumulative damage rules offer more accurate, and hence more conservative, fatigue life prediction than LDR. The nonlinear DCA and DLDR cumulative fatigue damage model, require only twice the effort of the classic linear rule.

Nor do they require additional material property or mission loading information to achieve the improved accuracy.

Linear damage rule

$$D = (n/N_f) \qquad (2.16)$$

Damage curve approach,

$$D = (n/Nf)^{g(N_f)} \qquad (2.17)$$

Equation (2-6) is appropriate to point out that this equation is of identical form to the classical LDR. For the LDR, $g(N_f)$is such asimple function that it is a constant and equal to unity. Equation (2.5) implies that damage accumulates linearly with applied cycle fraction, independent of life level N_f. This implication is at odds with common knowledge among fatigue researchers who recognize that damage in LCF and HCF does not accrue at the same rate. Nor does it accrue linearly applied cycle fraction [Gary (1997)].

- Omer G. Bilir model

Cumulative fatigue damage tests were conducted under a basic one-block loading sequence that comprised either a high-load followed by a low load. The data were analyzed first on the basis of Miner's linear damage rule.

$$\frac{n_1}{N_1} = \frac{n_2}{N_2} = 1 \qquad (2.18)$$

The crack propagation period ΔN_f cold be described in the terms of the life N_f by :

$$\Delta N_f = PN_f^{0.6} \qquad (2.19)$$

Where p: is an adjustable constant to be determined. Manson suggested that the crack initiation period be

$$No = N_f - PN_f^{0.6} \qquad (2.20)$$

Where : is No = cyclic life to initiate an effective crack at aparticular stress level.

Thus, the two equation for the double linear damage rule become [Omer (1991)]

$$\sum\left(\frac{n}{no}\right) = \sum\left(\frac{n}{N_f - PN_f^{0.6}}\right) = 1 \qquad (2.21)$$

For initiation, and

$$\sum\left(\frac{n}{\Delta N_f}\right) = \sum\left(\frac{n}{PN_f^{0.6}}\right) = 1 \qquad (2.22)$$

For propagation

- Kadhim model

A combination of effective strain damage (ESD) model based FORTRAN code with finite element software was proposed to predict fatigue life under random loadings.
To calculate steady state stress

$$S_{ss} = \alpha S_{max}\,[1-(S_{max}/Scy)^2] + \boldsymbol{\beta} S_{mix} \qquad (2.23)$$

To calculate the change in crack opening stress

$$\Delta S_{op} = m\,(S_{ss} - S_{cu}) \qquad (2.24)$$

Calculate crack opening stress

$$S_{op} = S_{cu} + \Delta S_{op} \qquad (2.25)$$

Calculate fatiguelife (N) for each cycle using damage equation of

$$Ni = (E\Delta\mathcal{E}/A)^{1/B} \qquad (2.26)$$

Then fatigue damage using

$$Di = 1/Ni$$

then total damage

$$D_T = \sum Di$$

$$E\Delta\varepsilon = E\varepsilon_{max} - S_{op} - S_i \qquad (2.27)$$

Ni : is the number of applied cycles.
$\mathcal{E}_{max}$: is the maximum strain.
m : is a material constant.
Scu : is the current opening stress.

σ, B: are materials constant which are obtained from a curve fitting procedure performed using a graph of the measured crack opening stress versus the max. stress [Kadhim (2011)].

- Shaik Jeelani model

Several investigators have concluded that when a metal is subjected to stress- cycling process its work hardening is confined primarily to the surface layer. With an increase in the number cycles and the stress amplitudes, there is an increase in the surface layer stress. As the fatigue damage accumulates, the surface layer stress reaches a critical value and crack is formed independently of the stress amplitude, leading to fatigue failure. Kramer has proposed that cumulative fatigue damage and fatigue life can be described in terms of the rate of increase in the strength of the surface layer with the number of cycles [Shaik (1984)].

$$D = \sum \frac{\sigma_{si}}{\sigma_{s*}} \qquad (2.28)$$

Where$\sigma_s$and σs* are the surface layer stress and the critical surface layer stress respectively, and that the failure will occur when

$$\frac{\sigma_{si}}{\sigma_{s*}} = 1 \qquad (2.29)$$

He further extended his investigation and proposed the failure equation

$$\frac{n1\sigma_1^p}{\beta} + \frac{n2\sigma_2^p}{\beta}\left(\frac{\sigma_1}{\sigma_2}\right)^{pf_1} + \frac{n3\sigma_3^p}{\beta}\left(\frac{\sigma_2}{\sigma_1}\right)^{pf_2}\left(\frac{\sigma_1}{\sigma_2}\right)^{pf_1f_2} + \cdots\cdots = 1 \qquad (2.30)$$

Where σ_1 ,σ_2 are the applied stresses, n_1 n_2… are the number of cycles applied at stressesσ_1 ,σ_2 …. m, is the slope of the S-N curve which is often of the $Y = CX^m$,

$p = -m^{-1}$ is a material constant, $\boldsymbol{\beta} = c^p$ is a material constant

$$f_1 = \sigma_1^p \, n_1 / \boldsymbol{\beta} \qquad (2.31)$$

and

$$f_2 = \left[\sigma_2^p \, n2 \left(\frac{\sigma_1}{\sigma_2}\right)^{pf_1}\right]/\beta \qquad (2.32)$$

f_1 f_2, are damage histories in the previous stress sequences

$$D_T = f_1 + f_2 + f_3 + f_4 \qquad (2.33)$$

DT: is the total cumulative fatigue damage.

- Alalkawi Model

Alalkawi et al model [Alalkawi (2012)], under different conditions of surroundings such as:

a. Life evaluation due to constant amplitude fatigue loading

The fatigue curve can be presented by the following equation (based on Basquin equation form).

$$\sigma_f = AN_f^{\alpha} \qquad (2.34)$$

Where: σ_f is the applied stress (MPa) at failure.

N_f is the fatigue life at failure (cycles).

α is the material constant.

Equation (4.34) can be written in the form

$$N_f = \left(\frac{\sigma f}{A}\right)^{\frac{1}{\alpha}}$$

A and $\boldsymbol{\alpha}$ are material constant and may be evaluated by linearizing the curve using equation (2.34) in logarithmic form as following

$$Log\sigma_f = logA + \boldsymbol{\alpha}\, logN_f \qquad (2.35)$$

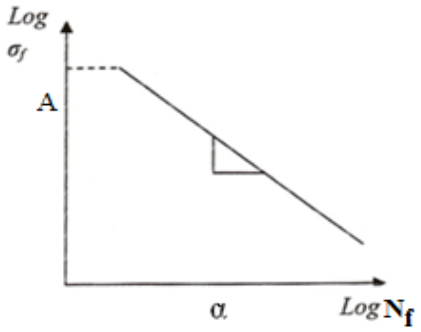

Fig. (2.13): Logarithm description of fatigue equation.

$$\boldsymbol{\alpha} = \frac{h \sum log\sigma_f logN_f - \sum log\sigma_f \sum logN_f}{h \sum (log_{Nf})^2 - [\sum log_{Nf})^2} \quad (2.36)$$

$$Log\ A = \frac{\sum log\sigma_f - \alpha \sum logN_f}{h} \quad (2.37)$$

Where: *h* is the number of tests.

b. Life estimation due to variable amplitude fatigue loading

Miner's rule can be specifying as:

$$\sum \frac{n}{(N_f)i} = \frac{n_1}{N_{f1}} + \frac{n_2}{N_{f2}} \quad (2.38)$$

Or $$\sum \frac{n_i}{(N_f)i} = D \quad (2.39)$$

Where: D is the fatigue damage

n_i : number of cycles at stress σ_i

N_{fi} : number of cycles to failure stress σ_{fi}

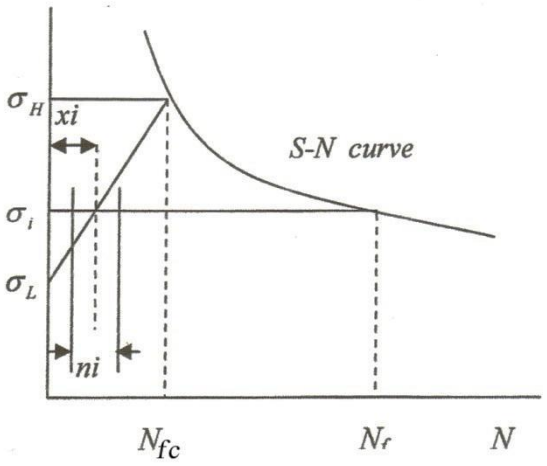

Fig.(2.14): constant and variable amplitude fatigue diagram

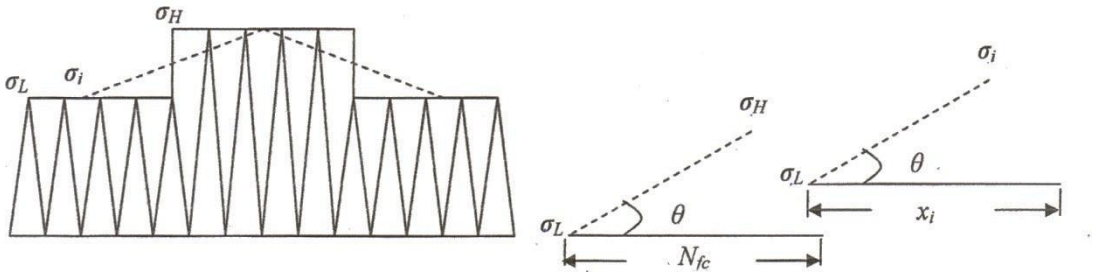

Fig.(2.15): Angle of the variable amplitude fatigue diagram

Take an element of n_i wide and x_i distance from σ-axis the slope of the line for the element can represents by

$$\theta = \frac{\sigma_{i-\sigma_L}}{x_i} \qquad (2.40)$$

OR

$$\theta = \frac{\sigma_{H-\sigma_L}}{N_{fc}} \qquad (2.41)$$

Equation (4.40) and (4.41) gives

OR $$\frac{\sigma_{i-\sigma_L}}{x_i} = \frac{\sigma_{H-\sigma_L}}{N_{fc}}$$

$$xi = \frac{N_{fc}(\sigma_{i-\sigma_L})}{\sigma_{H-\sigma_L}} \quad (2.42)$$

where N_{fc} is the number of cycle to failure.

Drive equation (4.42) w.r.t. σ_i, get:

$$dX_i = \frac{N_{fc} d\sigma_i}{\sigma_{H-\sigma_L}} \quad (2.43)$$

By substituting equation (4.43) in (4.38)

Equation (4.16) can be rewritten as:

$$\sum \frac{n}{(N_f)i} = \int_{\sigma_L}^{\sigma_H} \frac{dX_i}{(N_f)i} = \int_{\sigma_L}^{\sigma_H} \frac{N_{fc} d\sigma_i}{(\sigma_{H-\sigma_L})(N_f)i} \quad (2.44)$$

$$\therefore \sum \frac{n}{(N_f)i} = \frac{N_{fc}}{(\sigma_{H-\sigma_L})} \int_{\sigma_L}^{\sigma_H} \frac{d\sigma_i}{(N_f)i}$$

OR

$$D = \frac{N_{fc}}{(\sigma_{H-\sigma_L})} \int_{\sigma_L}^{\sigma_H} \frac{d\sigma_i}{(N_f)i}$$

By substituting equation (4.34) into (4.44) to get

$$D = \frac{N_{fc}}{(\sigma_{H-\sigma_L})} \int_{\sigma_L}^{\sigma_H} \frac{d\sigma_i}{(\frac{\sigma_f}{A})^{\frac{1}{\alpha}}} \quad (2.45)$$

Integrate equation (4.45) to get

$$D = \frac{N_{fc}}{(\sigma_{H-\sigma_L})} \left[\frac{(\sigma_f)^{1-\frac{1}{\alpha}}}{\left(1-\frac{1}{\alpha}\right)\times\left(\frac{1}{A}\right)^{\frac{1}{\alpha}}} \right]_{\sigma L}^{\sigma H} \qquad (2.46)$$

OR

$$D = \frac{N_{fc}}{(\sigma_{H-\sigma_L})} \times \frac{(\sigma_H)^{1-\frac{1}{\alpha}} - (\sigma_L)^{1-\frac{1}{\alpha}}}{\left(1-\frac{1}{\alpha}\right)\times\left(\frac{1}{A}\right)^{\frac{1}{\alpha}}}$$

Equation (2.46) will be half program so that to get one program multiply equation (2.46) by 2 to get full program

$$\mathbf{D = \frac{2N_{fc}}{(\sigma_{H-\sigma_L})} \times \frac{(\sigma_H)^{1-\frac{1}{\alpha}} - (\sigma_L)^{1-\frac{1}{\alpha}}}{\left(1-\frac{1}{\alpha}\right)\times\left(\frac{1}{A}\right)^{\frac{1}{\alpha}}}} \qquad (2.47)$$

Where D in the above equations is the experimental damage calculated from the test results while this value equal to unity in Palmgreen-Miner rule.

- Alalkawi , Shot peening model

A cumulative fatigue damage model for life predication will presented involving the effects of loading sequences and the surface shot peening treatment [Alalkawi (2014)]. Cumulative fatigue damage is an old, but not yet resolved problem. Miner first expressed the concept in a mathematical form as:

$$D = [\sum \frac{n_1}{(N_{f1}}] = 1 \qquad (2.48)$$

Following the work of Perieira et al and Alalkawi et al , they suggested the damage due to fatigue for low-high and high-low stress level as:

$$D= [\frac{n1}{Nf1}]^{x} \quad (2.49)$$

Where, (x) is a function of the applied load, (x) may be defined as the effect of loading sequences and surface treatment, here the surface treatment is shot peening technique. Equation (2.49) can be modified to take the form:

$$D= [\sum \frac{n}{(N_{f1}}]^{x} \quad (2.50)$$

Where (*x*) represents the effect of loading sequences and shot peening treatment, here (*x*) may be defined as:

$$X= \frac{\sigma_L}{\sigma_h} \boldsymbol{\beta}$$

Where, $\boldsymbol{\beta}$ is the inverse slope of the S-N curve, if the test program is low-high, also (*x*) it could be,

$$X= \frac{\sigma_h}{\sigma_L} \boldsymbol{\beta}$$

When the test program is represent from high to low.
In order to make the predication safe equation can be divided by the value (x) to become:

$$\mathbf{D} = \frac{[\sum \frac{n}{(N_{fL}}]^{x}}{x} \quad (2.51)$$

2.3.3 Proposed model for cumulative fatigue under laser peening

One of the major problems in fatigue process is concerning the fatigue damage to be proportioned to each cycle in the fatigue life. The fatigue damage is made more difficult should the stress range vary in magnitude. The most widely used theory to assess damage is

due to Palmgren and Miner [Walter (1999)]. This rule assumes a linear summation of cumulative damage which may be mathematically expressed for individual stress levels as:

$$\sum \frac{n}{N_f} = \left[\frac{n1}{N_{f1}}\right]_{\sigma 1} + \left[\frac{n2}{N_{f2}}\right]_{\sigma 2} + \left[\frac{n3}{N_{f3}}\right]_{\sigma 3} + \cdots = 1 \qquad (2.52)$$

Application of the above equation requires an experimental data and a conventional S-N curve. The fact that the summation is frequently less than unity as sometimes as large one [Miller, (1986).] illustrates the dangers of applying the Miner rule. Following the work of [Alalkawi(**2014**)],[Alalkawi (2015)] and [Perreira (2009)], they suggested the damage due to fatigue for low- high and high- low stress levels as:

$$\text{D = damage} = \left[\sum \frac{ni}{N_{fi}}\right]^{x} \qquad (2.53)$$

Where X: is a function of the applied load. In the present work **X** may be defined as the effect of loading sequences and surface treatment, here the surface treatment is used BPL and WLP.

Then:

$$X = \frac{\sigma_L}{\sigma_H}\alpha \quad \text{for low- high stress levels} \qquad (2.54)$$

And

$$X = \frac{\sigma_H}{\sigma_L}\alpha \quad \text{for high-low-stress levels} \qquad (2.55)$$

Where: $\boldsymbol{\sigma_L}$ is the applied low stress, and $\boldsymbol{\sigma_H}$ is the applied high stress in MPa. $\boldsymbol{\alpha}$ is the Basquin exponent determined from the S-N curve which may take the form:

$$\boldsymbol{\sigma_f} = A\, \boldsymbol{N_f^{\alpha}} \qquad (2.56)$$

2.3.4 Proposed model with laser peening

For two blocks testing

Low- high

$$D = \left[\frac{n_1}{N_{f_1}} + \frac{n_2}{N_{f_2}}\right]^{\frac{-\sigma_L \alpha}{\sigma_H}} \quad (2.57)$$

And

High- low

$$D = \left[\frac{n_1}{N_{f_1}} + \frac{n_2}{N_{f_2}}\right]^{\frac{-\sigma_H \alpha}{\sigma_L}} \quad (2.58)$$

Where *n* is the applied number of cycles

2.3.5 Proposed model for cumulative fatigue under ultrasonic peening

In order to estimate the fatigue life of components in service it is significant to formulate a method to predict the fatigue damage accumulation. For many years, the engineers used the Miner rule [http://www.weibull.com (1992)] or liner damage theory (LDT) in the case of variable loading.

$$\text{Damage} = \sum_{i=1}^{n} \frac{n_i}{N_{fi}} \quad (2.59)$$

Where n_i is the number of applied stress cycle σ_i and N_{fi} is the number of cycles to failure at the same applied stress σ_i . This theory is based on D (damage) equal to unity and because of the shortcomings occurred in the application of this rule, many workers tried to modify this theory. Marco and Starkey [Collins (1993)] suggested a non-linear damage rule as follows:

$$\text{Damage} = \sum_{i=1}^{n} \left(\frac{n_i}{N_{fi}}\right)^{x_i} \quad (2.60)$$

Where: x_i is a loading sequence coefficient

This theory can take the effect of different loading into account. The experimental results showed that only in some case and for some material, equation (2.60) have revealed good agreement. Recently, Alalkawi, et al [Alalkawi (2014)] proposed a non-linear damage model based on the above equation and taking into account, the loading sequences and the environment, as follows:

$$D = \sum_{i=1}^{n} \left(\frac{n_i}{N_{fi}}\right)^{\propto} \qquad (2.61)$$

Where $\propto = \frac{\sigma_h}{\sigma_L} \propto$ for high-low fatigue tests

And $\propto = \frac{\sigma_L}{\sigma_h} \propto$ for low-high fatigue tests

The model suggested here does not need too many factors and it takes into consideration the load history and based on the S-N curve. Following Marco and Starkey and Alalkawi et al, damage can be defined as:

$$\text{Damage } (D) = \sum_{i=1}^{n} \left(\frac{n_i}{N_{fi}}\right)^{\beta} \qquad (2.62)$$

All the parameters mentioned in the equation (2.62) have the same meaning except β which may be defined as:

For low-high cumulative fatigue testing

$$\beta = \left(\frac{Ault\ \sigma_L}{Adry\ \sigma_h}\right)^{\frac{\propto ult}{\propto dry}} \qquad (2.63)$$

And for high-low cumulative fatigue testing

$$\beta = \left(\frac{Ault\ \sigma_h}{Adry\ \sigma_l}\right)^{\frac{\propto ult}{\propto dry}} \qquad (2.64)$$

Where $Ault$, $\propto ult$ and $\propto dry$ are the coefficient constants of S-N curve equations as follow:

For unpeened S-N curve testing

$$\sigma_f = A\ N_f^{\propto dry} \quad (2.65)$$

And for ultrasonic peening S-N curve testing

$$\sigma_f = A\ N_f^{\propto ult} \quad (2.66)$$

The number of programs of cumulative testing for two applied stress is denoted by (R) and it can be obtained from the equation:

$$\left[\frac{n_1}{N_{f1}} + \frac{n_2}{N_{f2}}\right] R = D \text{ (Damage)} \quad (2.67)$$

Where n_1 and n_2 is the experimental applied cycles.
The cumulative fatigue life can be calculated from the equation:

$$[n_1 + n_2]\ R = N_{f\ cumulatie}$$

2.3.6 Proposed model with ultrasonic peening

Predication of fatigue loading in random condition required precise calculation and needs the equation of S-N curve with and without ultrasonic testing.
For low - high stress level tests:

$$\mathbf{D} = \left[\frac{n_1}{N_{f1}} + \frac{n_2}{N_{f2}}\right]^{\left(\frac{Ault\ \sigma_L}{Adry\ \sigma_h}\right)^{\frac{\propto ult}{\propto dry}}} \quad (2.68)$$

And for high-low stress level tests:

$$\mathbf{D} = \left[\frac{n_1}{N_{f1}} + \frac{n_2}{N_{f2}}\right]^{\left(\frac{Ault\ \sigma_h}{Adry\ \sigma_l}\right)^{\frac{\propto ult}{\propto dry}}} \quad (2.69)$$

Chapter 3
Experimental Work

3.1 Introduction

Throughout the present work, measurements were made to establish the influence of laser peening and ultrasonic peening on fatigue behavior of 2017A-T3. This chapter outlines the experimental program and describes the preparation of the test specimens, instrumentation and test methodology.

The experimental work of this thesis is presented in two sections. The first deals with the selection of material, and its chemical composition, mechanical properties. The second section describes the equipments; laser peening, ultrasonic peening, tensile test rig and fatigue test rig. The experimental testing details can be shown in flow chart as shown in figure (3.1).

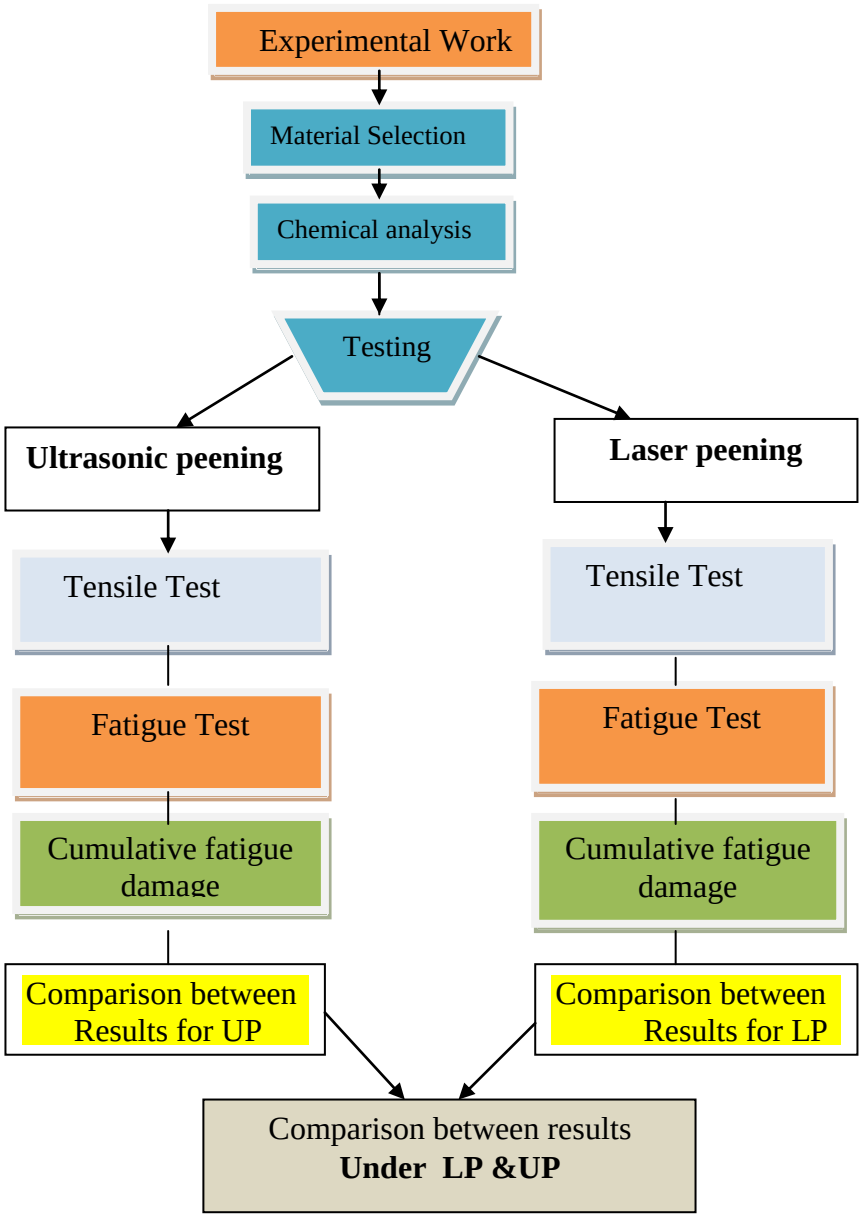

Fig.(3.1): The flow chart of the experimental plan

3.2 Material Selection

The selected material is from Aluminum alloys of 2xxx series alloy. The aircraft airframe has been the most demanding application for aluminum alloys; to chronicle the development of the high-strength alloys is also to record the development of airframes. Duralumin, the first high-strength, heat treatable aluminum alloy, was employed initially for the framework of rigid airships, by Germany and the Allies during World War I. Duralumin was an aluminum-copper-magnesium alloy; it was originated in Germany and developed in the United States as alloy (2017). It was utilized primarily as sheet and plate.

The material tested was a 2017A-T3 aluminum alloy supplied as round bar of 12 mm. The material is AA 2017A-T3, which is an aluminum copper alloy of widely industrial use (airplanes, aerospace industries) due to its mechanical properties such as good mechanical strength in weight and high in corrosion strength. The character (T3) in 2017A- T3 alloy is solution heat treated and cold worked, a letter (A) with a number which indicates to the type of alloy is the Aluminum Association (AA) designation for this material. In European standards, it will typically be given as EN AW-2017A. Chemical Analysis of the alloy was carried out at specialized Institute in wt% are reported in table (3.1) [www.makeitfrom.com/material (2013)].

Table (3.1) Experimental and standard chemical composition of 2017A-T3 Al-alloy, wt%

Material	Zn	Ti	Cr	Fe	Cu	Mg	Mn	Si	Al
Standard	max. 0.25	max. 0.25	max. 0.1	max. 0.7	3.5-4.5	0.4-0.1	0.4-1	0.2-0.8	Balance
Actual	0.02	0.08	0.01	0.39	4.07	0.70	0.56	0.52	Balance

Aluminum and its alloys are essential materials in various industries such as aerospace, marine, construction, and automobile. Aluminum 2017A-T3 alloy is a heat treatable wrought alloy with intermediate strength. It is stronger than aluminum 2011, but harder to machine. The reason of this compression coming from the 2011 can be replaced by 2017A-T3 aluminum alloy. Workability is fair with ductility and formability better than aluminum 2014. Arc and resistance weldability of this alloy are satisfactory while corrosion resistance is fair [Samer (2013)].

The standard mechanical properties of the material are known from handbooks. These properties known at room temperature, the mechanical properties of the alloy used can be illustrated in table (3.2).

Table (3.2): Mechanical properties of 2017A-T3 alloy

Property	σ_u (MPa)	σ_y (MPa)	E (GPa)	μ	EI %	Fatigue strength (MPa)	Shear modulus (GPa)	(HB)
Standard	**450**	**290**	**74**	**0.33**	**22**	**124**	**27**	**105**
Exp.	**435**	**270**	**73**	**0.33**	**22**	**122**	**26**	**103**

3.3 Specimens preparation

In this study, two types of specimens were manufactured**:**

1. Tensile test specimen

Tensile test specimens were manufactured by CNC (***Computer Numerical Control***) machine type CJK 6132 CNC LATHE 320x500 as shown in figure (3.2), and tensile specimen during manufacture in CNC machine can be seen in figure (3.3).

Fig.(3.2): CNC machine type CJK 6132 CNC LATHE 320x500

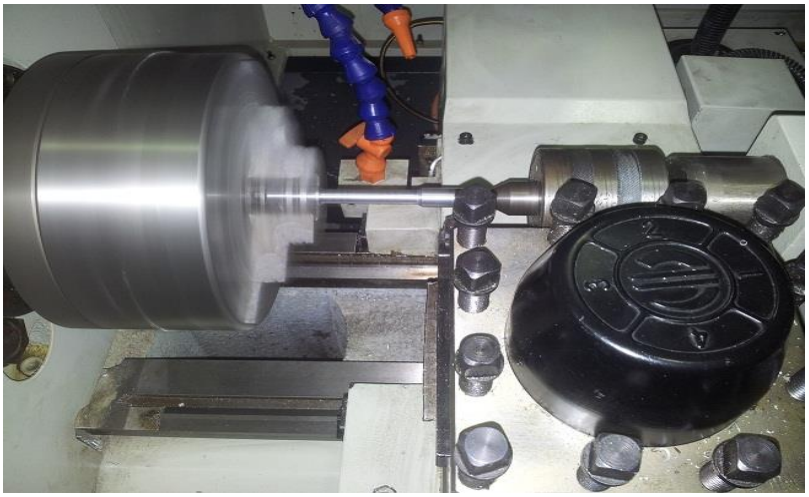

Fig.(3.3):Tensile specimen during manufacture in CNC machine

Machinery and structures manufacture requires us to know the mechanical behavior of materials that are used. The usual procedure is to put standard samples of the material in the test machine, and apply loads, and then measure the deviations from it. Most test materials laboratories are equipped with machines able to download the samples in a variety of ways, including download both static and dynamic stress and tension.
Tensile samples were manufactured in laboratory of the University of Technology in proportion to the tensile test machine in accordance to the American Society for Testing and Materials (ASTM-B211), as shown in figure (3.4).

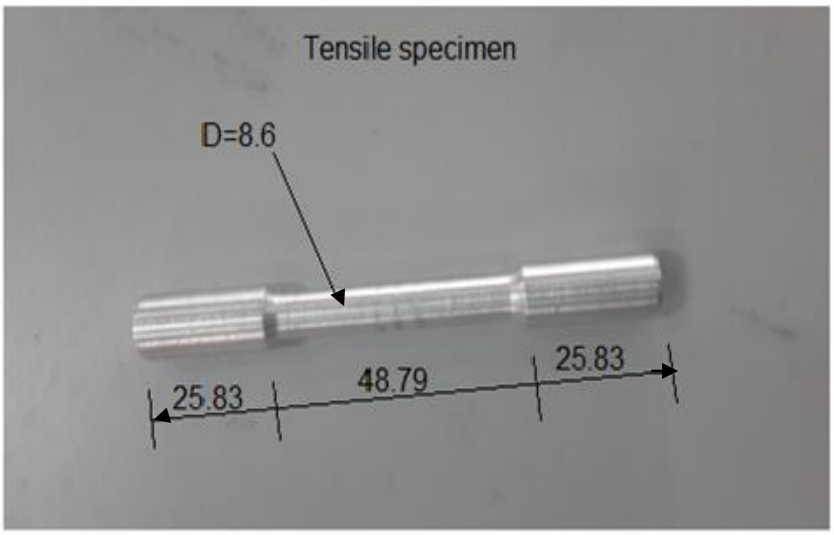

Fig.(3.4): Tensile test specimen, all dimension in mm.

2. Fatigue specimen

The material 2017A-T3 Al-alloy was received from aircraft repairing factory in the form of rolled rods of 12mm in diameter. Rotating bending fatigue specimen having an hour-glass profile with large curvature was adopted in this study. To obtain perfect dimensions of a fatigue specimen and to avoid mistake, an exact samples profile should be achieved .The specimens were manufactured by CNC machine. While specimens industrialization, careful notice was taken to produce a good surface finishing and to reduce tensile residual stresses. Shape and dimensions of fatigue specimen are detailed in figure (3.5). It was prepared according to DIN 50113.

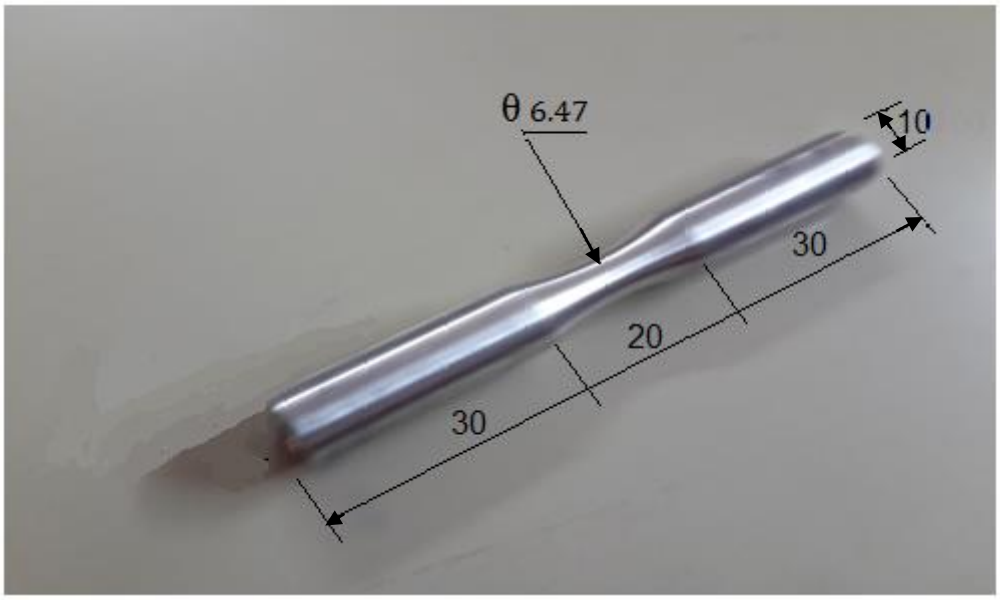

Fig.(3.5): Fatigue specimen configuration (in mm)

3.4 Roughness measurements

After preparing the specimens, they were numbered and polished. First, with grade 400,600,800,100 and 1200 emery papers and then with diamond pastes of 3 and 1µm respectively, to reduce the probability cracks growth at the surface of specimens.

Measurement of surface roughness for selected specimens was obtained by means of a Perthmeter M3A instrument. The output reading were Ra, (the center line average CLA) and Rt (the maximum surface roughness).The results are presented in table (3.3) for ten selected specimens.

$$\text{CLA or Ra (in microns)} = \frac{y_1 + y_2 + y_3 + \cdots y_n}{n} \qquad (3.1)$$

Where y_1, $y_2 \ldots y_n$ are the ordinates measured on both sides of the mean line and n is the number of ordinates.

Table (3.3): Selected roughness values for fatigue specimens

Spec. No.	Min. diam. (mm)	Ra (µm)	Rt (µm)
1	6.39	0.25	0.75
2	6.41	0.35	0.82
3	6.382	0.19	0.65
4	6.401	0.125	0.45
5	6.375	0.28	0.85
6	6.381	0.37	0.62
7	6.407	0.4	0.85
8	6.402	0.44	0.9
9	6.338	0.29	0.77
10	6.408	0.38	0.89

3.5 Tensile Test

Tensile test was used to ensure that material is meeting with standard specifications of selected material. Tensile test carried out to obtain the mechanical properties of 2017A-T3 AL-alloy by fixed the specimens between the two grips of test machine WDW-200E and then loaded in tension. The maximum load capacity of the tensile test machine is (200 KN). Measuring devices record the deformation of the specimens, and the automatic control and data- processing systems graph the results.

The tensile test was conducted in the production and Metallurgy Engineering Department, University of Technology (Baghdad) by tensile machine WDW2 Figure **(3.6)** shows the tensile test machine and tensile specimen during test.

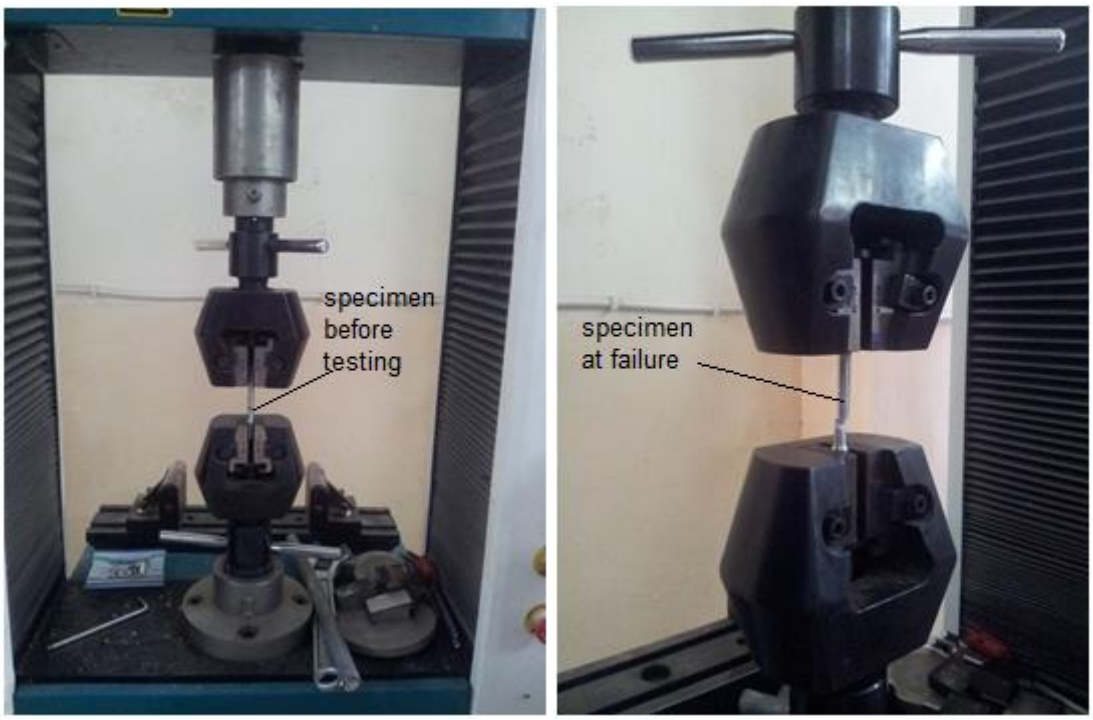

Fig.**(3.6):** Tensile test machine WDW-200E with tensile specimen during the test

3.6 Laser peening (LP)

Laser peening test has been done by using laser device (Nd-YAG laser system) as shown in figure (5.7) the following specifications of laser peening are listed below:

1. Laser wavelength is about 1.065μm**.**
2. Pulse duration (16, 26, 15) nano seconds.
3. Pulse energy (310, 610,1000). mJ
4. The laser spot is about (6) mm in diameter.
5. The water height to the area that peened is about (10) mm.
6. The specimens were shock laser peening with energy pulse 310 mJ at 16 nanoseconds.

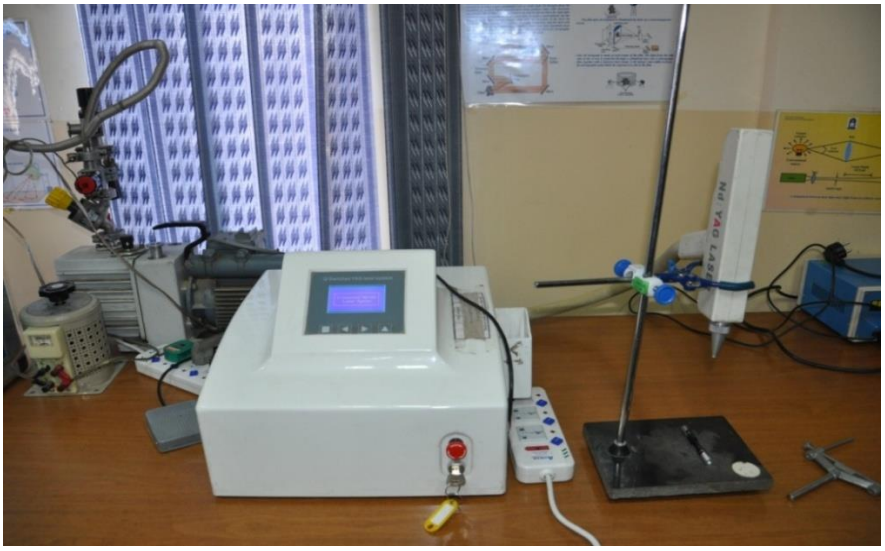

Fig.(3.7): Rig (Nd-YAG laser system)

The specimens have been shocked by laser peening with use pulse energy 310 mJ at 16 nanoseconds. The laser spot is about (6) mm in diameter. Figure (3.8) shows the data panel for laser device during working.

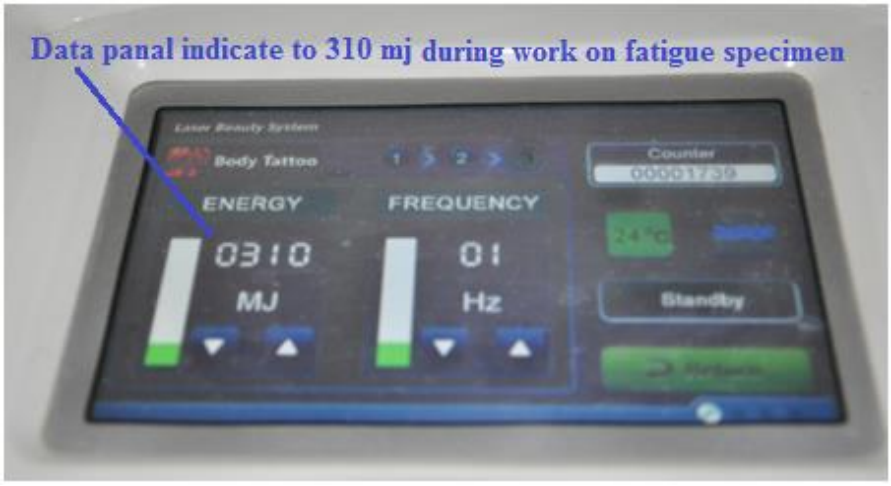

Fig.(3.8): Data panel of laser device during shock the specimen of 2017A-T3

3.6.1 Tensile test after laser peening

The tensile test specimen as described above has been done for cases of laser treatment [as received, black paint laser peening (BLP) and water laser peening (WLP)] as shown in figure (3.9).

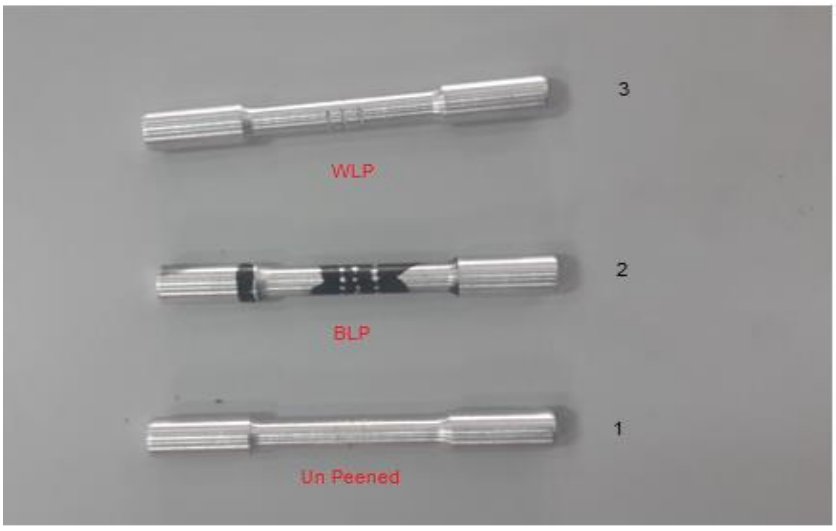

Fig. (3.9): Tensile specimens unpeening and under two cases of LP

The tensile stress-strain diagram for tested specimen three cases (as received, black paint laser and water leaser) can be seen in figure (3.10).

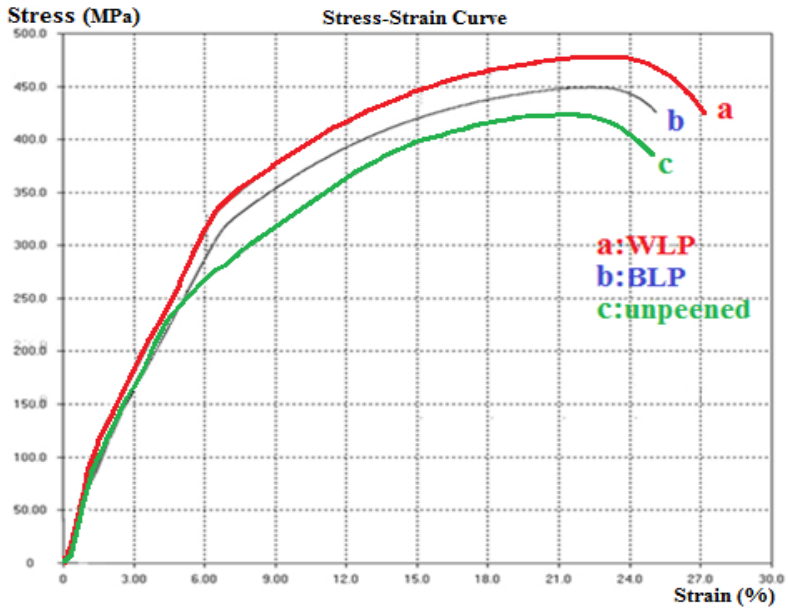

Fig.(3.10): stress-strain curves for tested specimen before and after LP

5.6.2 Fatigue test (after laser peening)

The fatigue test is a cyclic bending loading procedure. The purpose of the test is to generate S-N data (stress vs. Number of cycles) for each specimen. Rotating bending fatigue machine test of type (SCHENCK PUNN) has been used to test specimens of (2017A-T3) under different stresses after laser treatment**.**

The samples were tested by a fatigue test machine which used to execute all fatigue tests, with constant and variable amplitude, as illustrated in figure (3.11).

The specimen was subjected to an applied load. All tests were done at room temperature and R= -1 .The cycle frequency was 106 Hz, the rotating speed used is (6350 cycle /min).

Fig.(3.11): Fatigue testing machine type SCHENCK PUNN

The applied stress is calculated according to equation:

$$\sigma_{bending} = \frac{135.7+32*P}{\pi*d^3} \qquad (3.2)$$

where: $\sigma_{bending}$ is bending stress (MPa).

135.7 is the force arm distance (mm).

P is the force (N).

d is the minimum diameter of specimen.

3.6.3 Fatigue test procedure

Fatigue analysis are normally based on the results obtained from S-N curve then the first step was established the constant continuous cycling S-N curve.(12) specimens were tested under room temperature control stress unpeened. The second step (12) specimens were tested to find the S-N curve with black paint laser peening (BLP).The third step (12) specimens were tested to find the S-N curve which use water with WLP, in order to do a comparison in life and strength. The fourth step (18) specimens were examined to find the cumulative results under two block loadings without treatment and with BLP, WLP. Figures below (3.12), (3.13),(3.14) and (3.15) show the fatigue specimens under different laser shock treatment.

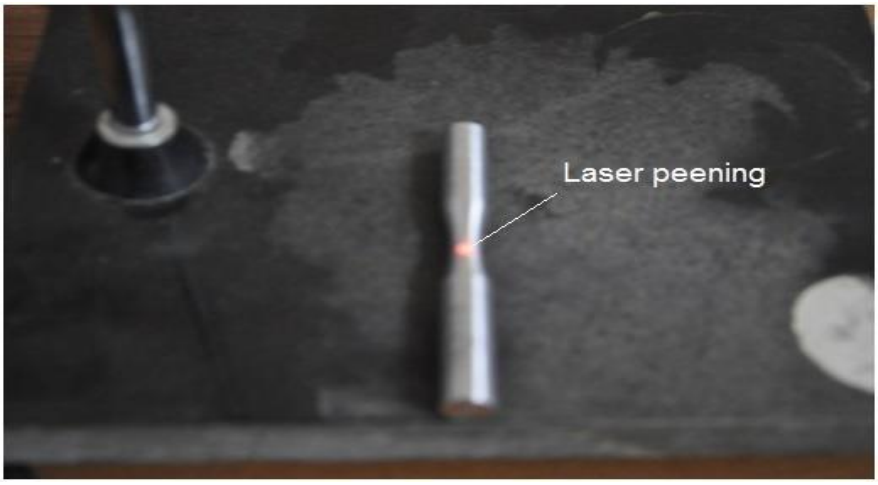

Fig.(3.12): Specimen under air laser spot peening (ALP)

Fig.(3.13): Specimen under black paint laser peening (BLP)

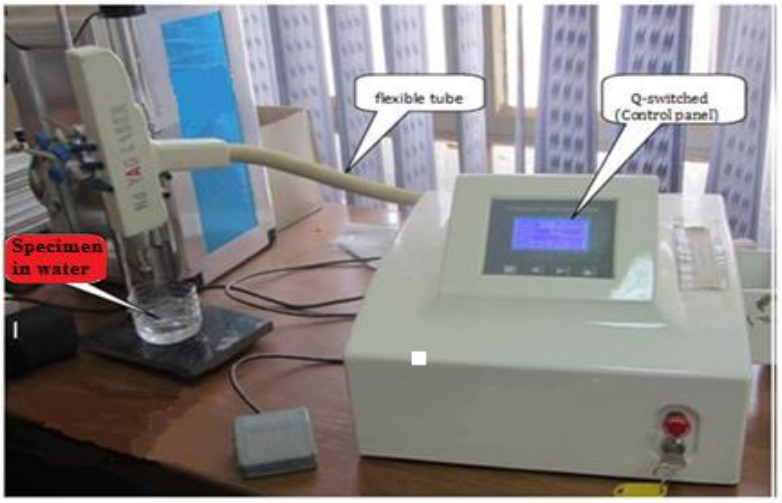

Fig. (3.14): Specimen under water laser peening (WLP)

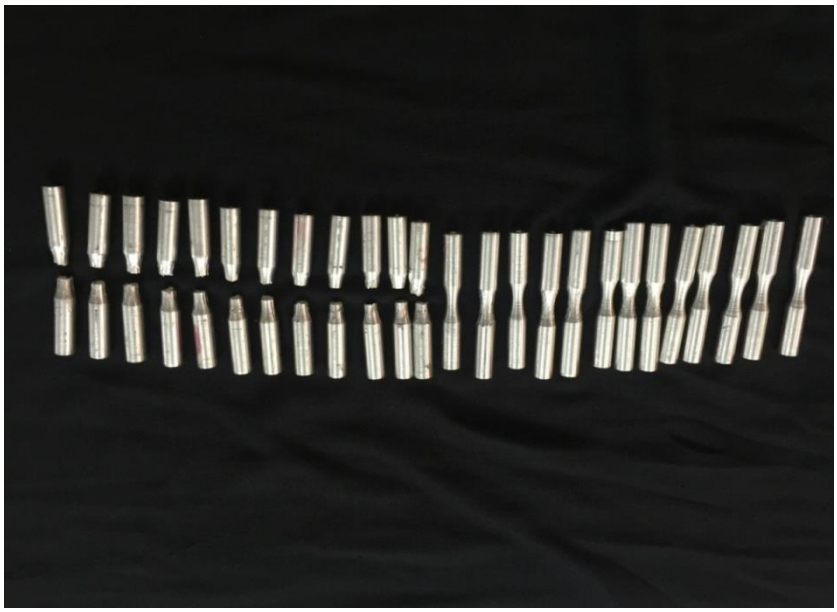

Fig.(3.15): Fatigue specimens before and after fatigue testing

3.7 Ultrasonic peening (UP)

3.7.1 Ultrasonic device

Ultrasonic peening (UP) device introduces the energy of ultrasound into metal through surface impulse contact. This energy is introduced into the metal by converting the resonant / harmonic oscillation of an acoustically tuned body to mechanical impulses on a surface [Hangzhou (2013)]. The main technical parameters of UP device are given below.

Ultrasonic prestressing force treatment machine

Place of Origin: China (Mainland)

Brand Name : HC

Mode Number: HC-S-1

Frequency : 20KHZ Voltage: 220v power: 500w

Usage : metal welding aging treatment

Type : portable

Length of gun: 450mm

System weight: 15kg

Shape of gun : needle

Working mode: impact the surface of weld seam.

Ultrasonic impact equipment specifications

Ultrasonic impact principle is the use of high-power ultrasonic drive impact tools more than twenty thousand times per second frequency impact metal surface, due to the high frequency ultrasound, efficient, and focus on the large energy, make the metal surface produces a larger plastic deformation pressure; Ultrasonic wave has changed the original stress field at the same time, have a certain value of compressive stress; And to strengthen ultrasonic impact areas.

Ultrasonic impact treatment improve the fatigue strength of welded joint and the fatigue life is the basic principle of using ultrasonic drive after welding the frequency of ultrasonic tool more than twenty thousand times per second impact weld toe area along the weld direction, make it produce larger compressive plastic deformation, make the welding toe joints smooth geometry, thereby greatly reducing the welding toe more than high, pits and bite edge caused by stress concentration; Eliminates the tiny crack on the surface of the weld toe area and slag defects, and suppresses the crack initiation in advance; Adjust the welding residual stress field, to eliminate the welding stress, near the weld toe and generate a certain numerical value of residual compressive stress; At the same time to strengthen weld toe part of the material. Therefore, ultrasonic impact can also improve the weld fatigue performance of several aspects influencing factors, such as: weld toe geometry, residual stress, micro cracks and crack in slag and slag defects, surface strengthening, etc., therefore, can greatly

improve the fatigue strength and fatigue life of welded joint [www.hzhccs.com. Device manual (2014)], as shown in figure (3.16).

Fig (3.16): Ultrasonic prestressing force treatment machine

The Ultrasonic Peening device which has been used in the current study to improved the fatigue life of 2017A-T3 AL-alloy can be illustrated in figure (3.17).

Fig.(3.17): ultrasonic peening device type HC-S-1

The tensile tests were done after Ultrasonic treatment for the alloy 2017A-T3 by using tensile test machine WDW-200E that has a maximum capacity 200 KN.

3.7.2 Mechanical properties under ultrasonic peening:

To improve the mechanical properties a number of different treatments processes are being used on specimens of selector alloy, one line peening (1UP) , two lines peening (2UP) and three lines peening (3UP) as shown in figure (3.18).

Fig.(3.18); A number of post treatment operation on tensile specimens under UP

The tensile stress-strain curves of one ultrasonic peening and as received alloy can be seen in figure (3.19), and all conditions in figure (3.20).

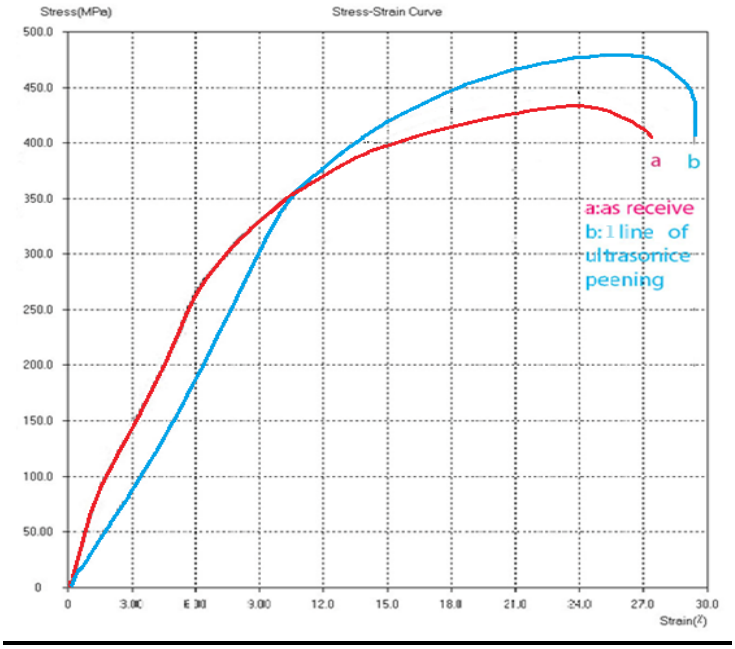

Fig.(3.19): Stress -Strain curves for as received and 1UP

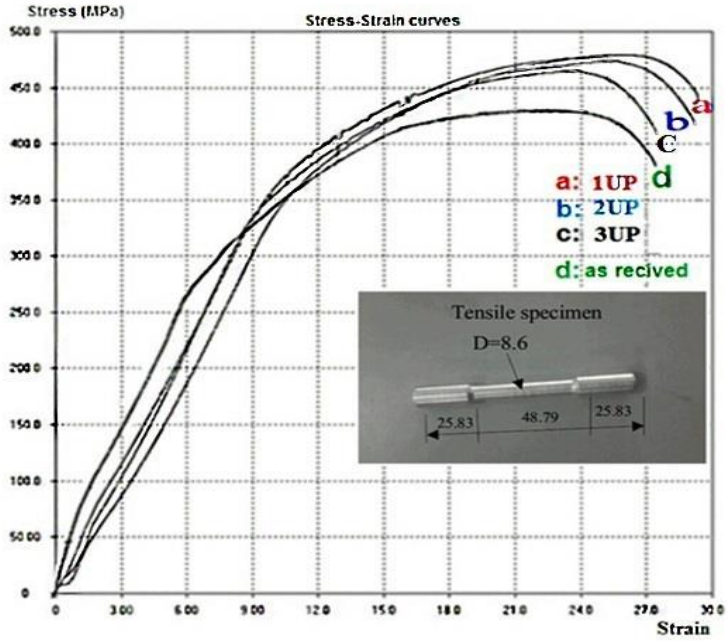

Fig.(3.20); All conditions of UP stress-strain curves compared with as received

3.7.3 Fatigue test (after ultrasonic peening)

Rotating bending fatigue machine test of type (SCHENCK PUNN) has been used to test specimens of metal genuine (2017A-T3) under different stresses after ultrasonic peening.

Fatigue analysis are normally based on the results obtained from S-N curve then the first step was established the constant continuous cycling S-N curve.(12) specimens were tested with one line ultrasonic peening (1UP).. The second step (12) specimens were tested to find the S-N curve with Two line ultrasonic peening (2UP).The third step (12) specimens were tested to find the S-N curve with three line ultrasonic peening (3UP), in order to do a comparison in life and strength. The fourth step (18) specimens were examined to find the cumulative results under two block loadings without treatment and with 1UP.

Figures below (3.21), and (3.22), show the fatigue specimens under different ultrasonic treatment.

Fig.(3.21):Specimen of 2017A-T3 under UP work

Fig.(3.22):Three specimens after 1UP.2UP and 3UP

3.8 Cumulative fatigue loading program

In this study two fatigue loading programs were used. The first program was the constant amplitude fatigue test, while the second one was the variable amplitude fatigue Test. The both program was carried out with and without treatments. As shown in figure (3.23), (3.24). Both of the programs were using stress ratio R= -1.

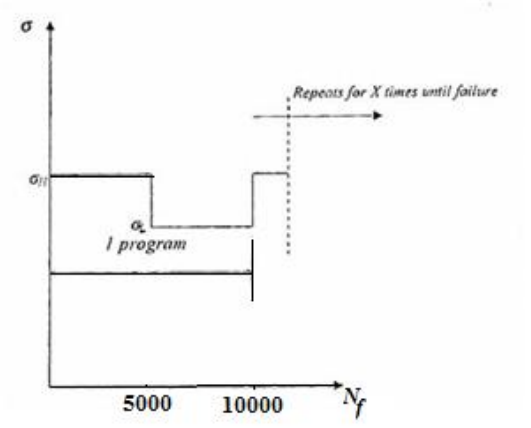

Fig.(3.23): Variable amplitude fatigue test (H-L) program

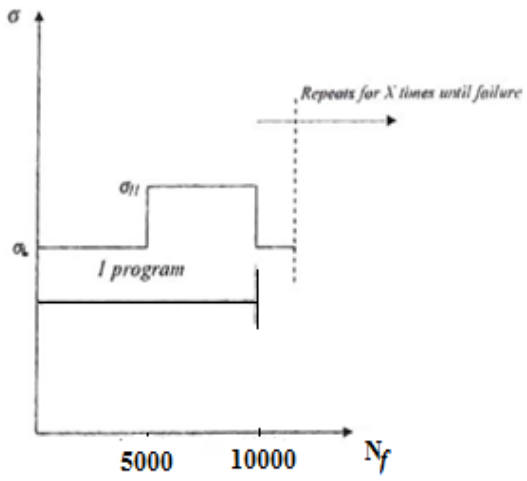

Fig.(3.24): Variable amplitude fatigue test (L-H) program

Chapter 4
Experimental Results analysis and Discussion

4.1 Introduction

This chapter includes the analysis and discussion of the experimental and theoretical results for the fatigue behavior of 2017A-T3 AL-alloy with the effect of laser peening and ultrasonic peening, and study the surface treatment on other properties of this alloy. Also, the empirical relationships which are derived to describe the experimental results were obtained.

1. Tensile tests to obtain the mechanical properties before and after laser peening and ultrasonic peening.
2. Constant amplitude tests to determine the S-N curves behavior in the above conditions.
3. Cumulative fatigue damage tests, Low-High and High-Low, were continued until failure for unpeened and peened specimens in order to know the effect of different peening on fatigue damage and life.

4.2 Laser peening

Laser peening test has been done according to the program outline in chapter five, and the results are presented below.

4.2.1 Tensile test with laser peening

The tensile test specimen prepared according to the American Society for Testing and Materials (ASTM-B211), have been installed in tensile test machine WDW-200E at **(**University of Technology Baghdad**)**, as display in chapter (3).

Figure (4.1) shows the behavior of stress-strain diagram for tested specimens. The first is untreated as received; the second is treated as air laser peening (ALP), Black paint leaser peening (BLP) and Water leaser peening (WLP). These figures present the average reading of three specimens.

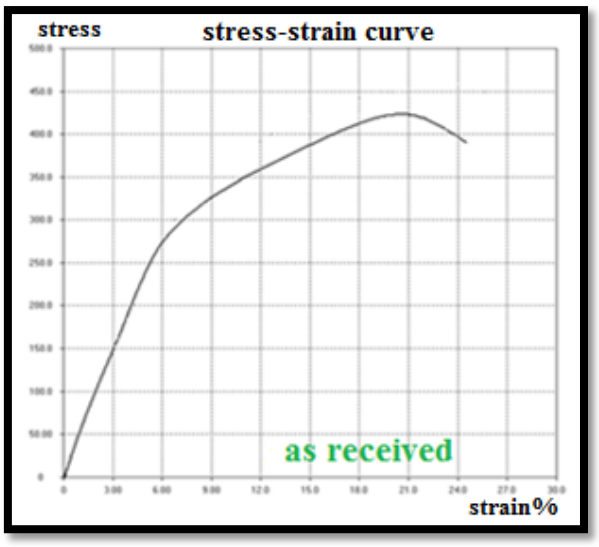

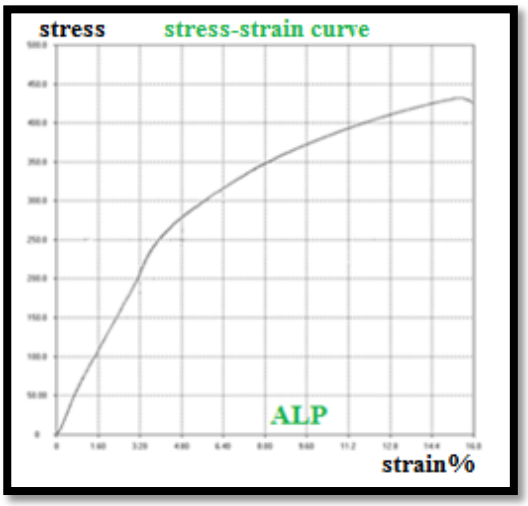

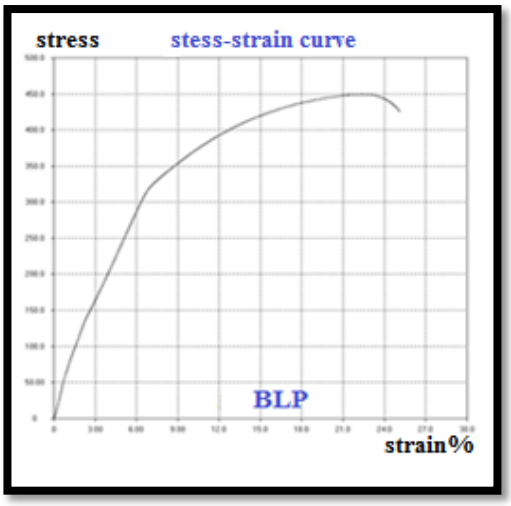

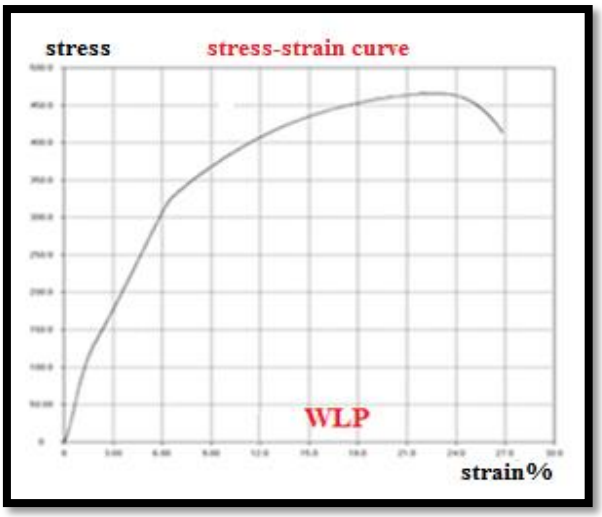

Fig.(4.1):stress-strain diagram for tested specimens before and after LP

The tensile test specimen as described above has been done for cases under laser pulse energy 310 mJ, the pulse duration is 16 nano second and the wavelength is about 1.065 μ m. The results are tabulated in table (4.1) and presented in one figure as illustrated in figure (4.2).

Table (4.1):Mechanical properties of 2017A-T3 AL-alloy in three conditions of LP

Condition	σu (MPa)	σy (MPa)	E (GPa)	RA%	∈%
As received	435	270	72	26.42	22
ALP	435	250	72	25.76	20
BLP	450	323	73	26.74	18
WLP	472	325	75	27.68	17

Where: RA% is reduction area percentage.

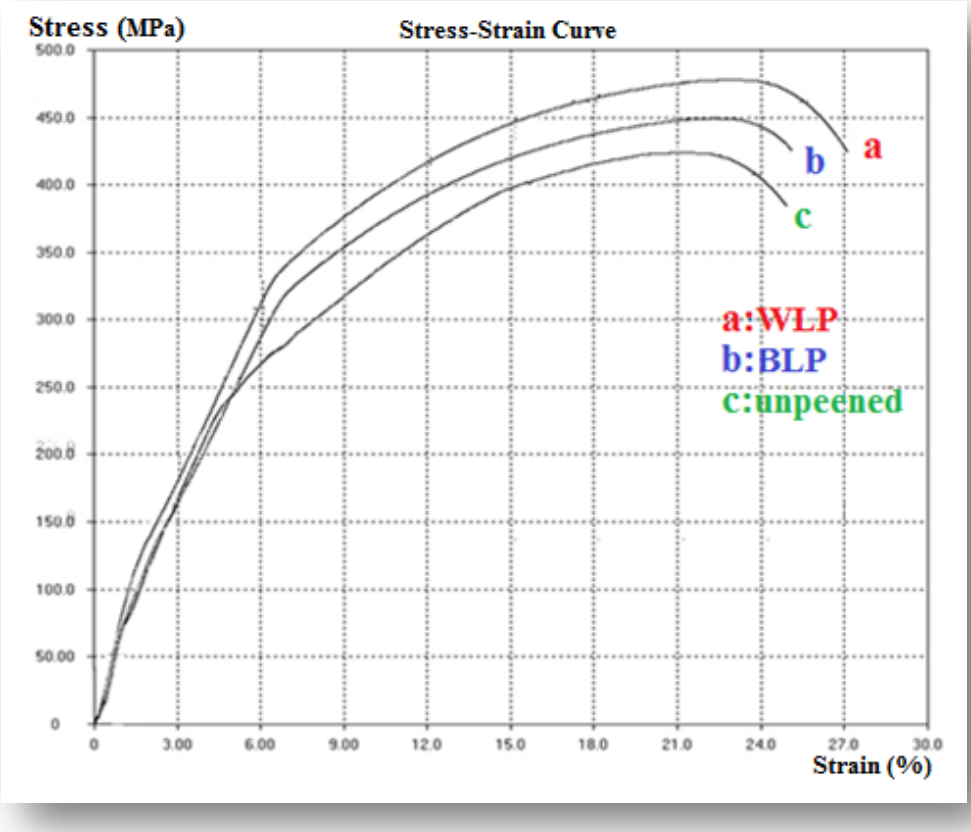

Fig.(4.2): Stress-strain diagram for tensile tested specimens with LP

Laser peening (LP) has been shown to be significant effect for improving the mechanical and fatigue characteristics particularly those that show positive response to shot peening like 7075, 2014 and 2017 Al-alloys. For ALP and WLP the specimens are completely immersed in Air or Water.

When the laser beam is directed to treated surface, it passes through the transparent overlay and strikes the specimen. Immediately vaporizes a very thin surface layer of the overlay. This process causes high pressure generating a shock wave propagating into the material. The shock waves cause plastic deformation produce compressive stresses. The principle of laser shock can be seen in figure (4.3) [Rubio (2011)]

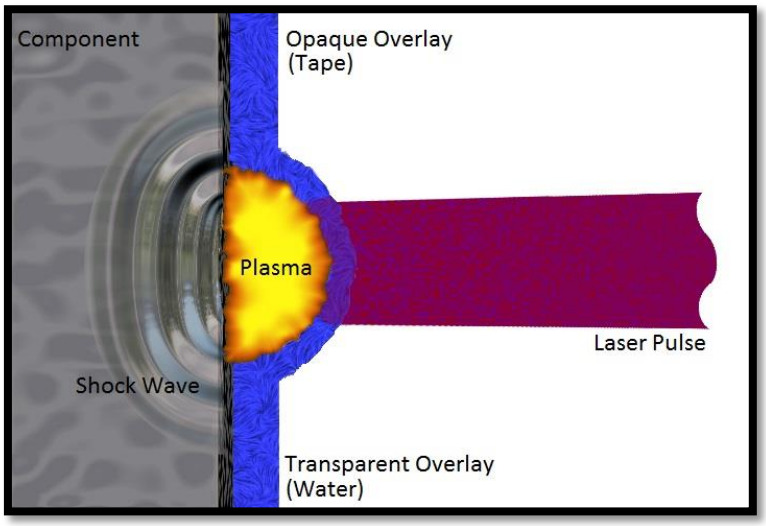

Fig.(4.3):laser shock peening principles

This figure shows the plasma gas is confine on the surface of the black layer limiting the thermal expansion of the gas. As a result the gas pressure increases to extremely high value. The high pressure has been transmitted to the specimen material producing a shock wave which travels through the part material and generates compression stress due to the surface material resists to stretching created by the stress waves resulting in a formation of a compression stressed skin. The effect of laser peening is cold work (not heating nor melting).The above explanation is obed to the current work [Dimitri (2015)]. The purpose of water is to confine the high pressure plasma gas (not cooling the surface), which can be explained the effect of water as a layer on the specimen surface not to cool the part but to increase the pressure developed by the plasma on the surface. This description is consistent with what presented by [Richard (2003)].

It is clear when using the water with the laser for 7075-T7351 aluminum alloy, an improvement in mechanical and fatigue properties were occurred.

4.2.2 Mechanical properties after laser peening (LP)

The mechanical properties of 2017A-T3 specimens which exposed to the laser peening lead to increase in σ_u and σ_y as follows in table (4.2):

Table (4.2) :Mechanical properties result under different LP

σ_u	σ_y	Percentage Increase (σ_u)	Percentage Increase (σ_y)	Condition
435	**270**	**-**	**-**	**As received**
435	**250**	**0%**	**-7.4%**	**ALP**
450	**323**	**3.4 %**	**19.6%**	**BLP**
472	**325**	**8.5%**	**20.4%**	**WLP**

Table (4.2) and figure (4.7) are shown the behavior of stress-strain diagram for tensile tested specimens with and without laser peening.

The water laser peening (WLP) treatment resulting in an increase in σ_u (tensile strength) value by 8.5% and 20.4% for yield strength (σ_y) as compared to the as received specimens. This improvement in σ_u and σ_y is due to compressive residual stress induced at the surface as a result of water laser peening when using the water with the laser.

The schematic diagram was shown in figure (4.4) which are introduce a deep residual compressive stress region on metallic targets. More precisely, LSP uses high energy laser pulses to impact the surface of a metal coated with a protective film (organic paint, tape or thin metallic film), and covered with a transparent layer (usually water). As the laser beam passes through the transparent layer and hits the surface of the material, a thin layer of the ablative layer is vaporized.

The vapor continues to absorb the remaining laser energy and is heated and ionized into high pressure plasma. Due to the confining effect of the transparent layer, the plasma pressure is amplified (up to several GPa), and the resulting pressure discontinuity propagates into the material as a shock wave. This plasma confined regime, allows obtaining maximum impact pressures of up to 5– 6 GPa in the 8–10 GW/cm^2 intensity regime for 10–20 ns pulse duration.

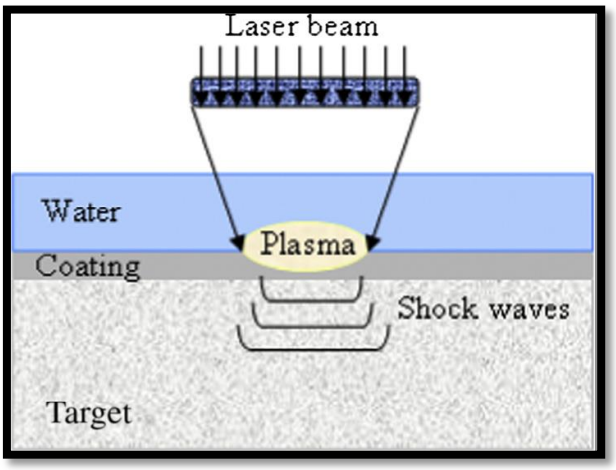

Fig. (4.4): Laser peening process

4.2.3 S-N curves experimental results

All fatigue specimens were tested under constant and variable loading, using the fatigue test machine of type PUNN rotary as shown in chapter (3), figure (3.11). The fatigue behavior at constant amplitude testing for three different surface treatments peened with laser. The empirical power law S-N equations with constants, and correlation coefficient (R^2) are illustrated in table (4.3) and figure (4.5). The average of three specimens at failure is calculated using the equation (4.1).

$$N_{f\,average} = \frac{N_{f1} + N_{f2} + N_{f3} + \cdots}{\text{No. of specimens tested}} \qquad (4.1)$$

Table (4.3 A,B& C): Constant fatigue results for three conditions of treatment

(Table A)

Without peening					
Specimens No,	**Applied Stress (MPa)**	**N_f Cycles**	**N_f Average**	**Basquin equation**	**R^2**
1,2,3	350	4000,5800 6200	5200	$\sigma_f = 1953\ N_f^{-0.2008}$	**0.97**
4,5,6	275	11000 ,22000 16000	16300		
7,8,9	200	89600,113500 102000	101700		
10,11,12	150	333000,287000 344000	321500		

(Table B)

BPLP					
Specimens No,	**Applied Stress (MPa)**	**N_f Cycles**	**N_f Average**	**Basquin equation**	**R^2**
13,14,15	350	6600, 5400 3900	5300	$\sigma_f = 1544\ N_f^{-0.1747}$	**0.96**
16,17,18	275	13000. 18000 20000	17000		
19,20,21	200	113000, 147000 126000	128600		
22,23,24	150	602000, 564000 710000	625300		

Table (C)

WLP					
Specimens No.	**Applied Stress (MPa)**	**N_f Cycles**	**N_f Average**	**Basquin equation**	**R^2**
25,26,27	350	6000, 4000 7000	5600	$\sigma_f = 1370\ N_f^{-0.1588}$	**0.94**
28,29,30	275	23000, 21000 26000	23300		
31,32,33	200	174000, 202000 188000	188000		
34,35,36	150	1080000 1200000 11120000	1133000		

R^2 means the correlation coefficient which indicated that the experimental data are well explained by power law formula. The correlation coefficient **R^2** mentioned in the above table gives relatively high description of the experimental data using Basquin equation. **R^2** is a hand measure of the goodness of fit [Mustafa (2014)].

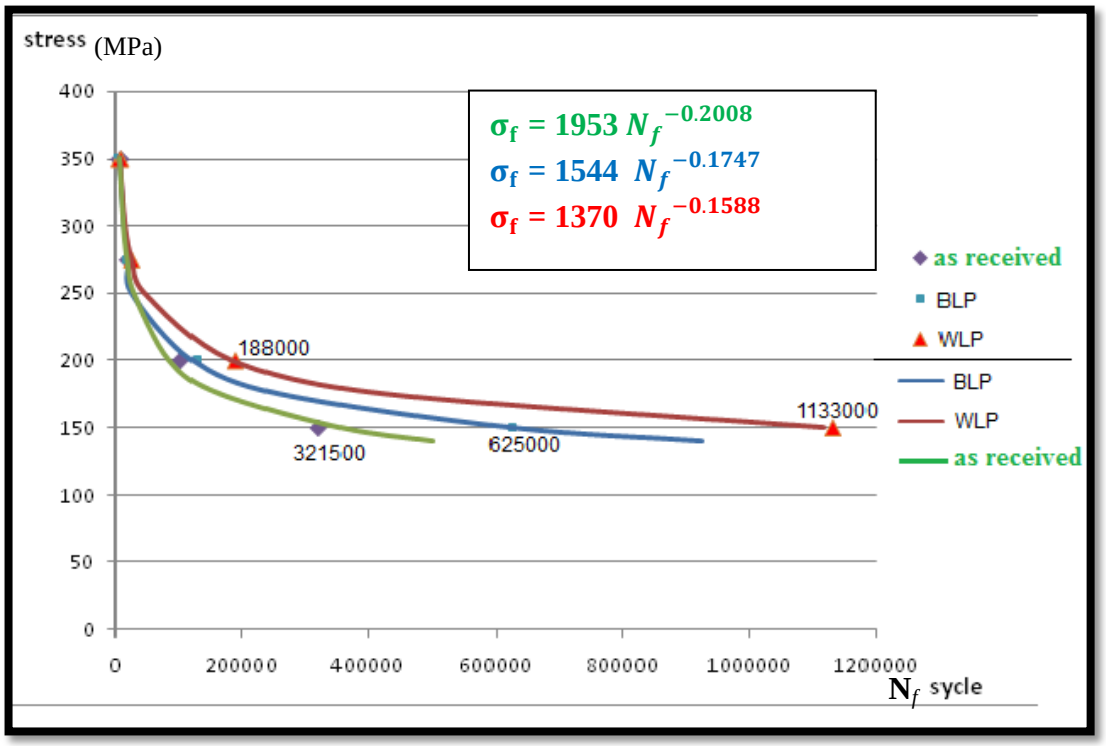

Fig. (4.5): Typical S-N curve of fatigue life without treatment and with(BPL, WL)

From above LP used to improve the mechanical and fatigue properties and improve the fatigue behavior which depends strongly on the generated surface profile and plastic deformation in the surface layers, [Luo (2015)] and **[Ren** (2010)], clarify that if the shock wave propagates into the metal target, the compressive residual stress will be generated near the target surface due to the plastic deformation. A water tamped layer with a thickness of about 2mm used as the plasma confinement layer. **[Sakion** (2009)], explain that there is many parameters effect of LP such as (material, time of pulses, area treatment, and means assist).In this study all parameters fixed except means assist (air, black paint, and water). Table (4.3) and figure (4.5) show three different laser shock processing were performed on fatigue specimens and their fatigue life were compared. LP with water coating can significantly improve surface compressive stress, and then improve the behavior of 2017A-T3 alloy, the reason is that water generates high pressure plasma, and the strength of material surface is improved due to the shock force by the plasma.

WLP samples displayed approximately 43% increase in fatigue life at load 275 MPa, and 85% at load 200 MPa.

LP with water covered was enhanced fatigue life more than others due to confining high pressure plasma gas to strike the surface [Rubio (2011)].

4.2.4 Endurance limits:

LP was used to improve the mechanical and fatigue properties of materials. [Mayer (2005), concluded that the LP is a good tool for improvement the endurance limit and they found that the laser peening was significantly improved the fatigue strength. For the present work, the S-N curves were done and the fatigue endurance limit for each case was calculated at 10^7 cycles. The results are given in table below with the improvement percentage with respect to as received case. The results showed that the existence of LP can improve the mechanical properties and fatigue life up to a limit value of LP [Y. TAN1 (2003)]. This limit depends on the material used and laser–peening process as shown in table (4.4).

Table (4.4): Improvement of Endurance limit

condition	σ_f at 10^7 cycles	Improve percentage
$\sigma f = 1953\ Nf^{-0.2008}$ Unpeened	77	---
$\sigma f = 1544\ Nf^{-0.1747}$ BLP	92.5	20%
$\sigma f = 1370\ Nf^{-0.1588}$ WLP	106	38%

Enforcement of laser peening keep away over $59 million in black replacement coasts, damage engine repair coasts, and cost avoidance from airfoil failures [Richard (2003)]. Figure (4.6) shows how the fatigue endurance limit and life of 7075-T351 Al-alloy specimens used in blades of fan of F101-GE aircraft subjected to laser peening and shot peening. The data illustrate the significant improvement of laser treated parts involving 30-50 percentage increase in fatigue strength and an increase in fatigue life of about an order of significance [Peyre (1995)].

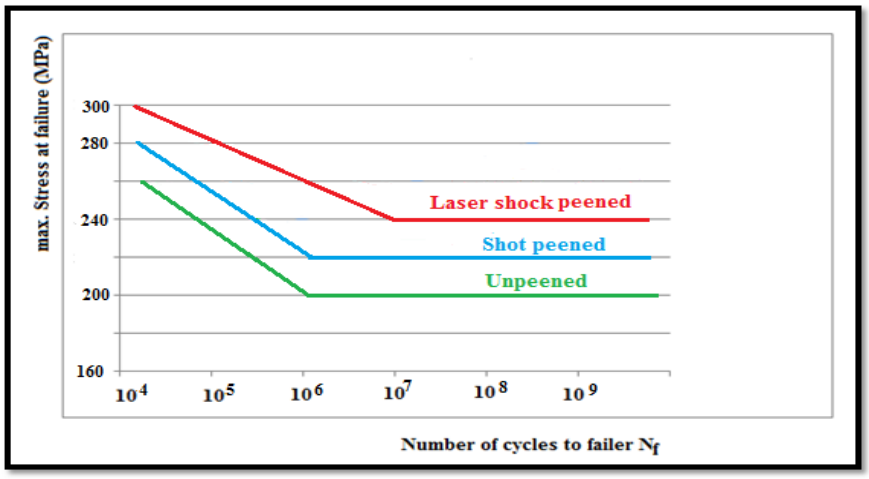

Fig.(4.6): Comparison of LP & SP fatigue strength and life of 7075-T351

4.2.5 Cumulative fatigue test results

Table (4.5) and figure (4.7) give the experimental results obtained from testing specimens at low to high and high to low loading sequences for three different laser coating interaction conditions.

Table (4.5) Cumulative fatigue results for 2017A-T3

Specimens No.	Applied stress Sequences (MPa)	N_f cycles	N_f av. cycles
		(unpeened)	
37,38,39	200-300 (L-H)	17600,22000,21000	20200
40,41,42	300-200 (H-L)	20700,15020,17680	17800
		(BLP)	
43,44,45	200-300 (L-H)	23700, 27000, 24300	25000
46,47,48	300-200 (H-L)	18000,21500,20500	20000
		(WLP)	
49,50, 51	200-300 (L-H)	25300, 29300,30000	28200
52, 53, 54	300-200 (H-L)	19800, 22000,21500	21100

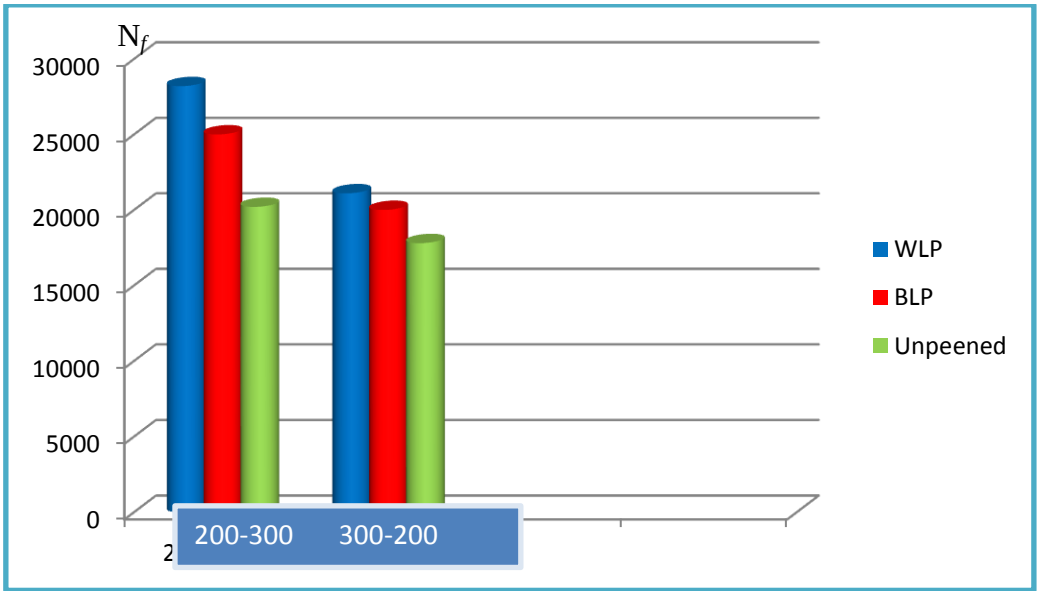

Fig.(4.7): Cumulative fatigue results for 2017A-T3

It is clear, as illustrated in the above table that an increase in fatigue life when using water as a layer coated for the specimen surface. For low-high testing the fatigue life improved by 1.396 times and 1.185 times for high-low tests. While for BLP the fatigue life were improved by 1.237 times for low-high tests and 1.123 times for high-low tests. [Ren, (2010)]. Identify the effect of laser shock peening (LSP) on the

fatigue crack initiation and propagation of 7050-T7451 aluminum alloy. The laser shocked specimen in which residual compressive stress is mechanically produced into the surface showed a very high dislocation density within the grains. The high dislocation density leads to retard the cracks initiation and propagation resulting in an increase in fatigue life.

The sum of the cycle ratio damage in low-high cumulative damage tests was always greater than for high-low tests. This leads to grater fatigue lives for low-high loading compared to high-low loading [Fatemi (2006)].

4.2.6 Application of the proposed model

The proposed model explained in chapter (4), now it can be applied to the cumulative fatigue damage results.

Low- high

$$D = \left[\frac{n_1}{N_{f_1}} + \frac{n_2}{N_{f_2}}\right]^{\frac{-\sigma_L \alpha}{\sigma_H}} \qquad (4.2)$$

And

High- low

$$D = \left[\frac{n_1}{N_{f_1}} + \frac{n_2}{N_{f_2}}\right]^{\frac{-\sigma_H \alpha}{\sigma_L}} \qquad (4.3)$$

Where: ***n*** *is the applied number of cycles.*

For the present work: ***n = 5000*** *cycles*

For the present experimental results given in table (6.5), the damage calculated from the proposed model can be presented in table (4.6) in comparison with Miner rule.

Table (4.6): damage values obtained from the present model in comparison with Miner rule

Applied loading sequences (MPa)	$N_f$aver cycles	Damage (present model)	R No. of program	Condition	D (Miner)
200-300 300-200	20200 17800	0.9121 0.8129	1.8136 1.6164	unpeend	1
200-300 300-200	25000 20000	0.9145 0.8178	1.970 1.7613	BPL	1
200-300 300-200	28200 21100	0.9022 0.7933	2.3848 2.0970	WLP	1

The predicated fatigue life under different conditions of laser surface treatments compared to the Miner theory lives can be illustrated in table (4.7).

Table (4.7):comparison of life predictions based on the experimental life

Condition	N_f**exp.**	N_f**Miner**	N_f**model**	Loading sequences
Unpeend	20200 17800	18924 18924	18136 16164	200-300 300-200
BLP	25000 20000	22222 22222	19700 17613	200-300 300-200
WLP	28200 21100	24138 24138	23848 20970	200-300 300-200

It can be seen from table (4.7) that the Miner rule gives non- conservation predictions for some specimens because the rule assumes that damage accumulation in a linear fashion at all stress levels, while in reality damage accumulates in a complex manner [Zainab (2014)] . Furthermore the Miner method doesn't taking into account the effect of surface treatments. The present model gives good correlation with the experimental lifetimes see table (4.7) which shows that a much better and conservative prediction of lifetime was obtained if the present model is available.

Many workers tried to improve the linear damage rule, but due to its shortcomings, the life predictions based on Miner rule is often unsatisfactory [Fatemi (1998)]. The comparisons of fatigue lives under different laser-coated interaction with proposed model have shown good agreement with the actual lives while Miner rule did not give safe lives for some specimens [Aid (2005)].

4.3 Ultrasonic peening (UP)

4.3.1 Mechanical properties under ultrasonic peening:

To improve the mechanical properties a number of post treatment operation are being used one line peening (1UP) , two lines peening (2UP) and three lines peening (3UP) by ultrasonic peening device type HC-S- as shown in chapter (3), figure(3.17).

The average three reading measured ultimate and yield strength for the four conditions above are summarized in table (4.8) and also the table comprises the results before and after tensile test of the specimens which treated with and without ultrasonic peening.

Table (4.8): Tensile test results for three categories of ultrasonic peening

Condition	One line 1UP		Two line 2UP		Three line 3UP		**unpeend**
		Increase%		Increase%		Increase%	
σ_u (MPa)	480	10.3%	476	9.4%	466	6.6%	435
σ_y (MPa)	353	30.7%	350	29.6%	343	27%	270
E (Gpa)	72		72		71		70

Where: E (GPa) is Young's modulus

It is well known that the hardening of this alloy grows from Al_2Cu and Al_2CuMg sedimentation, as long as that the particles are finely and densely distributed [May (2013)].

The tensile stress-strain curves of the four conditions are given in figure (4.8).

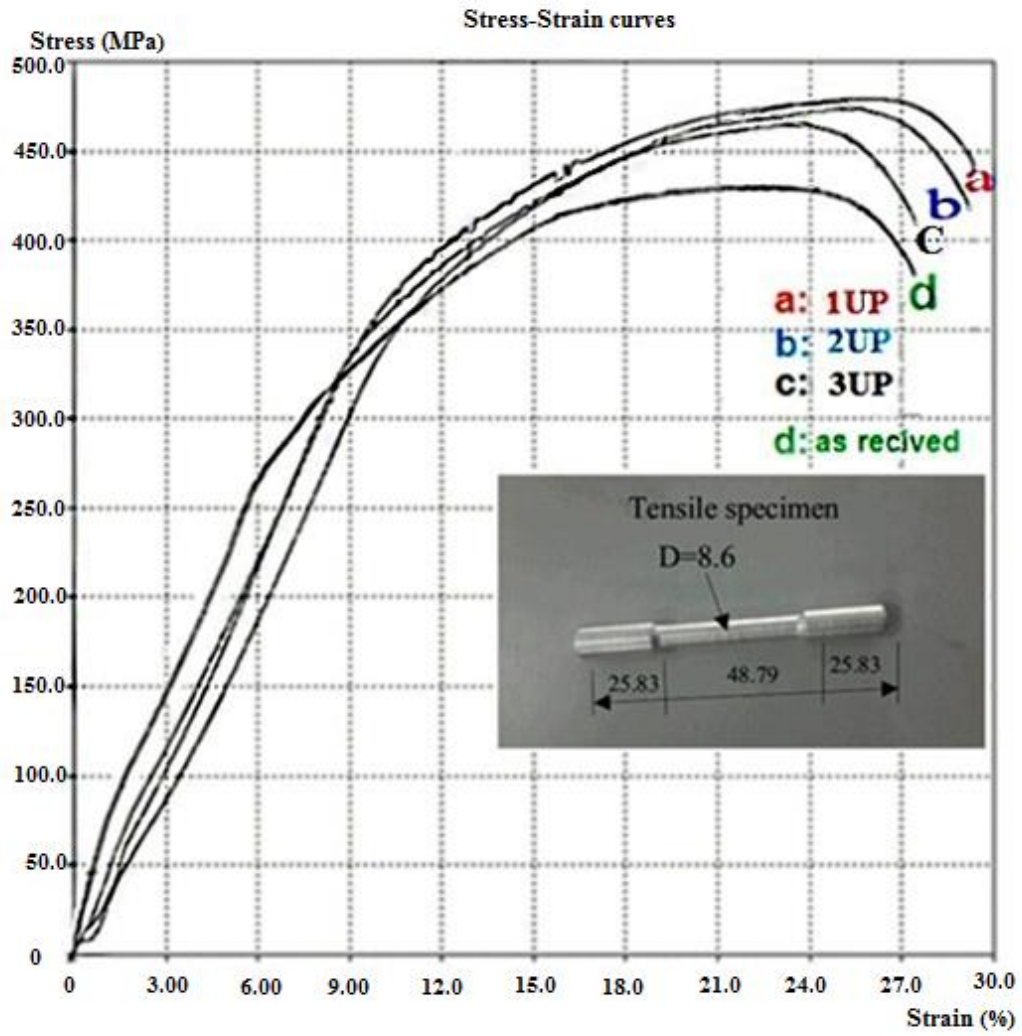

Fig.(4.8): The tensile stress-strain curves of the four conditions

As can be seen in figure (4.8) the lowest values of $\boldsymbol{\sigma_u}$ and $\boldsymbol{\sigma_y}$ are obtained for the as-received 2017A-T3.The maximum improvement for $\boldsymbol{\sigma_u}$ is found to be 10.3% and 30.7% $\boldsymbol{\sigma_y}$ increase for 1UP. The comparison reveals that the ultimate and the yield strengths are always higher under UP (ultrasonic peening) than under as-received condition. More specifically, the ultimate strength shown in the standard is (435) MPa. By comparison under 1UP, 2UP and 3UP, the ultimate strength values obtained in this research are 480,476 and 466 MPa respectively, indicating a 10.3%, 9.4% and 6.6% increase in ultimate strength.

The experimental results clearly indicate that percentage increase of ultimate strength reduce gradually as the number of peening line increases as plotted in figure (4.9)**.**

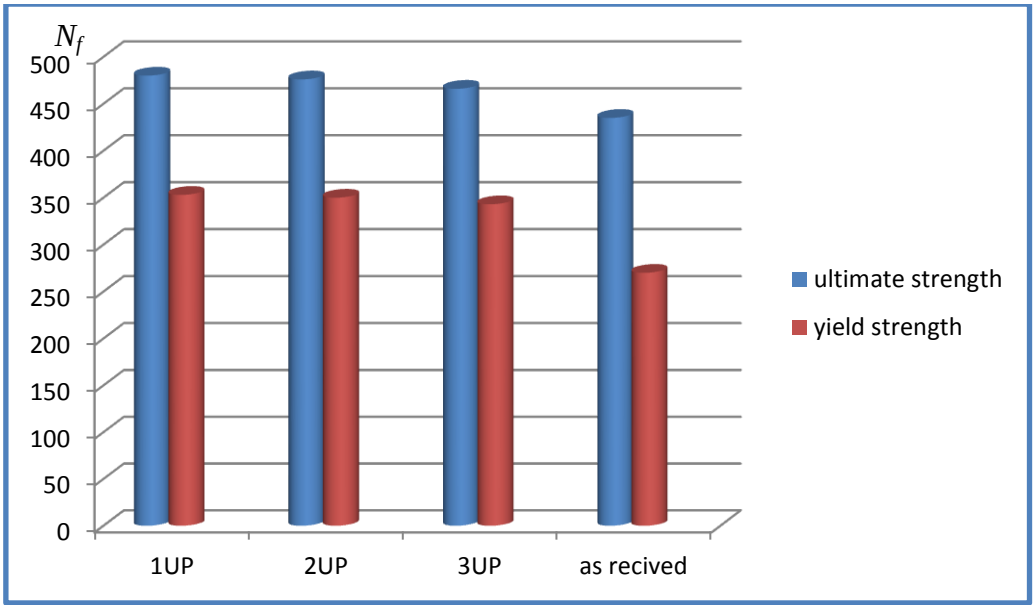

Fig.(4.9): conditions of UP stress-strain curves compared with as received data

6.3.2 The S-N curves

48 tests ranging from $\sigma_f = 350$ MPa to $\sigma_f = 175$ MPa provided the data for the basic S-N curves are given in table (4.9), and plotted in figure (4.10).

Table(4.9) S-N curves for four condition of ultrasonic peening

σ_f (MPa)	as received		1UP		2UP		3UP	
	N_f cycles	Avr. cycles	N_f cycles	Avr. cycles	N_f cycles	Avr. cycles	N_f cycles	Avr. cycles
350	5000, 4000 6600	5200	5600, 6000 5500	5700	4800, 5700, 5100	5200	4200, 5200 5600	5000
275	15000, 17000 16900	16300	38000, 47000 50000	45000	16000, 12000 17000	15000	10600, 14800 13600	13000
200	110000, 100000 95100	101700	226000 289000 340000	285000	240000, 226000 236000	234000	17000, 154000 162000	162000
175	172000, 155000 167800	164900	50500 530000 525000	520000	444000, 562000 447000	484300	38100, 345000 390000	372000

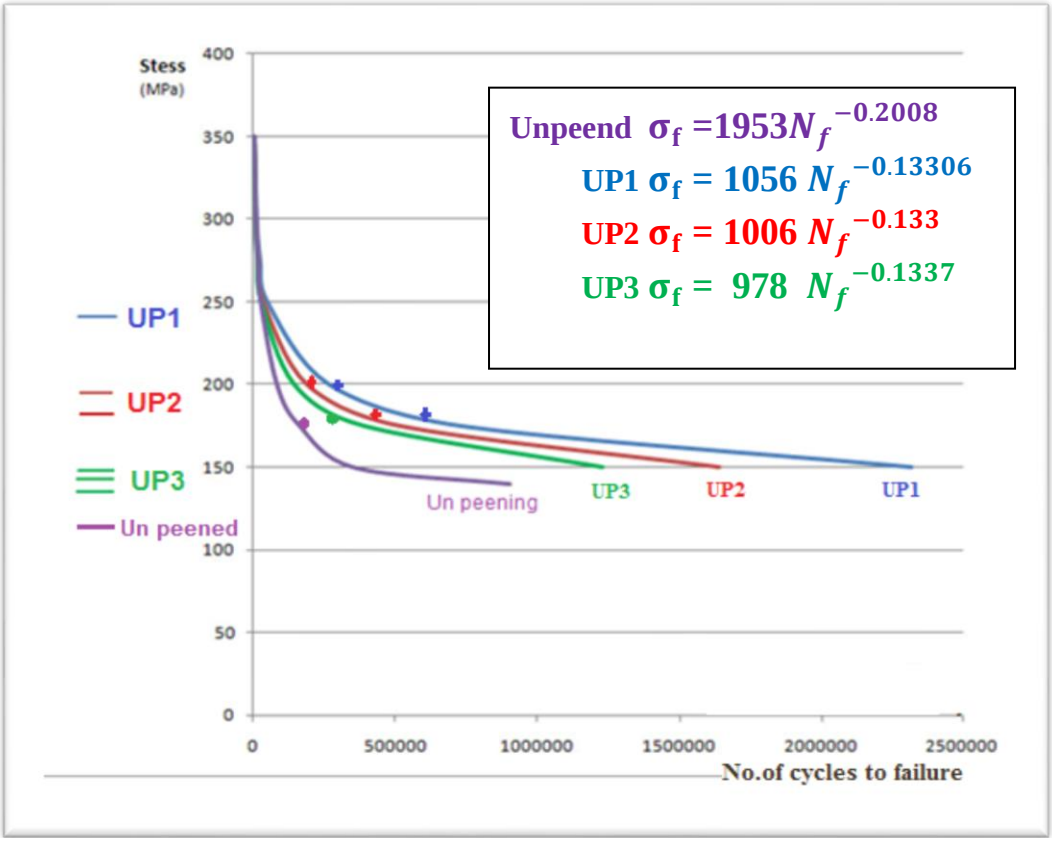

Fig.(4.10): four cases of fatigue test result with and without UP

Different methods have been used in order to improve the fatigue life and strength include optimization of geometric design, and surface treatments such as laser peening, shot peening and ultrasonic peening. Ultrasonic peening (UP) has long been widely employed as a low cost and simple method for raising the fatigue properties [Aggarwal (2005)]. Effect of UP on fatigue design for a rod aluminum alloy of 2017A-T3 is given in table (6.10).

Table (4.10) UP treatment effect on fatigue design

condition	S-N curve equation	Endurance fatigue limit at 10^7 (MPa) cycle	Increase In End. fatigue limit	Fatigue life predictions		
				Exp. σ_u 455 (MPa)	Exp. σ_y 270 (MPa)	σ_{EL} 77 (MPa)
As received	$\sigma_f = 1953\ N_f^{-0.2008}$	77	------	1415	19033	10^7
1UP	$\sigma_f = 1056\ N_f^{-0.13306}$	124	61%	560	28257	351,444,334
2UP	$\sigma_f = 1006\ N_f^{-0.133}$	118	53%	390	19724	245,976,913
3UP	$\sigma_f = 978\ N_f^{-0.1337}$	113	47%	306	15156	180,169,038

All increase in UP lines resulted in an increase in fatigue strength. The fatigue limit stress was 77 MPa as received and became 124 MPa at 1UP 61% increase compared to the dry fatigue. This increase generates high compressive residual stress filed, but an increase in the UP lines does not necessarily increase the strength and fatigue life of aluminum alloy used. The best fatigue life prediction was occurred at 1UP and it was observed that in all cases of UP, the strength and fatigue life are greater than that of unpeened fatigue. Also it was observed that at low cycle fatigue the fatigue life prediction is always less than that of as-received fatigue condition because the dominant factor which controls the crack initiation and propagation is the stress applied which is very high compared to high fatigue region. The present alloy usually used in low temperature environment. This environment improved the high cycle fatigue life as mentioned in Ref [Duaa (2016)].

4.3.3 Cumulative fatigue damage

In order to investigate cumulative damage in fatigue, a multi-level fatigue programmed has been carried out on 2017A-T3. All the tests have been performed under controlled amplitude conditions, with several changes of levels up to rupture;

4.3.4 Proposed model

Prediction of fatigue loading in random condition required precise calculation and needs the equation of S-N curve with and without ultrasonic testing.

For low - high stress level tests:

$$\mathbf{D} = \left[\frac{n_1}{N_{f1}} + \frac{n_2}{N_{f2}}\right]^{\left(\frac{Ault\ \sigma_L}{Adry\ \sigma_h}\right)^{\frac{\propto ult}{\propto dry}}} \qquad (4.4)$$

And for high-low stress level tests:

$$\mathbf{D} = \left[\frac{n_1}{N_{f1}} + \frac{n_2}{N_{f2}}\right]^{\left(\frac{Ault\ \sigma_h}{Adry\ \sigma_l}\right)^{\frac{\propto ult}{\propto dry}}} \qquad (4.5)$$

More details of the derivation of the above model can be seen in Appendix (A).

4.3.5 Application of proposed model to 1UP ultrasonic cumulative Testing

The cumulative damage tests were done for 1UP case because this condition revealed best improvement in strength and fatigue life. The experimental results of this type of ultrasonic are given in table (4.11).

Table (4.11): Experimental cumulative fatigue life under one line ultrasonic peening

Specimens No.	Loading Sequence (MPa)	$N_{fcycles}$	$N_{fav.}$	Loading programe
67,68,69	325-175	17900,19800 16900	18200	325 5000 175 5000
70,71,72	175-325	23000,22800 24700	23500	325 175 5000 5000
73,74,75	300-200	20200,19400 24000	21200	300 5000 200 5000
76,77,78	200-300	32200,27700 27400	29100	300 200 5000 5000

Now, comparison can be made between the prediction of the proposed model and the experimental results as shown in table (4.12).

Table (4.12): Comparison between the model predication and experimental results

Landing sequences (MPa)	$N_{fav.experimintal}$	$N_{f(model)}$	Repetition Of program (R)	Damage (D)	S.F (safety factor) model
175-325	23500	12048	1.2048	0.8629	1.950
200-300	29100	15549	1.5549	0.63307	1.871
325-175	18200	9990	0.99909	0.71563	1.821
300-200	21200	11234	1.1234	0.45739	1.887

It is clear that, the ultrasonic treatment of 2017A-T3 aluminum alloy specimens improved the cumulative fatigue life in both cases for low-high and high-low fatigue tests. The factor of safety is observed, table (4.12) more than unity and this indication gives increase in life and strength of the alloy used. [Mordyuk (2013)] tested Al-6Mg alloy specimens using ultrasonic impact peening and they found that the fatigue lives are improved in both regions, low cycle and high cycle fatigue and the causes of improvement are coming from combination of microhardness and compressive residual stresses in the surface layer. [Thibaut (2012)], uses ultrasonic peening technique as the final surface treatment to introduce surface compressive residual stresses in order to prevent cracks from propagation.

4.4 Comparison between mechanical properties and the fatigue behavior of 2017A-T3 AL-alloy under laser &ultrasonic peening

By survey the work there is no indication to use UP on the surface of aluminum alloy, but it is used in the welding area. While the present study investigates the use of UP to improve the surface of the aluminum alloy 2017A-T3. Previous research did not point to the existence of comparison between LP and UP, but there are comparisons between the SP (shot peening), and LP, Now, the comparison between WLP&1UP is made based on unpeened results for mechanical properties and fatigue behavior of the selected alloy.

4.4.1 Comparison between mechanical properties under WLP & 1UP

The comparison between water leaser peening (WLP) and one line ultrasonic peening (1UP) can be seen in table (4.13). It is clear that the improvement percentage due to 1UP is greater than that of WLP. A difference improvement of 1.84% in σ_u and 10.33% for σ_y as improvement percentages (IP%) are observed. This increase may be due to the amount of compressive residual stress which is larger in 1UP than that of WLP.

Table (4.13): Comparison mechanical properties results under WLP&1UP

condition	As received	WLP	1UP	Improvement%	
				WLP	1UP
σ_u	435	472	480	8.5 %	10.34 %
σ_Y	270	325	353	20.37 %	30.7 %

[Yongxiang (2006)] Compared LP with SP, the compressive residual stresses in the metal material treated by LSP can extend deeper below the surface than those from shot peening. LSP is well suited for precisely controlled treatment of localized fatigue critical areas, such as holes, notches, fillets and welds. It has been proposed as a competitive alternative technology to classical treatments for improving fatigue, corrosion and wears resistance of metals.

The difference improvement of σ_u & σ_y are clear in figure (4.11) below.

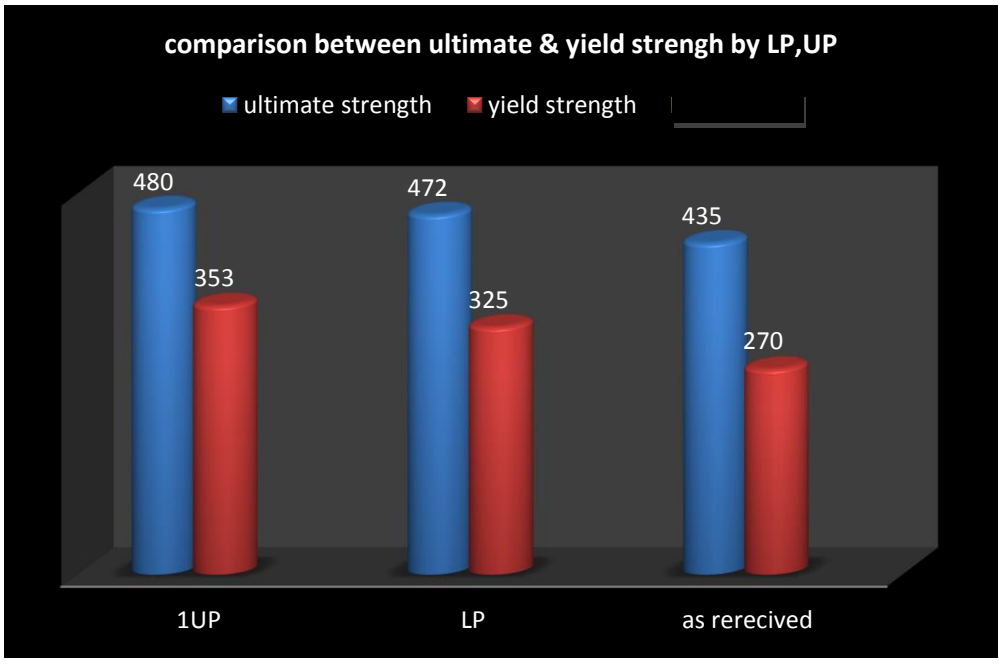

Fig. (4.11): Comparison between σ_u & σ_Y for 2017A-T3 after LP,UP

4.4.2 Comparison between the fatigue behavior of 2017A-T3 AL-alloy under laser &ultrasonic peening

The comparison for fatigue tests of water leaser peening (WLP) and one line of ultrasonic peening (1UP) is made based on unpeened results as given in table (4.14).

Table (4.14):Comparison of constant fatigue results between WLP,1UP with unpeend of 2017A-T3

Applied Stress (MPa)	$N_{fav.}$ As received (Cycles)	$N_{fav.}$ WLP (Cycles)	$N_{fav.}$ 1UP (Cycles)	Improvement%	
				WLP	1UP
350	5200	5600	5700	7.69%	9.61%
275	16300	23300	45000	43%	176%
200	101700	188000	285000	84.85%	180%

Mechanical surface enhancement techniques are used to introduce compressive residual stresses to enhance the fatigue life and corrosion resistance of metallic components. In this study, the effects of two advanced mechanical surface enhancements treatments: laser shock peening and ultrasonic peening modification on residual stress hardness, plastic deformation and changes in near surface microstructure introduced in 2017A-T3. Treatment for this alloy has been done in two ways of each treatment and results compared to achieve a better understanding of underlying mechanisms of these techniques. Results indicate that there are significant differences in mechanisms of these surface treatments.

The fatigue life of 2017A-T3 is enhanced by 7.69%, 43%, and 84.85% for 350, 275, and 200 (MPa) respectively under WLP while the enhancements are 9.61%, 176% and 180% for the same stresses but they are under 1UP. It is indicated that the improvement in fatigue life due to 1UP is much greater than the WLP.

These are high improvement in fatigue life may be coming from the reasons [Kudryavtsev (2010)].

1. The compressive residual stresses generated due 1UP is larger and deeper than that of WLP.

2. The plastic deformation created in 1UP is larger than that of WLP.

4.4.3 Comparison between the cumulative fatigue damage of 2017A-T3 AL-alloy under laser &ultrasonic peening

Table (4.15) give the experimental results obtained from testing specimens at low to high and high to low loading sequences for three different laser coating interaction conditions compare with one line ultrasonic peening (1UP).

Table (4.15):comparison of life predictions based on the experimental life

Loading sequences & Condition	$N_f$exp.	N_fMiner	$N_f$model	Safety factor model
200-300 300-200 Unpeend	20200 17800	18924 18924	18136 16164	1.113 1.101
200-300 300-200 BLP	25000 20000	22222 22222	19700 17613	1.269 1.135
200-300 300-200 WLP	28200 21100	24138 24138	23843 20970	1.182 1.006
200-300 300-200 1UP	29100 21200	24596 24596	15549 11234	1.871 1.887

Comparisons between the cumulative fatigue lives of specimens subjected to unpeened, BLP, WLP and 1UP can now be made using the Miner rule and the proposed models for laser and ultrasonic peening. Miner theory have been shown not to be satisfactory for predicting some of treated specimens due to their inability to take into account the effect of surface treatment and loading sequences. The proposed models give good correlation with the experimental fatigue lifetime. The proposed models gave better and conservative prediction of lifetime due to the following reasons:

1. The proposed models take into account the loading sequences and the surface treatments for calculation the fatigue lifetime, see table (4.15).

2. The present models showed non liner damage behavior while the Miner rule works in liner manner. Experimentally most of materials behave in non-liner fashion [Bruce (2013)].

Due to safe predications of fatigue lives using the proposed models. The factor of safety obtained from the application of the models showed safety factor greater than unity, as given in above table, but the higher safety factor is occurred in 1UP.

The 1UP generates deep compressive residual stresses more than other peening, these compressive residual stress work to raise the mechanical properties in greater manner compared to the other peening. This improvement leads to high fatigue properties due to ultrasonic peening.

Chapter 5
Conclusion and Recommendation

5.1 Conclusions

The experimental results analysis revealed the following conclusions drawn from this work.

5.1.1 Laser peening

1. The mechanical properties $\boldsymbol{\sigma_u}$ and $\boldsymbol{\sigma_y}$ were increased by 8.5% and 20.4% respectively when using WLP.
2. Constant fatigue lifetime was significantly increased about 2.6 and 6.88 times for BPL and WLP respectively.
3. Fatigue strength was improved by 18% and 35% for BLP and WLP respectively.
4. The non linear model showed safe and satisfactory estimations of cumulative fatigue lifetime.
5. Miner rule was not always applicable for life prediction under cumulative loading, because this rule does not tack the loading sequences and surface treatments into consideration.

5.1.2 Ultrasonic peening

Effect of three types of ultrasonic peening one line (1UP), two lines (2UP) and three lines (3UP) surface modification on mechanical and fatigue properties of 2017A-T3 aluminum alloy were investigated and compared. The main remarks arising from this treatment are listed below.

1. All ultrasonic peening showed an increase in mechanical and fatigue properties compared to unpeened results as wrote below.
2. The best type of ultrasonic peening is the one line (1UP) which gave an improvement by 10.3% for σ_u and 30.7% for σ_y .
3. The increase percentage in mechanical properties reduces gradually as the number of peening line increases.
4. The fatigue strength was enhanced under ultrasonic peening i-e an increase of 61% for 1UP, 53% for 2UP and 47% for 3UP.

5. The non- linear proposed cumulative fatigue model correctly follows the experimental results provided in this work. It gave a factor of safety slightly greater than unity for the variable test loading.

6. The proposed model based on load history and S-N curve equations for both cases as-received and ultrasonic peening. This model can satisfactorily for the above conditions.

5. 1.3 General conclusions

1. The treatment for this alloy has been done in two ways of each treatment and results compared to achieve a better understanding of underlying mechanisms of these techniques. Results indicate that there are significant differences in mechanisms of these surface treatments. The fatigue life of 2017A-T3 is enhanced by subjecting to mechanical treatments laser peening and ultrasonic peening to introduce compressive stresses in the surface layers.

The fatigue behavior of all average test groups unpeening, laser peening and ultrasonic peening can be seen that the best fatigue characteristic was achieved with ultrasonic peening as shown above.

2. Two separate cumulative fatigue models were proposed one for water laser peening cumulative fatigue lives and the other for one line ultrasonic peening. The applications of these models indicated satisfactory fatigue lives prediction compared to the experimental results.

5.2 Recommendations

The following suggestions for future work are recommended:

1. Repeating the work of this study with same aluminum alloy by use ultrasonic under different temperatures.

2. Study the effect of laser peening on the same alloy by using black paint and water together.

3. Study the effect of needle type of ultrasonic peening on the fatigue life and surface roughness of the same alloy.

4. Study the effect of the treatment time periods for mechanical properties and fatigue life of the same alloy by using ultrasonic peening.

5. Use of materials other than 2017A-T3 Al-alloy.

6. Study the crack growth behavior under the above two peening.

References

Aggarwal M L, R A Khan& V P Agrawal."Influence of shot peening intensity on fatigue design reliability of 65Si7 spring steel" Indian Journal of Eng. and material sciences Vol. 12,pp, 515-521 (2005).

Ahmad, Zaki (2003)."The properties and application of scandium-reinforcedaluminum" *JOM 55 (2): 35.* Bibcode:JOM....55b..35A. doi:10.1007/s11837-003-0224-6 (2003) .

Aid A., Chalet J., Amrouche A., Mesmacque G., Bonguediab M." Anew damage indicator: from blocks loading to random loading" Fatigue Des (16-18) (2005).

Alalkawi H.J, Amer H.M, A.B,"Interaction of corrosion cumulative fatigue and shot peeningof 1100 H12 aluminum alloy"Alkhawarizmi journal, Baghdad Iraq, vol.11 No.1, pp65-72 (2015).

Alalkawi H.J. Alsaraf S. A.Abdul-Jabbar H."A new cumulative damage theory for fatigue life predication under shot peening treatment" ISSN (printed) 18181171 ISSN(online)23120789 Year**: 2014** Volume**: 10** Issue**: 2** Pages: 57-64 Alkhawarizmi journal, Baghdad Iraq,(**2014**).

AlalkawiH.J., A.A. Talal, H.A. Safaa"Analysis the effects of shot peening upon the mechanical and fatigue properties of 2024-T351 AL-alloy" Engineering and Technology Journal, vol.30, No.1, pp.1-12, (2012).

AlalkawiHussain J. M.,*, Hazim Khalil Khalaf, " Cumulative fatigue damage under shot peening treatment," Department of Electromechanical Engineering, University of Technology, Baghdad-Iraq, *Elixir Orthopedics 73 (2014) 25954-25955.*

AnoopVasu, Ramana V. Grandhi "Effects of curved geometry on residual stress in laser peening", Wright State University, Dayton, OH 45435, USA, (2012) .

AuezhanAmanov,In-Sik Cho, Dae-Eun Kim, "Effectiveness of high-frequency ultrasonic peening treatment on the tribological characteristics of Cu-based sintered materials on steel substrate " Yonsei University, Seoul 120-749, South Korea, (2012).

BaptistaC.A.R.P, A.M.L. Adib,"Describing fatigue crack growth and load ratio effects in AL 2524 T3 alloy with an enhanced exponential model" Escola de Engenharia de lorena, EEL-USP, Department of materials Engineering, cx.postal 116, CEP 12602-810 Lorena /SP, Brazil (April 2012).

Bohdan N. Mordyuk_, Georgiy I. Prokopenko. " Ultrasonic impact peening for thesurface properties' management, Kurdyumov Institute for Metal Physics, National Academy of Science of Ukraine, (2007) .

Bruce W. Gonser," Modern Materials: Advances in Development and Applications," Volume 6 ,pp 128, Elsevier,22 Oct. (2013).

Charles S. Montross a, Tao Wei a, Lin Ye a, Graham Clark b, Yiu-Wing Mai." Laser shock processing and its effects on microstructure and properties of metal alloys: a review"International Journal of Fatigue 24 (2002) 1021–1036.

ChenHansong , Jianzhong Zhou 1, Jie Sheng , XiankaiMeng 1, Shu Huang and XiaojiangXie" Effects of Warm Laser Peening on Thermal Stability and High Temperature Mechanical Properties of A356 Alloy" journal/metals, Metals 2016, 6, 126; doi:10.3390/met6060126 (2016).

Clauer AH, Walters CT, Ford SC. The effects of laser shock processing on the fatigue properties of 2024-T3 aluminum. Lasers in materials processing. Metals Park (Ohio): ASM International; 1983.

CollinsJack A. ," Failure of Materials in Mechanical Design": Analysis, Prediction, Prevention, pp 258-262 (1993).

Duaa A. K. Q, "Fatigue of aluminum alloy under low temperature using electrical control circuit" A thesis submitted to the electromechanical engineering Department University of Technology, (2016).

Fatemi A. and L. Yang," cumulative fatigue damage and life prediction theories: a survey of the state of the art for homogeneous materials "Int. J Fatigue Vol. 20. No. 1,pp. 9-34, **(**1998**).**

Fatemi.A,Hamide AL-Amiri, "cumulative Fatigue Damage Application to Estimating the Fatigue life of Engineering parts Under High Temperature with using Leaning system" Msc Thesis, university of Technology, (2006).

Fengze Dai, Jianzhong Zhou, Jinzhong Lu, XinminLuo," A technique to decrease surface roughness in overlapping laser shock peening" Applied Surface ScienceVolume 370, 1 May 2016. Pages 501–507, (2016).

Fisher, J.W., E.Sh. Statnikov, L. Tehini, Fatigue Strength Enhancement by Means of Weld Design Change and the Application of Ultrasonic Impact treatment, Proc. of Intl. Symp. On Steel Bridges, Chicago (2001).

GarciaS., A.Amrouche, G. Mesmacque, "Fatigue damage accumulation of cold expanded hole in aluminum alloys subjected to block loading" Laboratoire de Mecanigue de Lille, France,(2005).

Gary R Halford, "Cumulative fatigue damage modeling- Crack nucleation and early growth" Senior Research National Aeronautics and Space Administration, Cleveland , OH 44135, USA (1997).

GouJ. Yu, G., L. Zhang,W. Zhang, H. Chen, and Y.P. Yang." Ultrasonic Impact Treatment to Improve Stress Corrosion Cracking Resistance of Welded Joints of Aluminum Alloy" JMEPEG (2016) 25:3046–3056 DOI: 10.1007/s11665-016-2087-3, June 8,(2016).

GyekenyesiJ. Z:, "NASA life-component Fatigue and creep life prediction", National Aeronautics and space Administration, (2005).

Halid Can Yildirim , Gary B. Marquis,"Fatigue strength improvement factors for high strength steel welded jointstreated by high frequency mechanical impact" Contents lists available at SciVerse Science Direct International Journal of Fatigue (2012).

Hangzhou Create Ultrasonic Technology Co. Ltd "Ultrasonic Generator, Ultrasonic prestressing force impact treatment system" Operation Instruction. WW. hzcreate. en. alibaba . Com (2013).

http://www.weibull.com/hotwire/issue116/hottopics116.htm. Copyright© 1992- 2016 ReliaSoft Corporation. All Rights Reserved.

https://en.wikipedia.org/wiki/Aluminium_alloy, sited on (2015).

https://en.wikipedia.org/wiki/Laser_peening, sited on (2015).

https://www.google.iq/search?q=laser+peening+mechanism, sited on (2015).

Joseph Edward shigley "Mechanical Engineering Design", 1st metric edition, Mcgraw-Hillcompany (1986).

KadhimN.A, S. Abduyah, A.K. Ariffin, "Effective strain damage model associated with finite element modeling and experimental Validation" University kebangsao Malaysia,(2011).

KalainathanS' , S. Prabhakaran, "Recent development and future perspectives of low energy laser shock peening", Optics & Laser TechnologyVolume 81, July 2016, Pages 137–144, (2016).

Kaufman J. G, "(ALUMINUM ALLOYS)" chapter3 Columbus, ohio (2006).

Khurml R.S, Gupta " Machine Design" tenth Edition, p 140 (1990).

Kim, W.H>; Laird, C. Crack Nucleation and State I Propagation in High Strain Fatigue- II Mechanism. ActaMetallurgica. pp. 789–799, (1978).

KnudE. Hansen andBrik-Sorensen,"Aluminum fatigue tests", **(**2000**).**

Kudryavtsev Y. and J. Kleiman." Fatigue Improvement of Welded Elements and Structures by Ultrasonic Impact Treatment (UIT/UP)". International Institute of Welding. IIW Document XIII-2276-09. 2009.

Kudryavtsev Y. and J. Kleiman. "Increasing Fatigue Strength of Welded Elements and Structures by Ultrasonic Impact Treatment". International Institute of Welding. IIW Document XIII-2318-10. (2010).

Kudryavtsev Y., J. Kleiman and Y. Iwamura. "Fatigue Improvement of HSS Welded Elements by Ultrasonic Peening. Proceedings of the International Conference on High Strength Steels for Hydropower Plants", July 20-22, 2009. Takasaki, Japan.

Kudryavtsev Y., J. Kleiman," Fatigue Life Improvement of Welded Elements by Ultrasonic Peening" INTERNATIONAL INSTITUTE OF WELDING, Canadian Delegation Ukrainian Delegation IIW Document XIII (2010).

Kuilin Yuan, Yoichi Sumi," Simulation of residual stress and fatigue strength of welded joints under the effects of ultrasonic impact treatment (UIT)" International Journal of FatigueVolume 92, Part 1, November 2016, Pages 321–332. (2016).

KyunTaekChoa, Kyung Song, Sang Ho Oh, " Surface hardening of aluminum alloy by shot peening treatmentwith Zn based ball, Korea Institute of Industrial Technology, Korea ,(2012) .

Liang Li, Miru Kim, Seungjun Lee, MunkiBae, Deugwoo Lee' ," Influence of multiple ultrasonic impact treatments on surface roughness and wear performance of SUS301 steel" Surface and Coatings Technology Available online 13 September (2016).

LuoK.Y. , B. Liu, L.J. Wu, Z. Yan, J.Z. Lu,," Tensile properties, residual stress distribution and grain arrangement as a function of sheet thickness of Mg–Al–Mn alloy subjected to two-sided and simultaneous LSP impacts"Applied Surface ScienceVolume 369, 30 April 2016, Pages 366–376, (2016).

Luo K.Y. , X. Jing a,J.Shenga,G.F. Sun b, Z.Yan a, J.Z. Lu," Characterization and analyses on micro-hardness, residual stress and microstructure in laser cladding coating of 316L stainless steel subjected to massive LSP treatment" Contents lists available at ScienceDirect Journal of Alloys and Compounds, 673 (2016) 158e169, (2016).

Luo K.Y., T. Lin, F.Z. Dai, X.M. Luo," .Effects of overlapping rate on the uniformities of surface profile of LY2 Al alloy during massive laser shock peening impacts" Volume 266, 25, Pages 49–56 China, March(2015).

LynnA.K, D.L. Du Quesnay, "Computer Simulation of Variable amplitude Fatigue crack initiation behavior Using a new strain-based cumulative damage model" Kyoto university, sakyou-ku, Kyoto 606- 8507, (2012).

MahirH.Majeed "Accumulated Damage in Fatigue-creep interaction of Aluminum Alloy 2024-T_4"phD thesis, university of Technology (2009).

Manson S.S. "Re- Examination of cumulative fatigue damage analysis- an engineering perspective Eng. Fract.(1986, Pages 539–571),(1986).

Mao-ZhongGe,Jian-Yun Xiang,"Effect of laser shock peening on microstructure and fatigue crack growth rate of AZ31B magnesium alloy" Contents lists available at Science Direct Journal of Alloys and Compounds 680 (2016) 544-552. (2016).

Martinez SA, Sathish S, Blodgett MP, Shepard MJ. Residual stress distribution on surface-treated Ti–6Al–4V by X-ray diffraction. ExpMech 2003;43(2):141–7.

MassoudMalaki. Hongtao Ding," A review of ultrasonic peening treatment" Materials & DesignVolume 87, 15 December 2015, Pages 1072–1086. (2015).

May A., L. Taleb, M.A.B elouchrani,"Analysis of the cyclic behavior and fatigue damage of extruded AA2017 aluminum alloy" Material science and engineering A571,123,136 (2013).

Mayer H., C.E de, J.E.Alison" Influence of cyclic loads below endurance limit or threshold stress intensity on fatigue damage in cast aluminium alloy 319-T7 "International Journal of FatigueVolume 27, Issue 2, February 2005, Pages 129–141 (2005).

MillerK.J.,MohamedAlalkawiH.J.and de los Rios" Fatigue damage accumulation above and below the fatigue limit" European Group on Facture publication No.1, EGF1(1986).

Montross CS, Wei T, Ye L, Clark G, Mai Y-W. Laser shock processing and its effects on microstructure and properties of metal alloys: a review. Int J Fatigue;24:1021–36. (2002).

MordyukB.N , O.P. Karasevskaya ," Structurally induced enhancement in corrosion resistance of Zr–2.5%Nb alloy in saline solution by applying ultrasonic impact peening", KurdyumovInsttitute for Metel Physics, Ukraine (2012).

Mordyuk B.N., G.I. Prokopenko,Yu.V.Milman, M,o,lefimov, A.V. Sameljuk "Enhanced fatigue durability of Al-6Mg alloy by applying ultrasonic impact peening: Effects of surface hardrning and reinforcement with AlCuFequasicrystalline particles" Materials science and Engineering A 563 (Pages 138–146) (2013).

MordyukB.N., G.I. Prokopenko, P.Yu. Volosevich, L.E. Matokhnyuk, A.V. Byalonovich,T.V., "Improved fatigue behavior of low-carbon steel 20GL by applying ultrasonic impact treatment combined with the electric discharge surface alloying"Materials Science and Engineering: AVolume 659, 6 April 2016, Pages 119–129 (2016).

Mustafa B. H. Al-Khafaji "Experimental and theoretical study of composite material under static and dynamic loadings with different temperature conditions" PhD. Thesis, University of Technology (2014).

NallaR.K. ,I. Altenberger b, U. Noster," On the influence of mechanical surface treatments* deep rolling and laser shock peening* on the fatigue behavior of Ti_ 6Al_ 4V at ambient and elevated temperatures." Department of Materials Science and Engineering,University of California, Berkeley, CA 94720-1760, USA, (2003).

NouguierC.-Lehona,n, M.Zarwel a, C.Diviani , " Surface impact analysis in shot peening process " University of Lyon, ,France (2012).

OmerG.Bilir, " Experimental investigation of fatigue damage accumulation in 1100 AL-alloy" Middle East Technical university, Ankara, Turkey (1991).

PantB.K, A.H.V. Pavan, Raghu V. Prakash, M. Kamaraj," Effect of laser peening and shot peening on fatigue striations during FCGR study of Ti6Al4V "International Journal of FatigueVolume 93, Part 1, December 2016, Pages 38–50, (2016).

PerreiraH.F.S.G, Jesus A.M.P, Ribeir A.S, Fethades A.A." Fatigue damage behavior of structural components under variable amplitude loding" Mech. Exp. Vol.17 pp.75-85 (**2009)**.

PeyreP., p. Merrien, H. Lieurade, R. Fabbro," Laser induced shock waves as surface treatment for 7075-T735 aluminum alloy" surface Engineering. 11.47-52 (1995).

PolmearI. J, "Light Alloys; Metallurgy of the light Metals" Halsted press, London 1996).

PrabhakaranS. , S. Kalainathan," Warm laser shock peening without coating induced phase transformations and pinning effect on fatigue life of low-alloy steel" Materials & DesignVolume 107, 5 October 2016, Pages 98–107, (2016).

Ramos R., N. Ferreira, J.A.M. Ferreira,C. Capela, A.C. Batista" Improvement in fatigue life of Al 7475-T7351 alloy specimens by applying ultrasonic and microshot peening"International Journal of FatigueVolume 92, Part 1, November 2016, Pages 87–95, (**2016**).

Ren **X.D**. , Y.K. Zhang," Effect of laser shock processing on the fatigue crack initiation and propagation of 7050-T7451 aluminum alloy" School of Mechanical Engineering, Jiangsu University. PR China.(2010).

Richard D. T. ,Dovid F. L. "Preventing fatigue failures with laser peening" The AMPTIAC Quarterly,vol.7. No.2, (2003).

Richard D.T, David F.L "preventing fatigue failures with laser peening" The AMPTIAC Quarterly, vol.7, No.2 (2003).

Robert A. Brockman, William R. Braisted," Prediction and characterization of residual stresses from laser shock peening", a University of Dayton Research Institute, Dayton, OH, USA, (2011).

Roncobden, Alcan, Banbury, "Aluminim: Physical properties, Characteristics and alloys", TALAT Lecture 1501 (1997).

RubioC-González[a,,], C. Felix-Martinez[a], G. Gomez-Rosas[b], J.L. Ocaña[c], M. Morales[c], J.A. Porro," Effect of laser shock processing on fatigue crack growth of duplex stainless steel"Materials Science and Engineering: A528, Pages 914–919 (2011).

Ryder G.H "Strength of Materials " Third Edition in SI Units, p327 (1982) .

Sakion Y., K.Youshikawa, Y.sano and Y-c kim "Effect of laser peening on residual stress and fatigue life of welded joints of high strength steel" proceeding of national symposium on welding mechanics and design 471-477 (**2009**).

Salimianrizi A., E. Foroozmehr a, M. Badrossamay a, H. Farrokhpour," Effect of Laser Shock Peening on surface properties and residual stress of Al6061-T6" Contents lists available at Science Direct journal homepage Optics and Lasers in Engineering 77 (2016) 112–117, (2016).

SamerS.murdhi "fatigue behavior under shot peening and laser peening stainless steel turbine shaft "A thesis submitted to the material engineering department ,AL – Mustansiriya University , Degree of master of science ,(2013).

Sanders R.E., Technology Innovation in aluminum Products, The Journal of The Minerals, 53(2):21–25, (2001).

Sanjeev Kumar' , K. Chattopadhyay, G.S. Mahobia, Vakil Singh," Hot corrosion behaviour of Ti–6Al–4V modified by ultrasonic shot peening" Materials & Design, Volume 110, 15 November 2016, Pages 196–206, (**2016**).

SchijveJ., "Fatigue of structures and materials" 2nd Ed, springer, (2009).

Schulze V. "Modern Mechanical surface treatment Wiley- VCH, Weinheim (2005).

Schwarz, James A.; Contescu, Cristian I.; Putyera, Karol (2004). Dekker encyclopedia of nanoscience and nanotechnology *3. CRC Press. p. 2274.* ISBN 0-8247-5049-7,(2004).

Sealy M.P., Y.B. Guo, R.C. Caslaru, J. Sharkins, D. Feldman," Fatigue performance of biodegradable magnesium–calcium alloy processed by laser shock peening for orthopedic implants" International Journal of FatigueVolume 82, Part 3, January 2016, Pages 428–436, (2016).

Shaikjeelani and Muhammad Aslam, "AStudy of cumulative fatigue damage in Aluminum alloy 2024-T4" school of Engineering, Tuskegee Institute, Tuskegee, AL 36088 (U.S.A),(1984).

Sheng J., S. Huang, J.Z.Zhou, J.Z. Lu, S.Q. Xu, H.F. Zhang," Effect of laser peening with different energies on fatigue fracture evolution of 6061-T6 aluminum alloy" Optics & Laser TechnologyVolume 77, March 2016, Pages 169–176, (2016).

Stephens R. 1, Ali Fatemi "Metal Fatigue in Engineering" second Edition, P 248-252 (2001).

TAN1 Y.,G.WU1, J.-M.YANG1 and T.PAN2." Laser shock peening on fatigue crack growth behaviour of aluminium alloy" 1Department of Materials Science and Engineering, University of California, Los Angeles, CA, USA; 2Research and Advanced Engineering, Ford Motor Company, Dearborn, MI, USA Received in final form 21 November (2003).

Technology.open.ac.uk/materials/mem/mem_mftext.htm© 2005 Materials Engineering - Page last modified 18-Dec-2007.

ThibautChaisea, Jun Li, Daniel Néliasa, RégisKublerd, Said Taherib, Gérard Douchetc, Vincent Robine, Philippe Gilles," Modelling of multiple impacts for the prediction of distortions and residual stresses induced by ultrasonic shot peening," Journal of Materials Processing Technology, Journal of Materials Processing Technology 212 (2012) 2080– 2090, (2012).

Thomas Rousseau, Thierry Hoc, Philippe Gilles, Cécile Nouguier-Lehon," Effect of bead quantity in ultrasonic shot peening: Surface analysis and numerical simulations"Journal of Materials Processing TechnologyVolume 225, , Pages 413–420, November (2015).

ttp://www.totalmateria.com/page.aspx?ID=CheckArticle&LN=AR&site=kts&NM=282, sited on (2016).

UmapathiA.,S. Swaroop," Residual stress distribution in a laser peened Ti-2.5Cu alloy," Surface and Coatings TechnologyVolume 307, Part A, 15 December 2016, Pages 38–46, (2016).

VaibhavPandey, K. Chattopadhyay, N.C. SanthiSrinivas, Vakil Singh," Low Cycle Fatigue behavior of AA7075 with surface gradient structure produced by Ultrasonic

Shot Peening" Procedia Structural IntegrityVolume 2, 2016, Pages 3288–3295, 21st European Conference on Fracture, ECF21, 20-24 June 2016, Catania, Italy. (**2016**).

Vinodh Krishna Caralapatti, SivakumarNarayanswamy," Effect of high repetition laser shock peening on biocompatibility and corrosion resistance of magnesium" science direct, Optics & Laser TechnologyVolume 88, February 2017, Pages 75–84, (2017).

Walterschutz, "A history of fatigue" Engineering Fracture Mechanics, volume 54, Issue 2, May 1996 pp 263-300, Germany, (1999)

WangG.Q., M.K. Lei, D.M. Guo," Interactions between Surface Integrity Parameters on AISI 304 Austenitic Stainless Steel Components by Ultrasonic Impact Treatment" Procedia CIRPVolume 45, 2016, Pages 323–326,(2016).

WeijuJia' , Hengzhang Zhao, Quan Hong, Lei Li, Xiaonan Mao," Research on the thermal stability of a near α titanium alloy before and after laser shock peening" Materials CharacterizationVolume 117, July 2016, Pages 30–34, (2016).

WWW.aircraftmaterials.com/data /aluminum /2017 a.html, sited on (2013).

www.appliedultrasonics.com/solutions.html,sited on (2015).

www.appliedultrasonics.com/Ultrasonic-Peening.htm, sited on (2015).

www.hzhccs.com. Device manual, international department: David Wang, (2014).

www.makeitfrom.com/material.../2017A-T3-Aluminum *sited on (2013).*

www.substech.com,"Laser peening", Dr. Dmitri Kopeliovich, sited on (2015).

Yanjun Fan, Xiaohui Zhao, Yu Liu," Research on fatigue behavior of the flash welded joint enhanced by ultrasonic peening treatment"Materials& DesignVolume 94, 15 March 2016, Pages 515–522, (**2016**).

YanyanFeng, Shengsun Hu, Dongpo Wang' , Hai Zhang**,**" Influence of surface topography and needle size on surface quality of steel plates treated by ultrasonic peening" VacuumVolume 132, October 2016, Pages 22–30. (2016).

YanyanFeng, Shengsun Hu, Dongpo Wang," Formation of short crack and its effect on fatigue properties of ultrasonic peening treatment S355 steel" Materials & DesignVolume 89, 5 January 2016, Pages 507–515(2016).

Ya-zhang HE, Dong-po WANG, Ying WANG, Hai ZHANG', "Correction of buckling distortion by ultrasonic shot peening treatment for 5A06 aluminum alloy welded structure" Transactions of Nonferrous Metals Society of ChinaVolume 26, Issue 6, June 2016, Pages 1531–1537 (**2016)**.

Yiliang Liao a,n, ChangYe b, GaryJ.Cheng." [INVITED] A review: Warm laser shock peening and related laser processing technique"Department of Mechanical Engineering, University of Nevada, Reno, Reno, NV 89557, USA. ScienceDirectOptics &LaserTechnology78(2016)15–24, (2016).

Yongxiang Hu , Zhenqiang Yao, Jun Hu," 3-D FEM simulation of laser shock processing" science direct Surface & Coatings Technology 201 (2006) 1426 1435, (2006).

Zainab A.B," Corrosion- fatigue behavior of 1100-H12 Al-alloy under different shot peening times" MSC thesis, university of Al-Mustansrriya (**2014**).

ZHAOJibin, QIAO Hongchao," Study on Mechanism and Application of Online Detection of Laser Peening" Shenyang Institute of Automation, Chinese Academy of Sciences,(2013).

ZoranBergant, UrošTrdan, JanezGrum," Effects of laser shock processing on high cycle fatigue crack growth rate and fracture toughness of aluminum alloy 6082-T651" Contents lists available at Science Direct International Journal of Fatigue 87 (2016) 444–455, (2016).

Appendix A

Application of proposed model with ultrasonic peening

Predication of fatigue loading in random condition required precise calculation and needs the equation of S-N curve with and without ultrasonic testing.

For low-high stress level tests:

$$\mathbf{D} = \left[\frac{n_1}{N_{f1}} + \frac{n_2}{N_{f2}}\right]^{\left(\frac{Ault\ \sigma_L}{Adry\ \sigma_h}\right)^{\frac{\propto ult}{\propto dry}}}$$

Where n_1 and n_2 is the experimental applied cycles, in this tests.
$n_1 = n_2 = 5000$ for each stress level, low and high.

The S-N curve equations for both cases i-e dry and ultrasonic are given below:

For dry or unpeened S-N curve

$$\sigma_f = 1953\ N_f^{-0.2008}$$

And for ultrasonic S-N curve

$$\sigma_f = 1056\ N_f^{-0.133}$$

1. From σ_f =175 MPa to σ_f =325 MPa

N_{f175} =740231, N_{f325} = 7047

Damage (D) = $\left[\frac{5000}{740231} + \frac{5000}{7047}\right]^{\beta}$

$D = [0.716276]^{\beta} \rightarrow \beta = \left(\frac{Ault\ \sigma_L}{Adry\ \sigma_h}\right)^{\frac{\propto ult}{\propto dry}}$

$$\beta = \left(\frac{1056*175}{1953*325}\right)^{\frac{-0.133}{-0.2008}}$$

$$\beta = (0.291149)^{0.6623}$$

$\beta = (0.44165)$

D = $[0.716276]^{0.44165}$ = 0.8629

R = $\frac{D}{\frac{n_1}{N_{f1}}+\frac{n_2}{N_{f2}}} = \frac{0.8629}{0.7162}$ = 1.2048

N_f= 10000* R =12048 cycles

$N_{f175-325}$ =12048 cycles

---

2. From σ_f =325 MPa to σ_f =175 MPa

N_{f175} =740231, N_{f325} = 7047

Damage (D) = $[\frac{5000}{740231} + \frac{5000}{7047}]^{\beta}$

D = $[0.716276]^{\beta}$

$\beta = (\frac{Ault\ \sigma_h}{Adry\ \sigma_l})^{\frac{\propto ult}{\propto dry}}$

$\beta = (\frac{1056*325}{1953*175})^{0.6623}$ = 1.0027

D = $[0.716276]^{1.0027}$ =0.71555

R = $\frac{0.71555}{0.716276}$ = 0.99909

$N_{f325-175}$ = 9990 cycles

---

3. From σ_f =200 MPa to σ_f =300 MPa

N_{f200} = 271230, N_{f300} = 12863

Damage (D) = $[\frac{5000}{271230} + \frac{5000}{12863}]^{\beta}$

$$D = [0.407146]^{\beta}$$

$$\beta = \left(\frac{\boldsymbol{Ault\ \sigma_h}}{\boldsymbol{Adry\ \sigma_l}}\right)^{\frac{\propto ult}{\propto dry}}$$

$$\beta = \left(\frac{\boldsymbol{1056*200}}{\boldsymbol{1953*300}}\right)^{\boldsymbol{0.6623}} = 0.50876$$

$$D = [0.407146]^{0,5087} = 0.63307$$

$$R = \frac{0.63307}{0.407146} = 1.5549$$

$\boldsymbol{N_{f200-300}}$ = 15549 cycles

---

4. From $\boldsymbol{\sigma_f}$ =300 MPa to $\boldsymbol{\sigma_f}$ =200 MPa

$\boldsymbol{N_{f200}}$ = 271230, $\boldsymbol{N_{f300}}$ = 12863

$$\text{Damage (D)} = \left[\frac{\boldsymbol{5000}}{271230} + \frac{\boldsymbol{5000}}{12863}\right]^{\beta}$$

$$D = [0.407146]^{\beta}$$

$$\beta = \left(\frac{\boldsymbol{Ault\ \sigma_h}}{\boldsymbol{Adry\ \sigma_l}}\right)^{\frac{\propto ult}{\propto dry}}$$

$$\beta = \left(\frac{\boldsymbol{1056*300}}{\boldsymbol{1953*200}}\right)^{\boldsymbol{0.6623}} = 0.87049$$

$$D = [0.407146]^{0.87049} = 0.45739$$

$$R = \frac{0.45739}{0.407146} = 1.1234$$

$\boldsymbol{N_{f2300-200}}$ = 11234 cycles

Table (1): Cumulative fatigue life for L-H and H-L fatigue tests under 1UP.

Landing sequences (MPa)	$N_{f(model)}$	Repetition Of program (R)	Damage (D)
175-325	12048	1.2048	0.8629
200-300	15549	1.5549	0.63307
325-175	9990	0.99909	0.71555
300-200	11234	1.1234	0.45739

Appendix B

Papers published:

First paper

SUST Journal of Engineering and Computer Sciences (JECS), Vol. 17, No. 2, 2016

7049 AL-Alloy Fatigue Behavior under Black Paint Laser Peening

Hussian J. Alalkawi, Madlool Awad Saeed, Ali Yousuf Khenyab
School of Mechanical Engineering, Sudan University of Science and Technology, Khartoum, Sudan
Alalkawi2012@yahoo.com

Received:15/06/2014
Accepted:28/08/2014

ABSTRACT- Black Paint Laser (bPL) peening technique is currently applied to engineering components due to their improvements of fatigue behavior and economic advantages. In the current work, the experimental examinations of bPL peening, which aims to understanding the fatigue behavior of bPL surface treated bars was carried out. The application of bPL was associated with significant extension of fatigue life and strength. This extension is due to compressive residual stresses (CRS) generating from peening process. A series of fully rotating bending fatigue tests was conducted at room temperature using 7049 Aluminum alloy. Improvements in fatigue life and strength for constant and cumulative fatigue were demonstrated. Finally, the fatigue strength of 7049 Aluminum alloy at 10_7 cycles increased by 53% and cumulative fatigue life improved by factors of 1.55 and 1.787 for Low-high sequence and high-low sequence due to bPL treatment respectively.

Keywords*: Aluminum alloy, black Paint Laser (bPL), fatigue strength, residual stress cumulative fatigue life, Laser shock peening (LSP), fatigue crack growth (FCG)*

المستخلص - إن تقنية معالجة سطوح المعادن بواسطة أشعة الليزر وبعد طلائها بطبقة من طلاء أسود تعتبر من الطرق الرائده الحديثة والمستخدمة مع المواد الهندسية, حيث يتم تحسين قابليتها على تحمل الكلال(التعب) وبالتالي الحصول على مزايا اقتصادية. في هذا البحث تم تصميم,واجراء التجارب اللازمة على عمدان من سبيكة الألمونيوم نوع . 7049 كانت النتائج مشجعه وواضحة بزيادة قابليتها على التحمل ومقاومة التعب وزيادة عمر الأشتغال ، أن هذه الزيادة أو التحسين نتيجة لتوليد إجهادات ضغط متبقية (CRS) علي السطح والتي تولدت بتأثير التعرض لاشعة الليزر . تم اجراء التجارب علي عينات من عمدان الألمونيوم مطلية بطبقة رقيقة من الطلاء الأسود وتعريضها الي أحمال مختلفة خلال دورانها. النتائج المحددة التي تم الحصول عليها هي أن مقاومة التعب عند 10^7 دورة ا زادت بمقدار % 53 ونسبة زيادة عمر التعب التراكمي كانت بمقدار 1.55 و 1.787عند الزيادة أو النقصان المضطرد للدو ا رت وعلى التوالي.

Second Paper

Available online at www.elixirpublishers.com
(Elixir International Journal)

Mechanical Engineering
Elixir Mech. Engg. 82 (2015) 32362-32366

ISSN: 2229-712X

Fatigue life prediction under different laser coatings for cumulative bending based on a new non-linear model

Alalkawi H.J.M1, Elkhawad Ali Elfaki2, Ali Yousuf Khenyab2 and Zainab K. Hantoosh1
1University of Technology Baghdad, Iraq.
2 Sudan University of Science and Technology, Sudan

ARTICLE INFO
Article history:
Received: 8 March 2015;
Received in revised form:
28 April 2015;
Accepted: 6 May 2015

ABSTRACT

A non-linear cumulative fatigue model was developed for estimating the fatigue life of high strength aluminum alloy 7049 in high cycle fatigue (HCF) and low cycle fatigue (LCF) regimes with different laser surface coatings. These coatings are water laser peening and the black paint laser peening (bPLP). The results of the application the new non-liner model to the experimental data that the proposed model is quite applicable for interaction cumulative fatigue with laser coating. The paper also indicated that the fatigue limit increased by 2.59 due to bpLp while it reduced by 2.3 due to WLP. The new non linear model showed satisfactory prediction for bpLp cumulative fatigue loading.

Keywords
Non-linear fatigue model,
Cumulative fatigue life prediction, 7049 aluminum alloy,
Laser coating

Third paper

MINISTRY OF HIGHER EDUCATION
AND SCIENTIFIC RESEARCH
UNIVERSITY OF BABYLON
COLLEGE OF ENGINEERING

وزارة التعليم العالي والبحث العلمي
جامعة بابل
كلية الهندسة

The Iraqi Journal for Mechanical and Materials Engineering
Editorial Board

المجلة العراقية للهندسة الميكانيكية وهندسة المواد
هيئة تحرير المجلة

Date / 19/5/2016
Ref. / 3644

العدد / ٣٦٤٤
التاريخ / ١٩/٥/٢٠١٦

قبول نشر

الى / أ.د. حسين جاسم العلكاوي المحترم / الجامعة التكنولوجية / قسم الكهروميكانيك
د. الخواض علي الفكي المحترم / جامعة السودان للعلوم والتكنولوجية
السيد علي يوسف خذياب المحترم / جامعة السودان للعلوم والتكنولوجية
م / قبول بحث للنشر .

تهديكم هيئة تحرير المجلة العراقية للهندسة الميكانيكية وهندسة المواد أطيب تحياتها وتود بعد أن تدارست واطلعت على آراء المقيمين بنصوص بحثكم الموسوم :-

Laser surface coating fatigue interaction of 2017A-T3 Aluminum alloy

أن تعلمكم بقبول بحثكم الموسوم اعلاه للنشر في مجلتنا وسينشر بالأعداد القادمة للمجلة متمنين لكم التوفيق مع التقدير.....

أ . د . هارون عبد الكاظم شهد
رئيس هيئة التحرير

تعنون المراسلات إلى/مدير هيئة التحرير/المجلة العراقية للهندسة الميكانيكية وهندسة المواد/كلية الهندسة/جامعة بابل محافظة بابل/العراق ص.ب (٤)
البريد الالكتروني.. (engineering _ mech _mat @yahoo.com)

Laser surface coating fatigue interaction of 2017A-T3 Aluminum alloy

Alalkawi H.J.M* Elkhawad Ali Elfaki ** Ali Yousuf Khenyab***
University of Technology Baghdad
Sudan University of Science and Technology
Sudan University of Science and Technology
Alalkawi2012@yahoo.com
Iraq
Sudan
Sudan

Abstract

The interaction of fatigue and laser peening with different surface coatings was studied for 2017A-T3 aluminum alloy under stress ratio R= -1 and room temperature (RT). This interaction is a major issue in the practice life assessment of aircrafts. The current work examined the effect of laser surface with different coatings i.e. ALP (Air laser peening), BPL (Black paint laser peening) and WLP (Water laser peening) on

cumulative fatigue. The experimental results observed that the fatigue strength was improved by 18% and 35% under BPL and WLP respectively. A new non-liner damage model was derived to predict the cumulative fatigue lives. This model showed safe and satisfactory predictions for unpeend and peened specimens for all cases of surface coatings. While Miner theory indicated not always suitable for life prediction of cumulative fatigue loading.

التداخل الكلالي مع التغطيه السطحيه الليزريه لسبيكة الالمنيوم 2017A-T3

د. حسين جاسم العلكاوي* **الجامعة التكنلوجية**

د. الخواض علي الفكي** **جامعة السودان للعلوم والتكنلوجيا**

علي يوسف خنياب*** **جامعة السودان للعلوم والتكنلوجيا**

الخلاصه:

تمت انجاز دراسة التداخل الكلالي مع التصليد الليزري لعدة حالات من تغطية سطح عينة سبيكة الالمنيوم 2017A-T3 عند نسبة اجهاد R= - 1 وبدرجة حرارة الغرفه.

يعتبر هذا التداخل عمليه مهمة الاستخدام في تحديد اعمار اجزاء الطائرات. في هذا العمل اجريت الفحصات الكلاليه لبيان تاثير الليزر باختلاف التغطية والتي هي التغطيه الهوائيه, الصبغ الاسود والتغطيه المائية.اوضحت النتائج العمليه ان مقاومة الكلال تحسنت بنسبة 18% و35% عند استخدام الصبغ الاسود والتغطيه المائيةعلى التوالي. تم اشتقاق انموذج جديد لاخطي لتخمين اعمار الكلال التراكمي حيث اعطى هذا الانموذج تخمين امين ومقنع للعينات غير المصلده والمصلده ليزريا لجميع حالات التغطيه بينما اعطت نظرية ماينرالخطية تخمين غير ملائم في بعض حالات التحميل الكلالي التراكمي.

الكلمات المرشدة :التداخل الكلالي, مقاومة الكلال, الكلال التراكمي المصلد ليزريا, التغطيه السطحيه, سبيكة الالمنيوم 2017A-T3.

Keywords: Interaction of fatigue, fatigue strength, cumulative fatigue laser peening, surface coatings, 2017A-T3 AL-alloy.

Fourth paper

International Journal of Energy and Environment (IJEE)-

Applied Mechanics Researches (AMR).

Analysis of ultrasonic peening mechanical properties and fatigue damage of 2017A-T3 aluminum alloy

Alalkawi H.J.M* **Elkhawad Ali Elfaki** ** **Ali Yousuf Khenyab***

University of Technology Baghdad Iraq

Sudan University of Science and Technology Sudan

Sudan University of Science and Technology Sudan

Abstract

Mechanical surface treatment like laser peening (LP), shot peening (SP) and ultrasonic peening (UP) are used to improve the mechanical and fatigue properties of materials. In the current work, ultrasonic peening (UP) technique has been selected using 2017A-T3 Al-alloy in order to enhance the mechanical and fatigue properties of the above alloy. Mechanical properties and constant fatigue testes has been performed at room temperature (RT) and stress ratio R= -1. While variable fatigue tests were carried out for the best group of the fatigue tests. Three type of UP surface treatment were done, i-e one line (1UP), two lines (2UP) and three lines (3UP) at surface test specimens. The experimental analysis of results indicate that, all the above three types of UP improved the mechanical properties i-e and by different percentages. But the best enhancement was obtained for the (1UP). Fatigues at constant amplitude tests have also done for the above three types and compared to the unpeened one. The results showed that the (1UP) is better for fatigue life improvement.

In cooperation with

International Energy and Environment Foundation

International Journal of Energy and Environment

Issue on Applied Mechanics Research

Publication Certificate

Awarded December, 2016 to

Alalkawi H. J. M., Elkhawad Ali Elfaki, Ali Yousuf Khenyab

Published a research paper entitled

Analysis of ultrasonic peening mechanical properties and fatigue damage of 2017A-T3 aluminum alloy

The Editors of International Journal of Energy and Environment (IJEE)
Official Journal of the International Energy and Environment Foundation (IEEF)
Foundation Homepage: www.IEEFoundation.org, Journal Homepage: http://www.IJEE.IEEFoundation.org